THROUGHPUT ANALYSIS OF WIRELESS AD-HOC COGNITIVE RADIO NETWORKS

A Dissertation

by

ARMIN BANAEI

Submitted to the Office of Graduate and Professional Studies of
Texas A&M University
in partial fulfillment of the requirements for the degree of

DOCTOR OF PHILOSOPHY

Chair of Committee,	Costas N. Georghiades
Co-Chair of Committee,	Shuguang Cui
Committee Members,	Jim Ji
	Natarajan Sivakumar
Head of Department,	Chanan Singh

May 2014

Major Subject: Electrical Engineering

ABSTRACT

In this dissertation we consider the throughput performance of cognitive radio networks and derive the optimal sensing and access schemes for secondary users that maximizes their sum-throughput while guaranteeing certain quality of service to primary networks. First, we consider a cognitive radio network where secondary users have access to N licensed primary frequency bands with their usage statistics and are subject to certain inter-network interference constraint. In particular, to limit the interference to the primary network, secondary users are equipped with spectrum sensors and are capable of sensing and accessing a limited number of channels at the same time. We consider both the error-free and erroneous spectrum sensing scenarios, and establish the jointly optimal random sensing and access scheme, which maximizes the secondary network expected sum throughput while honoring the primary interference constraint. We show that under certain conditions the optimal sensing and access scheme is independent of the primary frequency bandwidths and usage statistics; otherwise, they follow water-filling-like strategies.

Next, we study the asymptotic performance of two multi-hop overlaid ad-hoc networks that utilize the same temporal, spectral, and spatial resources based on random access schemes. The primary network consists of Poisson distributed legacy users with density $\lambda^{(p)}$ and the secondary network consists of Poisson distributed cognitive radio users with density $\lambda^{(s)} = (\lambda^{(p)})^{\beta}$ that utilize the spectrum opportunistically. Both networks employ ALOHA medium access protocols where the secondary nodes are additionally equipped with range-limited *perfect* spectrum sensors to monitor and protect primary transmissions. We study the problem in two distinct regimes, namely $\beta > 1$ and $0 < \beta < 1$. We show that in both cases, the

two networks can achieve their corresponding stand-alone throughput scaling even without secondary spectrum sensing ; this implies the need for a more comprehensive performance metric than just throughput scaling to evaluate the influence of the overlaid interactions. We thus introduce a new criterion, termed the *asymptotic multiplexing gain*, which captures the effect of inter-network interference . With this metric, we clearly demonstrate that spectrum sensing can substantially improve the overlaid cognitive networks performance when $\beta > 1$. On the contrary, spectrum sensing turns out to be redundant when $\beta < 1$ and employing spectrum sensors cannot improve the networks performance.

Finally, we present a methodology employing statistical analysis and stochastic geometry to study geometric routing schemes in wireless ad-hoc networks. The techniques developed in this section enable us to establish the asymptotic connectivity and the convergence results for the mean and variance of the routing path lengths generated by geometric routing schemes in random wireless networks.

DEDICATION

To my Parents.

ACKNOWLEDGEMENTS

First and foremost, I would like to express my deepest gratitude to my supervisors Prof. Costas Georghiades and Prof. Shuguang Cui for their invaluable guidance throughout the course of my Ph.D. study at the Texas A&M University. I am thankful for their support and all I have learned from their great professional vision and scientific insight. This would not be possible without them.

I wish to thank my dissertation committee members, Prof. Ji and Prof. Sivakumar for their invaluable comments. I would also like to thank Ms. Tammy Carda for her administrative support and kindness through the course my PhD study.

I would not have been here today if it were not for the love and support of my family. I want to express my deepest thanks to my parents for their unconditional love, devotion and support.

TABLE OF CONTENTS

LIST OF FIGURES

FIGURE Page

1. INTRODUCTION AND BACKGROUND

1.1 Background

The demand for wireless services has been the fastest growing segment of the communications industry in the last decade. The extensive use of voice over IP networks, gaming consoles, PDA's and Wi-Fi networks has shown that wide-band wireless communication is becoming more and more popular and demanded as the last mile connection rather than cable, fiber, etc. Fig. 1.1 shows the devices responsible for mobile data traffic growth, based on the Cisco visual networking index (VNI) global mobile data traffic forecast [1]. Laptops generate a disproportionate amount of traffic today, but smartphones and newer device categories such as tablets and M2M nodes will begin to account for a more significant portion of the traffic by 2017. In 2012 alone, global mobile data traffic grew 70 percent and mobile network connection speeds more than doubled.

The Federal Communications Commission (FCC) licenses certain frequency segments exclusively to a particular user in a particular geographic area and prohibits the transmission of of other unlicensed users in that band. However, with the emergence of personal wireless communications, static spectrum allocation is no longer reasonable due to economical and technological factors. Therefore, Industrial, Scientific and medical (ISM) bands have been provided to support unlicensed networks at 900 MHz, 2.4 GHz, and 5.8 GHz; however, due to the recent boom in wireless technologies, these open channels have become overcrowded with everything from wireless networks to wireless controllers. Fig. 1.2 shows the NTIA's chart of frequency allocation [2].

From the chart it appears that almost all usable frequency spectrum has been

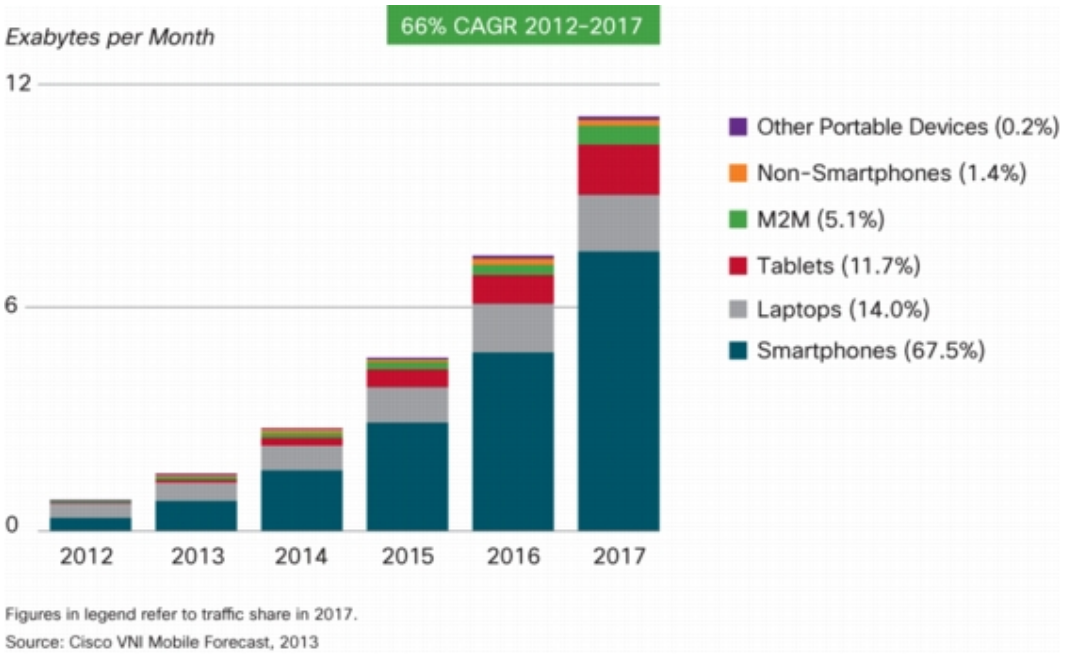

Figure 1.1: Cisco visual networking index (VNI) global mobile data traffic forecast: device diversification.

allocated and we are running out of spectrum. The FCC Spectrum Policy Task Force published a report in 2002 [3], indicating that there is a spectrum shortage for further licensing. However, measurements of actual spectrum usage in different countries show an inefficient utilization of the seemingly crowded radio spectrum mostly in the range of $5\% - 50\%$ [3]–[9]. For example, Fig. 1.3 shows the actual measurements taken in downtown Berkeley, which are believed to be typical and indicate low utilization, especially in the 3-6 MHz bands [9]. Another example could be the current television broadcast frequency bands where on average only 8 channels out of the 68 allocated channels are being used in any given TV market [10], which suggests utilization factor of about 12%. Therefore the real problem is the inefficient spectrum usage due to static spectrum allocations and rigid regulations.

As such, a change to the current spectrum allocation policies is desired. However,

there is still a strong debate going on among economists about the approaches to fix this problem. Some suggest that the introduction of a secondary market in the already existing market could greatly reduce the inefficiencies in spectrum usage [11], while others believe that a common band for all the users is the best solution [12]. They argue that "wireless transmissions can be regulated by a combination of (a) baseline rules that allow users to coordinate their use, to avoid interference-producing collisions, and to prevent, for the most part, congestion, by conforming to equipment manufacturer's specifications, and (b) industry and government sponsored standards" [12]. More specifically, in the first proposed approach primary or licensed users have a higher priority and secondary or unlicensed users have a lower priority in accessing the spectrum. Therefore the secondary user activity should be transparent to primary users. In the second proposed approach, all the users are treated equally and should limit their interference to their neighbors.

From the technological point of view there are still many challenges that need to be addressed until any one of these two approaches become applicable [9, 13, 14]. In particular, both approaches require an acute interference management in order for the users to be able to coexist peacefully along side each other in a shared medium. In order to limit the interference to the primary users two main approaches have been suggested.

The first one, *spectrum sharing/underlay*, is based on controlling the interference temperature at the primary users and makes use of ultra-wideband signaling. For example, secondary users could spread their power over a vast bandwidth to minimize the interference they cause to the primary users [15]. Essentially in this method, the secondary users transmit their packages while the channels are occupied by the primary users but they schedule their transmissions such that the perceived interference at each primary receiver does not exceed the tolerable threshold, as shown in Fig.

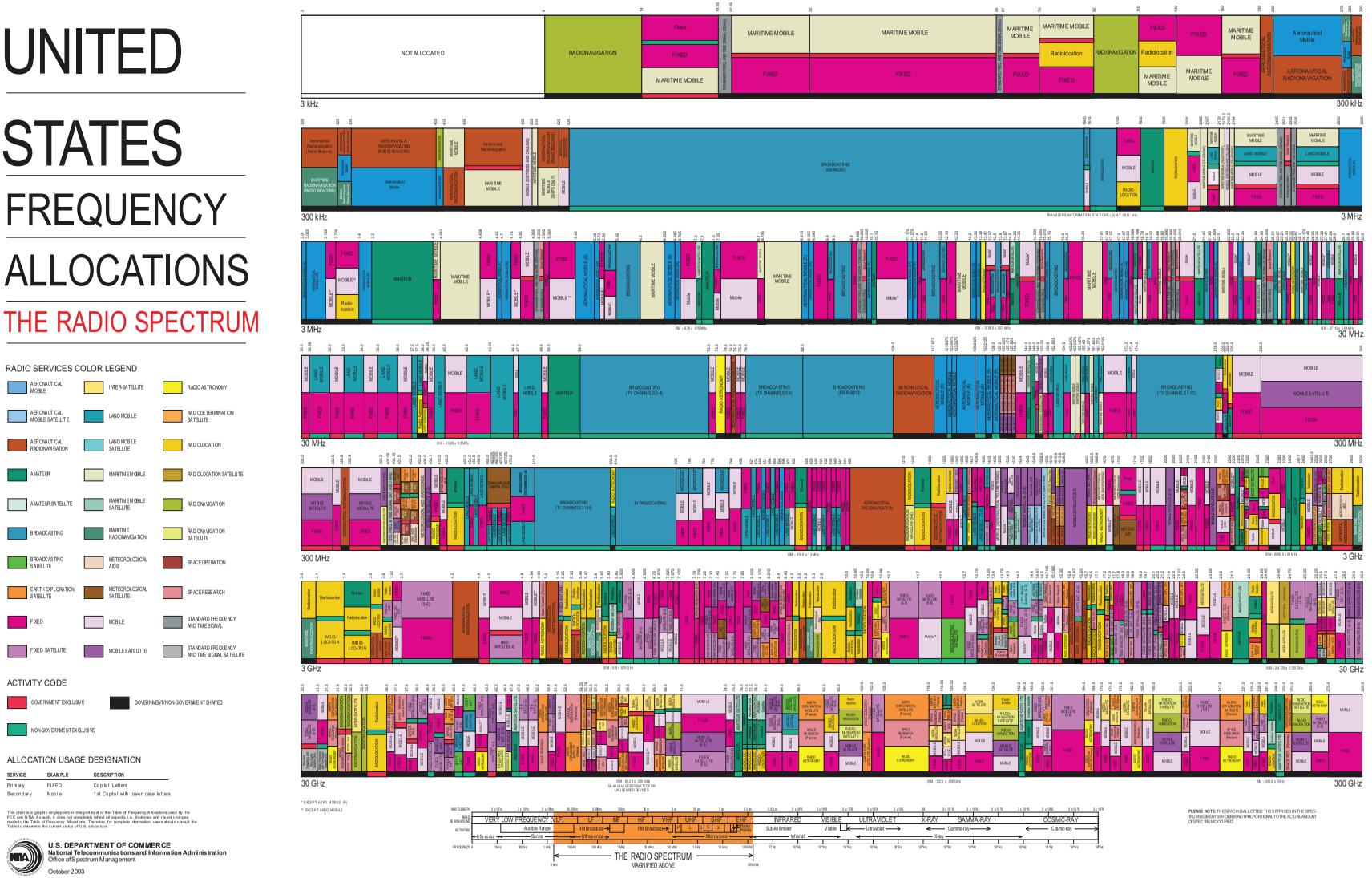

Figure 1.2: NTIA's chart of frequency allocation.

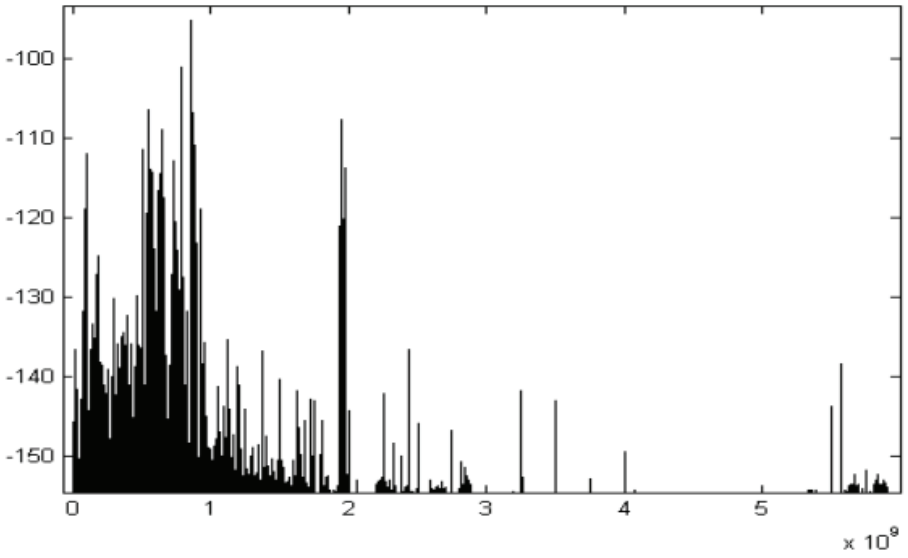

Figure 1.3: Measurement of 0-6 GHz spectrum utilization at Berkeley Wireless Research Center; Power spectral density (PSD) of the received 6 GHz wide signal collected for a span of 50's sampled at 20 GS/s.

1.4. However, implementation of this model results in poor performance compared to the amount of generated interference it can cause to primary users. Hence, this model has been abandoned by the FCC in 2007 [16].

The second strategy is called *opportunistic/dynamic spectrum access*, in which secondary users only make use of locally or temporally unused channels to transmit their data, as shown in Fig. 1.5. Primary signal detection is of fundamental importance to this strategy. The performance of the sensing scheme and the detector characteristics highly affect the system performance. In this dissertation we take the second approach (opportunistic spectrum accessing) and study the performance of the resulting cognitive radio system with randomized medium access protocols.

In Section 2 these effects will be studied in details. Since in this strategy secondary users presumably use the vacant channels they can transmit in higher power or bit

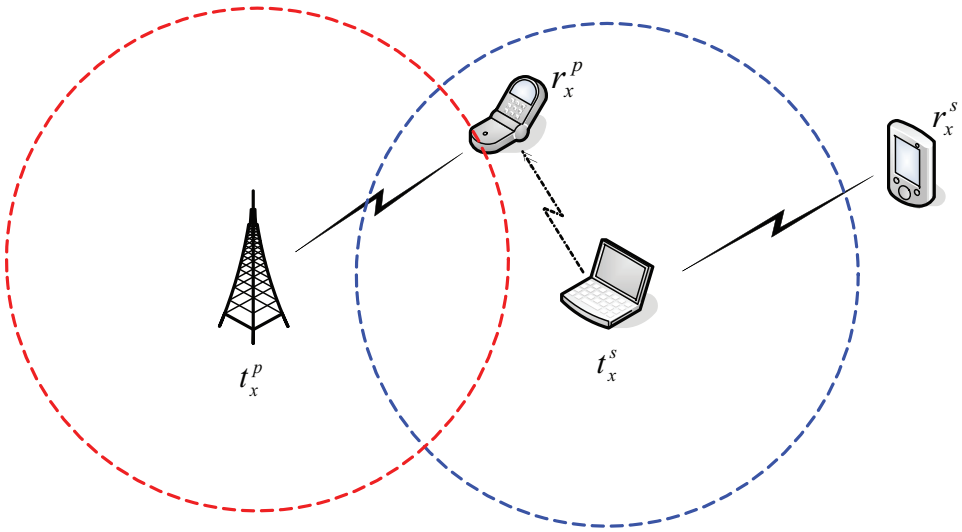

Figure 1.4: Spectrum sharing.

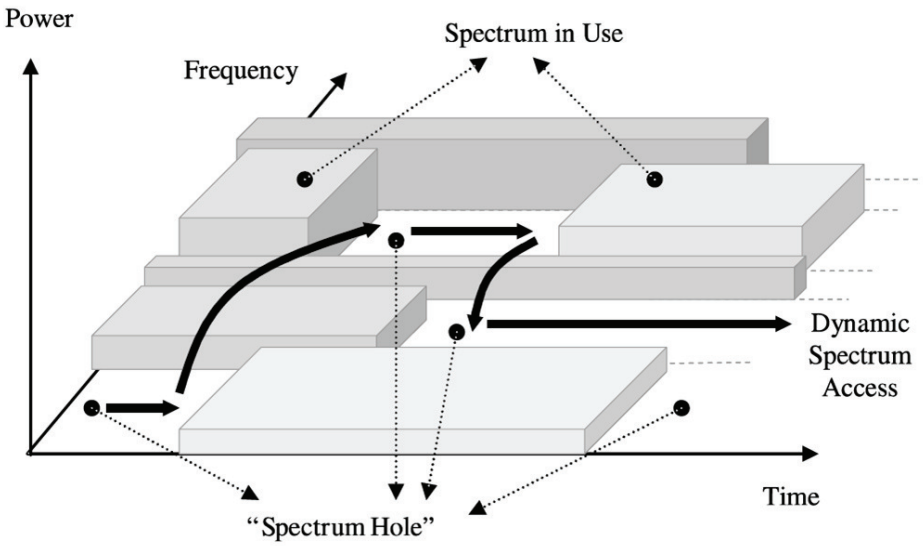

Figure 1.5: Opportunistic spectrum access.

rates compared with the first strategy; But they could only use the channel over a fraction of time or frequency.

1.2 Cognitive Radios

The term *Cognitive radio* was first coined by Joseph Mitola III as a radio that is sufficiently intelligent about the radio resources and can identify the user communication needs in order to provide wireless services most appropriate to user needs [17, 18]. Mitola's CR-1 cognitive radio prototype modeled a cognition cycle at the application layer. His research pointed to the potential use of cognitive radio technology to enable spectrum rental applications and create secondary wireless access markets [19]. A more common definition that restricts the radio's cognition to more practical sensory inputs is the FCC definition of cognitive radios as "a radio that can change its transmitter parameters based on interaction with the environment in which it operates" [20].

The main idea of cognition for a radios is to periodically search the spectrum for available opportunities (idle frequency bands), dynamically adopts the proper transmission policy (power, modulation scheme, ...) in order to avoid interference to other users. When we have multiple cognitive radios working together, we have a cognitive radio network.

To support the cognitive radio idea, the FCC allowed the unlicensed users to use the un-utilized television spectrum [21]. The IEEE also supported the cognitive radio paradigm by developing the IEEE 802.22 standard for wireless regional area network (WRAN) which works in unused TV channels [22].

1.3 Motivation

As mentioned earlier, cognitive radios offer a novel solution to overcome the spectrum under-utilization problem by allowing an opportunistic usage of the spectrum

resources. The underlying idea is to let unlicensed users (secondary users) to use the licensed band as long as they can guarantee low interference to the licensed users. Although seemingly simple, sophisticated interference management protocols are needed to meet the expected level of transparency accepted by licensed users. Essentially, secondary users are allowed to access the spectrum resources of primary users when the primary users are not using them. The secondary users have to vacate the occupied channel whenever the primary users become active in that channel. As such, spectrum sensing plays a key role in successful implementation of cognitive radio networks not only for exploring opportunities but also for limiting the interference imposed to the primary users. Therefore, cognitive radios need to periodically scan the spectrum for primary users activity. One of the key challenges in this regard is the design of wide-band detectors [9].

Due to the present practical limitation, secondary users are capable of sensing and accessing only a limited number of frequency bands at a time. Hence, secondary users can only obtain partial information about the channel state, which together with inherent hierarchy in accessing the channels, imposes substantial complications in identifying transmission opportunities; this differentiates the cognitive medium access control (MAC) layer from the MAC layer in conventional radios.

Furthermore, due to deployment difficulties, the cognitive schemes that make use of a central authority to coordinate the action of secondary users are less appealing. Therefore, recently, distributed techniques for dynamic spectrum allocation, where no central spectrum authority is required, are being widely studied. Though they are less efficient, decentralized approaches require much less cooperation. Some of the decentralized protocols require control channels as a common medium among locally adjacent users to negotiate the communication parameters in order to make the best use of the available opportunities [23, 24]. These protocols face serious challenges:

How to set up the control channel? What if the control channel is corrupted by interference? How to negotiate a transition to a new frequency?

Due to aforestated difficulties and the desired autonomous nature of secondary users, in this dissertation we focus on randomized cognitive MAC protocols, which need no (or minimal) information to be exchanged among secondary users in order for them to take an appropriate actions. This fact rids us from the need of control channels and the complications that they incur.

In additions, the design and deployment of cognitive radio networks necessitate an understanding of the following fundamental questions:

- What is an appropriate metric to evaluate the performance of cognitive radio networks?

- What type of performance assurances can secondary users give to primary users?

- What mechanisms (e.g., spectrum sensing and medium access schemes) can secondary users employ to honor these assurances?

- What are the optimal values for these parameters to maximize the secondary users' throughput while satisfying the primary users' quality of service (QoS) requirements?

In this dissertation, with the above issues under consideration, we focus on the design and analysis of optimal sensing and access schemes that maximize the secondary network throughput while satisfying the primary network QoS requirements in : 1) single-hop multi-channel setup and 2) multi-hop single-channel setup. In the end, we dedicate one section to develop a methodology to characterize the asymptotic statistics of geometric routing schemes in wireless ad-hoc networks. Employing

this method, we can obtain an accurate and more rigorous characterization for the asymptotic throughput of cognitive radio networks.

1.4 Overview of Contributions

In this dissertation, the analysis and design of decentralized sensing and access schemes for cognitive radio networks is investigated. We first consider one of the key issues in design of cognitive MAC which is how to decide which channel(s) to sense and how to share the idle channels between secondary users in such a way that maximizes the spectrum utilization while guaranteeing the desired QoS for the licensed users. We consider a cognitive radio network with access to N licensed primary frequency bands and their usage statistics, where the decentralized secondary users are subject to certain inter-network interference constraint. In particular, to limit the interference to the primary network, secondary users are equipped with spectrum sensors and are capable of sensing and accessing a limited number of channels at the same time due to hardware limitations. We consider both the error-free and erroneous spectrum sensing scenarios, and establish the optimal cognitive MAC framework for a decentralized cognitive radio network, which integrates a random spectrum sensing scheme deciding which channel(s) to sense, and a slotted-ALOHA access protocol to jointly control the inter- and intra-network interferences, and maximize the secondary network expected throughput. Specifically, secondary users seek communication opportunities over a multi-band licensed frequency spectrum while controlling the probability of collision to the primary users at each channel and maximize the secondary expected throughput over all channels. In order to satisfy the collision constraint, secondary users sense the frequency bands that they intend to access, and access them with different probability depending on whether they are idle or busy. We show that under certain conditions the optimal sensing and access scheme

is independent of the primary frequency bandwidths and usage statistics; otherwise, they follow water-filling-like strategies. Moreover, we show that the performance of the secondary network depends on the ratio between the "opportunity-detection" probability and the "mis-detection" probability if the former is larger; otherwise, it depends on the ratio between the "false-alarm" probability and the "detection" probability. Finally, we demonstrate a binary behavior for the optimal access scheme at each channel, depending on whether the opportunity-detection probability or mis-detection probability is larger in that channel.

So far we have studied the throughput performance of the multi-band cognitive network when sources and destinations are in one-hop distance from each other. Next, we study the spatial throughput of multi-hop overlaid ad-hoc networks when both primary and secondary users share a single frequency band. The primary network consists of Poisson distributed legacy users with density $\lambda^{(p)}$ and the secondary network consists of Poisson distributed cognitive radio users with density $\lambda^{(s)} = (\lambda^{(p)})^{\beta}$ ($\beta > 0$, $\beta \neq 1$) that utilize the spectrum opportunistically. Both networks are decentralized and employ ALOHA medium access protocols where the secondary nodes are additionally equipped with range-limited *perfect* spectrum sensors to monitor and protect primary transmissions. We study the problem in two distinct regimes, namely $\beta > 1$ and $0 < \beta < 1$. We show that in both cases, the two networks can achieve their corresponding stand-alone throughput scaling even without secondary spectrum sensing (i.e., the sensing range set to zero); this implies the need for a more comprehensive performance metric than just throughput scaling to evaluate the influence of the overlaid interactions. We thus introduce a new criterion, termed the *asymptotic multiplexing gain*, which captures the effect of inter-network interferences with different spectrum sensing setups. With this metric, we clearly demonstrate that spectrum sensing can substantially improve the overlaid cognitive

network performances when $\beta > 1$. On the contrary, spectrum sensing turns out to be unnecessary when $\beta < 1$ and employing spectrum sensors cannot improve the network performances.

Finally, we present a methodology employing statistical analysis and stochastic geometry to study geometric routing schemes in wireless ad-hoc networks. In particular, we analyze the network layer performance of one such scheme, the random $\frac{1}{2}$disk routing scheme, which is a localized geometric routing scheme in which each node chooses the next relay randomly among the nodes within its transmission range and in the general direction of the destination. The techniques developed in this section enable us to establish the asymptotic connectivity and the convergence results for the mean and variance of the routing path lengths generated by geometric routing schemes in random wireless networks. Furthermore, these techniques enable us to obtain an accurate and rigorous characterization of the asymptotic throughput performance of large scale wireless ad-hoc networks. In particular, we approximate the progress of the routing path towards the destination by a Markov process and determine the sufficient conditions that ensure the asymptotic connectivity for both dense and large-scale ad-hoc networks deploying the random $\frac{1}{2}$disk routing scheme. Furthermore, using this Markov characterization, we show that the expected length (hop-count) of the path generated by the random $\frac{1}{2}$disk routing scheme normalized by the length of the path generated by the ideal direct-line routing, converges to $3\pi/4$ asymptotically. Moreover, we show that the variance-to-mean ratio of the routing path length converges to $9\pi^2/64 - 1$ asymptotically. Through simulation, we show that the aforementioned asymptotic statistics are in fact quite accurate even for finite granularity and size of the network.

1.5 Outline

The rest of the dissertation is organized as follows. In Section 2 we consider the design of the optimal ad-hoc sensing and scheme for cognitive radio networks that maximizes the secondary network sum-throughput. In Section 2.2, we introduce the mathematical models, notations, and definitions. In Section 2.3, we consider the case where the secondary users are equipped with error-free spectrum sensors and investigate how the primary channel bandwidths, their usage statistics, the secondary network population, and their ability to sense and access multiple channels, affect the optimal random sensing and access scheme. In Section 2.4, we extend the analysis to the case where the spectrum detections are error-prone and investigate the effect of spectrum detection errors on the optimal sensing and access scheme. Section 2.5 concludes this study.

In Section 3 we derive the asymptotic throughput and optimal sensing and access schemes for multi-hop overlaid cognitive radio networks in which a primary ad-hoc network and a cognitive secondary ad-hoc network coexist over the same spatial, temporal, and spectral dimensions. Section 3.2 introduces the mathematical model, notations, and definitions. In Section 3.3 we consider the *spatial throughput* of the single-tier network. Section 3.4 studies the cognitive overlaid scenario and addresses the trade-off between the primary and secondary networks by introducing the notion of asymptotic multiplexing gain (AMG). In particular, we show that both networks can achieve their corresponding single-tier throughput scaling regardless of the setting for the spectrum sensing range. However, for the case with a denser secondary network, spectrum sensing can improve the overlaid networks performances; whereas, for the case with a sparser secondary network, the spectrum sensing turns out to be redundant and the primary network AMG cannot be enhanced by employing spec-

trum sensors. Section 3.5 concludes this study.

In Section 4 we present a methodology employing statistical analysis and stochastic geometry to study geometric routing schemes in wireless ad-hoc networks. In Section 4.2 we introduce the system model and describe the random $\frac{1}{2}$disk routing scheme. Then we define the notion of connectivity based on generic geometric routing schemes and state the main results of the section in a theorem regarding the connectivity and the statistical performance of the random $\frac{1}{2}$disk routing scheme. In Sections 4.3 and 4.4 we prove the claims made in this theorem. In Section 4.3, we establish sufficient conditions on the transmission range that ensure the existence of a relaying node in every direction of a transmitting node for both dense and large-scale networks. In Section 4.4, we study the stochastic properties of the paths generated by the random $\frac{1}{2}$disk routing scheme. Specifically, in Section 4.4.1, we prove that the routing path progress conditioned on the previous two hops can be approximated with a Markov process. In Section 4.4.2, using the Markovian approximation, we derive the asymptotic expression for the expected length, and in Section 4.4.3 we derive the asymptotic expression for the variance of the length of the random $\frac{1}{2}$disk routing paths. In Section 4.5, we present some simulation results to validate our analytical results. In Section 4.6, we present some guidelines on how to generalize the results derived for the random $\frac{1}{2}$disk routing scheme to other variants of the geometric routing schemes. We conclude the part in Section 4.7.

In Section 5, we present a summary of dissertation accomplishments and contributions. Recommendations for further research and unanswered questions are also discussed.

2. JOINTLY OPTIMAL RANDOM SPECTRUM SENSING AND ACCESS SCHEME FOR MULTICHANNEL DECENTRALIZED COGNITIVE RADIO NETWORKS

2.1 Introduction

One of the key issues in designing the cognitive MAC is how to decide which channel(s) to sense and how to share the idle channels among secondary users. A considerable amount of literature exists on cognitive MAC protocol design, for example [25]–[28]. In [25] the authors proposed schemes integrating the spectrum sensing policy at the physical layer with packet scheduling at the MAC layer. They analyzed the throughput and the delay-QoS performance of the proposed schemes for the saturation network and the non-saturation network cases under random and negotiation-based channel sensing policies, respectively. In [26], the authors presented two heuristic spectrum sensing policies in which secondary users collaboratively sense the licensed channels. The sensing policies are then incorporated into p-Persistent CSMA to coordinate opportunistic spectrum access for CR network users. In [27], an optimal strategy for dynamic spectrum access of a single secondary user is developed by integrating the design of spectrum sensors at the physical layer with that of spectrum sensing and access policies at the MAC layer, based on a partially observable Markov decision processes framework. In [28], the authors considered a similar problem to ours and proposed a heuristic MAC protocol for opportunistic spectrum access in cognitive radio networks. They considered two channel selection schemes: uniform channel selection vs. spectrum-opportunity-based channel selection, where in the latter case, they considered spectrum availability and selected each channel with different probabilities based on the estimation of spectrum availabil-

ity. However, as shown in this section, these schemes are strictly suboptimal. To the best of our knowledge, none of the existing results provided the design of jointly optimal sensing and access policies for multi-channel, multi-user, decentralized cognitive radio networks.

We note that the problem of medium access design for multi-channel, decentralized cognitive radio networks is similar to the problem of medium access scheduling in the traditional multi-channel wireless networks using CSMA protocol, which has been extensively studied in the literature, for example [29]–[32]. However, the key difference is that the goal of spectrum sensing in the cognitive setup is to detect and protect the primary users, where primary users are oblivious to the existence of the secondary network. Furthermore, the spectrum sensing errors have not been considered in the traditional multi-channel random access protocols. Recently, distributed CSMA scheduling with collision has been considered in [33, 34] for single-channel wireless networks, where the source of collision is not the spectrum detection errors but the simultaneous access attempts by the users.

In this section, we derive the optimal cognitive MAC framework for a decentralized cognitive radio network, which integrates a random spectrum sensing scheme deciding which channel(s) to sense, and a slotted-ALOHA access protocol to jointly control the inter- and intra-network interferences, and maximize the secondary network expected throughput. Specifically, secondary users seek communication opportunities over a multi-band licensed frequency spectrum while controlling the probability of collision to the primary users at each channel and maximize the secondary expected throughput over all channels. In order to satisfy the collision constraint, secondary users sense the frequency bands that they intend to access, and access them with different probability depending on whether they are idle or busy.

The rest of this section is organized as follows. In Section 2.2, we introduce the

mathematical models, notations, and definitions. In Section 2.3, we consider the case where the secondary users are equipped with error-free spectrum sensors and investigate how the primary channel bandwidths, their usage statistics, the secondary network population, and their ability to sense and access multiple channels, affect the optimal random sensing and access scheme. In Section 2.4, we extend the analysis to the case where the spectrum detections are error-prone and investigate the effect of spectrum detection errors on the optimal sensing and access scheme. Section 2.5 concludes the study.

2.2 System Model

Consider a frequency band consisting of N orthogonal channels with bandwidths W_j, $j = 1, \ldots, N$, which are licensed to N time-slotted primary networks. Primary users in channel j access the channel with probability θ_j independent of the users at other frequency bands. as shown in Fig. 2.1. In order to utilize the spectrum more efficiently, the N frequency channels are also made available to an unlicensed (secondary) network comprised of M secondary users who seek opportunities to access the vacant frequency bands while abiding by a certain interference constraints:[1] The *probability* of inter-network interference disturbing primary users in each channel should be no greater than ϵ_j, with $0 \leq \epsilon_j \leq 1$, $j = 1, \ldots, N$, where secondary users interfere with a primary network if they initiate transmission in an already occupied primary channel.

A secondary transmission in an idle channel j is deemed successful if there are no other secondary users transmitting in channel j at the time. Here, we assume that all the secondary users adopt the same physical-layer transmission scheme, such that

[1]Here we are assuming that there is an ideal control mechanism such that every secondary receiver knows in which channel its corresponding secondary transmitter is attempting to establish a connection at any given time [35, 36].

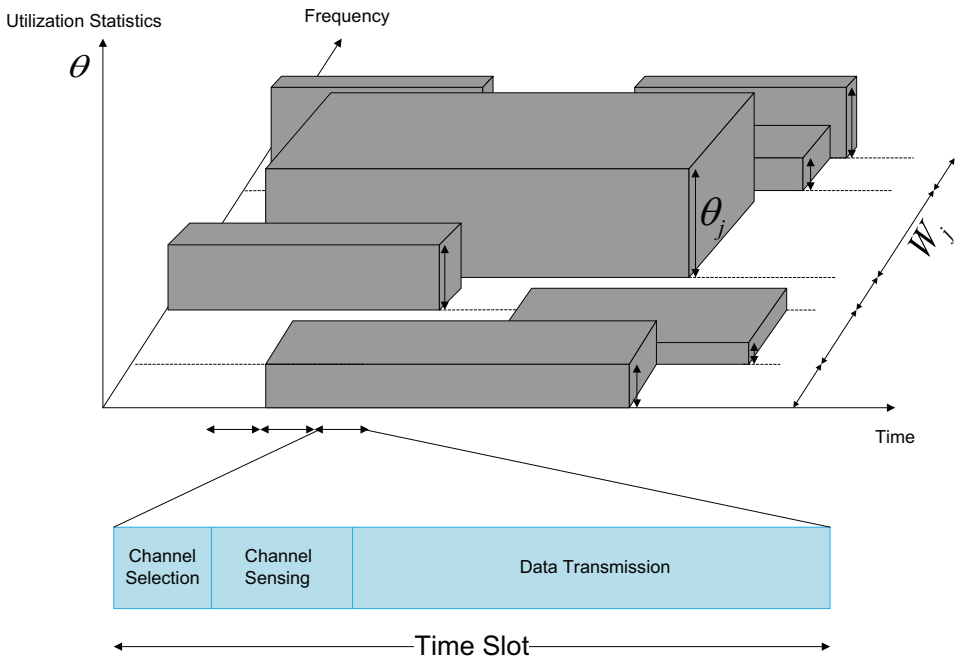

Figure 2.1: Primary channel configuration and utilization statistics, and the secondary time-slot structure.

the achievable rate C_j at channel j only depends on the bandwidth of channel j, constant across different secondary users. We leave the cases with per-user adaptive modulation to a future study. Here we assume that no acknowledgment is required to complete a packet transmission, and secondary transmitters do not re-transmit the data lost in the channel. These assumptions are suitable for delay sensitive applications, e.g., online video or audio streaming and gaming. The interference constraint thresholds and the spectrum occupancy statistics of primary networks are assumed to be available to the secondary network. The secondary network is time-slotted and synchronized with the primary network clock. The basic secondary time slot structure is illustrated in Fig. 2.1. We assume that the secondary users operate under a heavy traffic model, i.e., they always have packets to transmit, to focus on the maximum usage of spectrum opportunities.

In order to satisfy the primary interference constraint, the secondary users are equipped with spectrum sensors. However, due to practical limitations [9], secondary users are only capable of sensing and accessing a limited number of channels at the same time. The partial information obtained about the general channel state and the inherent primary vs. secondary hierarchy in accessing the channels impose substantial complications in identifying transmission opportunities, which differentiates the cognitive MAC layer from the MAC layer in conventional wireless networks. In particular, secondary users need to decide on which channel(s) to sense such that their aggregate expected throughput is maximized while the inter-network interference is limited below the acceptable threshold. To enable autonomous features of the cognitive radio networks, in this section we focus on the class of random sensing and access schemes, which are more appealing due to their decentralized nature [25, 24]. Next, we explicitly define our sensing and access scheme in detail.

We define $\{G_1, \cdots, G_U\}$ to be the set of all sensing actions available to secondary users where U is the cardinality of the action set. Assuming secondary users are capable of sensing $1 \leq S \leq N$ channels simultaneously, G_i corresponds to a specific subset of $\{1, \ldots, N\}$ with cardinality S. We define the secondary user random *sensing scheme* as adopting probability p_i to sense the channel group G_i, where we must have $\sum_{i=1}^{U} p_i = 1$. For example, when $S = 1$ we have that G_i is simply the i^{th} channel, $U = N$, and p_i is the probability of sensing channel i.

Intuitively, for each secondary user to maximize its own throughput, it should sense the channels with highest expected throughput, i.e., S largest $C_j\overline{\theta}_j$'s, where $\overline{\theta}_j = 1 - \theta_j$. However, since all secondary users follow the same strategy, those channels may become too congested. As such, the optimal sensing scheme should spread the secondary users properly over different channels to reduce the intra-network interference, and strike a balance between individual and aggregate gain of the secondary

users.

Let H_{j0} and H_{j1} represent the idle and busy states of channel j. We assume the Receiver Operating Characteristic (ROC) of the secondary spectrum sensor, i.e., the probability of *mis-detection* α_j and the probability of *false-alarm* $1-\beta_j$ at each frequency band are given, where

$$\alpha_j := \Pr(\text{detect } H_{j0} \mid H_{j1} \text{ is true}), \tag{2.1a}$$

$$1-\beta_j := \Pr(\text{detect } H_{j1} \mid H_{j0} \text{ is true}), \tag{2.1b}$$

and β_j is defined as the probability of (spectrum) *opportunity-detection* in channel j.

Given group G_i is chosen for spectrum sensing, in order to control the intra- and inter-network interferences, the secondary user initiates transmissions according to the ALOHA protocol with probability $0 \leq q_{j0} \leq 1$ or $0 \leq q_{j1} \leq 1$ in channel $j \in G_i$, depending on whether channel j is detected idle or busy, respectively. We consider the transmission with probability q_{j1} for secondary users in channel j to compensate for the false alarms of the spectrum sensors, which may conceivably improve the secondary network throughput. Setting $q_{j0} = 0$ or $q_{j1} = 0$ means that the packet transmission should be postponed to the next time slot when channel is detected idle or busy respectively.

In the following sections, we will determine p_j, q_{j0}, and q_{j1} such that the secondary network expected sum throughput is maximized, while the probability of interference to the primary users is limited by ϵ_j in channel j, $j = 1, \ldots, N$. We will first assume that the secondary users are equipped with perfect spectrum sensors and we will later consider erroneous spectrum sensors for secondary users and study how the spectrum detection errors affect the optimal sensing and access scheme.

2.3 Perfect Spectrum Sensors

In this section we consider the scenario where the secondary users are equipped with error-free spectrum sensors, i.e., $\alpha_j = 0$ and $\beta_j = 1$, $j = 0, \ldots, N$, and focus on the question of how the channel bandwidths, their usage statistics, the secondary network population, and their ability to sense and access multiple channels, affect the optimal sensing and access scheme. In this case, without loss of generality, we set $q_{j1} = 0$ for $j = 1, \ldots, N$.

Let us first consider the single-channel sensing and access case as the starting point, i.e., $S = 1$. The perfect detection capability of secondary users and the setup of $q_{j1} = 0$, $j = 1, \ldots, N$, together guarantee collision-free communications for the primary network. Each secondary user initiates a transmission in channel j with probability $q_{j0}p_j$ independent of other secondary users if channel j is idle. Hence, the expected throughput that the secondary network can achieve in channel j equals $C_j\overline{\theta}_j M f_M(q_{j0}p_j)$, where $f_M(t) := t(1-t)^{M-1}$. As such, the problem of deriving the optimal random sensing and access scheme can be formulated as the following optimization problem $(P1)$:

$$\text{maximize} \sum_{j=1}^{N} MC_j\overline{\theta}_j f_M(q_{j0}p_j)\,, \tag{2.2a}$$

$$\text{such that} \sum_{j=1}^{N} p_j = 1\,, \tag{2.2b}$$

$$p_j \geq 0\,, \quad j = 1, \ldots, N\,, \tag{2.2c}$$

$$0 \leq q_{j0} \leq 1\,, \quad j = 1, \ldots, N\,. \tag{2.2d}$$

Note that $P1$ is not a convex problem and cannot be optimized using conventional convex optimization methods. In the following theorem we present the random

sensing and access scheme that optimizes $P1$.

Theorem 2.3.1. *Assume secondary users can sense and access a single channel, and are equipped with perfect spectrum sensors. The optimal random sensing and access scheme that maximizes the secondary network expected sum throughput is*

$$(q_{j0}^*, q_{j1}^*, p_j^*) = \begin{cases} (\frac{N}{M}, 0, \frac{1}{N}) & \text{if } N \leq M \\ (1, 0, g^{-1}(\frac{\nu}{MC_j\overline{\theta}_j})^+)\,, & \text{otherwise} \end{cases} \tag{2.3}$$

for $j = 1, \ldots, N$, where $t^+ := \max\{0, t\}$, $g(t) := \partial f_M(t)/\partial t = (1 - Mt)(1 - t)^{M-2}$, and $\nu > 0$ is chosen such that $\sum_{j=1}^N p_j^* = 1$.

Proof. Define $x_j := q_{j0}p_j$, $j = 1, \ldots, N$, and consider the following optimization problem $\widetilde{P1}$ that has the same objective function as $P1$ but with possibly a larger feasible set.

$$\text{maximize} \sum_{j=1}^{N} MC_j\overline{\theta}_j f_M(x_j)\,, \tag{2.4a}$$

$$\text{such that} \sum_{j=1}^{N} x_j \leq 1\,, \tag{2.4b}$$

$$x_j \geq 0\,, \quad j = 1, \ldots, N\,. \tag{2.4c}$$

Observe that the optimal value of $\widetilde{P1}$ is no less than optimal value of $P1$ and if we can find p_j^*'s and q_{j0}^*'s such that $q_{j0}^* p_j^* = x_j^*$ satisfying constraints (2.2b)–(2.2d) then p_j^* and q_{j0}^* are the optimal solution of $P1$.

Moreover, note that for any $\frac{1}{M} < t \leq 1$ with $f_M(t) = c$, there exists a $0 \leq t' < \frac{1}{M}$ such that $f_M(t') = c$ (using intermediate value theorem). Hence, given $(x_1^*, \ldots, x_N^*)$ as the global maximizer for $\widetilde{P1}$, we can, without loss of generality, assume that $x_j^* \leq \frac{1}{M}$ for $j = 1, \ldots, N$ (by replacing any $x_i^* > \frac{1}{M}$ with $x_i'^* < \frac{1}{M}$, which also satisfies

the conditions (2.4b) and (2.4c)). In other words, $\widetilde{P1}$ should have an optimal solution lying in $0 \leq x_j \leq \frac{1}{M}$, $j = 1, \ldots, N$. In this region, the objective function in (2.4a) is concave; applying KKT conditions [37] (which are necessary and sufficient conditions for optimality), we can find the optimal x_j^*'s. After some algebraic manipulations, we obtain the following KKT conditions

$$\begin{aligned} g(x_j^*) &\leq \frac{\nu^*}{MC_j\overline{\theta}_j}\,, \\ x_j^*(g(x_j^*) - \frac{\nu^*}{MC_j\overline{\theta}_j}) &= 0\,, \\ x_j^* &\geq 0\,, \end{aligned}$$

for $j = 1, \ldots, N$, and

$$\begin{aligned} \nu^*(\sum_{j=1}^{N} x_j^* - 1) &= 0\,, \\ \sum_{j=1}^{N} x_j^* &\leq 1\,, \\ \nu^* &\geq 0\,, \end{aligned}$$

where ν is the Lagrangian multiplier associated with (2.4b) and $g(t) := \partial f_M(t)/\partial t = (1 - Mt)(1 - t)^{M-2}$. Hence, given $N \leq M$, the optimal solution is achieved when $\nu^* = 0$ as

$$x_j^* = g^{-1}(0) = \frac{1}{M}\,, \tag{2.5}$$

with $\sum_{j=1}^{N} x_j^* = \frac{N}{M} \leq 1$. However, when $N > M$, the optimal solution is obtained by

$$x_j^* = g^{-1}(\frac{\nu}{MC_j\overline{\theta}_j})^+\,, \tag{2.6}$$

with $\nu^* > 0$ chosen such that $\sum_{j=1}^{N} x_j^* = 1$. Furthermore, note that in both these case $x_j^* = g^{-1}(\frac{\nu}{MC_j\overline{\theta}_j})^+ \leq \frac{1}{M}$ when $\nu \geq 0$ for all j. Now it is straightforward to verify that by setting $(q_{j0}^*, p_j^*) = (\frac{N}{M}, \frac{1}{N})$ when $N \leq M$ and setting $(q_{j0}^*, p_j^*) = (1, g^{-1}(\frac{\nu}{MC_j\overline{\theta}_j})^+)$ when $N > M$, we satisfy $q_{j0}^* p_j^* = x_j^*$ and (2.2b)–(2.2d) for $j = 1, \ldots, N$. □

Remark 2.3.2. *Observe that the function $f_M(t)$ is quasi-concave over $0 \leq t \leq 1$ and $t = \frac{1}{M}$ is its maximizer. Hence, intuitively, to maximize the individual summands in* (2.4a)*, we need to assign the sensing and access probabilities at each channel in such a way that their product is as close as possible to $\frac{1}{M}$ while satisfying conditions* (2.2b)–(2.2d)*. When the number of secondary users is larger than the number of primary frequency bands, this assignment is possible in a manner that is independent of the primary channel bandwidths and usage statistics, depending only on N and M. However, when there are fewer secondary users than primary channels, the probability of sensing channel j should be inversely proportional (via the function g^{-1}) to the expected secondary achievable-throughput in channel j, i.e., $C_j\overline{\theta}_j$. Furthermore, due to proper spreading of secondary users in N channels, secondary users should access the channels with probability one when detected idle.*

Next, we assume that secondary users can sense and access up to $0 < S \leq N$ channels simultaneously. Again, perfect detection capability of secondary users guarantees zero collisions to the primary network. Each secondary user initiates a transmission in channel j with probability $q_{j0} \sum_{i:j \in G_i} p_i$ independent of the other secondary users if channel j is idle. Hence, the expected throughput that secondary network can achieve in channel j equals $C_j\overline{\theta}_j M f_M(q_{j0} \sum_{i:j \in G_i} p_i)$. Recall that here p_i is the probability of sensing channel group G_i, $i = 1, \ldots, U$, and q_{j0} is the probability of accessing channel j, $j = 1, \ldots, N$, when detected idle. As such, the problem of deriving the optimal random sensing and access scheme can be formulated as the

following optimization problem ($P2$):

$$\text{maximize } \sum_{j=1}^{N} MC_j\overline{\theta}_j f_M(q_{j0}\sum_{i:j\in G_i} p_i)\,, \tag{2.7a}$$

$$\text{such that } \sum_{i=1}^{u} p_i = 1\,, \tag{2.7b}$$

$$p_i \geq 0\,, \quad i = 1,\ldots,U\,, \tag{2.7c}$$

$$0 \leq q_{j0} \leq 1\,, \quad j = 1,\ldots,N\,. \tag{2.7d}$$

$P2$ is not a convex problem either; however, we can find its optimal solution in a manner similar to $P1$.

Theorem 2.3.3. *Assume secondary users can sense and access up to $0 < S \leq N$ channels at the same time and they are equipped with perfect spectrum sensors. The optimal random sensing and access scheme that maximizes the expected secondary network sum throughput is*

$$\begin{aligned}(q_{j0}^*, q_{j1}^*) &= (\frac{N}{MS}, 0)\,,\\ p_i^* &= \frac{1}{U}\,,\end{aligned} \tag{2.8}$$

if $N \leq MS$, and is

$$\begin{aligned}(q_{j0}^*, q_{j1}^*) &= (\frac{1}{S}, 0)\,,\\ (p_1^*,\ldots,p_U^*)^T &= S(\mathcal{G}^T\mathcal{G})^{-1}\mathcal{G}^T\,(x_1^*,\ldots,x_N^*)^T\,,\end{aligned} \tag{2.9}$$

otherwise, for $j = 1,\ldots,N$ and $i = 1,\ldots,U$, where $x_j^* = g^{-1}\left(\frac{\nu}{MC_j\overline{\theta}_j}\right)^+$, $\mathcal{G}_{N\times U}$ is the sensing matrix, i.e., $\mathcal{G}_{ji} = 1$ if channel j is in group G_i and zero otherwise, A^T is the transpose of matrix A, $g(t) := (1-Mt)(1-t)^{M-2}$, and ν is chosen such that

$\sum_{j=1}^{N} x_j^* = 1$.

Proof. Defining $x_j := q_{j0} \sum_{i:j\in G_i} p_i$, $j = 1, \ldots, N$, and reformulating $P2$ with respect to x_j, we again obtain the optimization problem $\widetilde{P1}$ in the proof of Theorem 2.3.1. Hence, the optimal value of problem $\widetilde{P1}$ is an upper bound for $P2$ as well. So, if we can find p_i^*'s and q_{j0}^*'s such that $q_{j0}^* \sum_{i:j\in G_i} p_i^* = x_j^*$ satisfying constraints (2.7b)–(2.7d), p_i^* and q_{j0}^* are then the optimal solution of $P1$, where x_j^*, $j = 1, \ldots, N$, is the optimal solution for $\widetilde{P1}$.

Assume $(x_1^*, \ldots, x_N^*)$ is the maximizer of $\widetilde{P1}$ obtained in (2.5) and (2.6). Now we need to find appropriate p_i^* and q_{j0}^* such that

$$\Lambda(q_{10}^*, \ldots, q_{N0}^*)\, \mathcal{G}\, (p_1^*, \ldots, p_U^*)^T = (x_1^*, \ldots, x_N^*)^T\,, \tag{2.10}$$

and satisfy conditions (2.7b)–(2.7d), where $\Lambda(t_1, \ldots, t_N)$ is the matrix with diagonal elements equal q_{j0}, $j = 1, \ldots, N$, and all elements outside the main diagonal equal zero. From (2.10) and (2.5), we have that if $N \leq MS$,

$$\begin{aligned} S &= S \sum_{i=1}^{U} p_i^* \\ &= \mathrm{tr}(\mathcal{G}(p_1^*, \ldots, p_U^*)^T) \\ &= \sum_{j=1}^{N} \frac{x_j^*}{q_{j0}} \\ &= \frac{1}{M} \sum_{j=1}^{N} \frac{1}{q_{j0}}\,, \end{aligned}$$

where $\mathrm{tr}(\cdot)$ is the trace operator, and the second equality is due to the fact that each column of $\mathcal{G}$ consists of S elements equal to one and the rest equal to zero. Hence, setting $q_{j0}^* = \frac{N}{MS} \leq 1$ and $p_i^* = \frac{1}{U}$ satisfies (2.10) and (2.7b)–(2.7d). Now, when

$N > MS$, if we set $q_i^* = \frac{1}{S}$, from (2.10) and (2.6), we must have

$$\begin{aligned} 1 &= \sum_{j=1}^{N} x_j^* \\ &= \frac{1}{S} \operatorname{tr}\left(\mathcal{G}(p_1^*, \ldots, p_U^*)^T\right) \\ &= \sum_{i=1}^{U} p_i^* \,. \end{aligned}$$

Consequently, setting $q_i^* = \frac{1}{S}$ and $\mathcal{G}(p_1^*, \ldots, p_U^*)^T = S(x_1^*, \ldots, x_N^*)^T$ satisfies (2.10) and (2.7b)–(2.7d); we obtain (2.9). □

Remark 2.3.4. *Based on Theorems 2.3.1 and 2.3.3, it is easy to show that the secondary network expected throughput is an increasing function over $M \leq N/S$, achieves its supremum at $M = N/S$, and is slowly decreasing over $M > N/S$ with value $\sum_{j=1}^{N} C_j \overline{\theta}_j (1 - \frac{1}{M})^{M-1} \to e^{-1} \sum_{j=1}^{N} C_j \overline{\theta}_j$ as $M \to \infty$. Consequently, the optimal number of secondary users that can coexist in the network equals $M^* = N/S$ with the optimal expected sum throughput of $\sum_{j=1}^{N} MC_j \overline{\theta}_j f_M(\frac{1}{M}) \approx e^{-1} \sum_{j=1}^{N} C_j \overline{\theta}_j$.*

2.4 Erroneous Spectrum Sensors

In this section we consider the scenario where the secondary users are equipped with erroneous spectrum sensors with mis-detection and false-alarm probabilities α_j and $1 - \beta_j$, respectively, for $j = 1, \ldots, N$, and investigate the effect of spectrum detection errors on the optimal sensing and access scheme.

Each secondary user initiates a successful transmission in channel j with probability $p_j(\beta_j q_{j0} + (1 - \beta_j) q_{j1})$ independent of other secondary users if channel j is idle. Hence, the expected throughput that secondary network can achieve in channel j equals $C_j \overline{\theta}_j M f_M(p_j(\beta_j q_{j0} + (1 - \beta_j) q_{j1}))$. On the other hand, secondary users interfere with primary network in channel j if channel j is already occupied by primary

users and at least one secondary user initiates a transmission in that channel, which happens with probability $\theta_j[1-(1-p_j(\alpha_j q_{j0}+(1-\alpha_j)q_{j1}))^M]$. As such, the problem of deriving the optimal random sensing and access scheme can be formulated as the following optimization problem $(P3)$:

$$\text{maximize} \qquad \sum_{j=1}^{N} MC_j\overline{\theta}_j f_M\left(p_j(\beta_j q_{j0}+(1-\beta_j)q_{j1})\right)\,, \tag{2.11a}$$

$$\text{such that} \qquad \sum_{j=1}^{N} p_j = 1\,, \tag{2.11b}$$

$$p_j \geq 0\,, \quad j=1,\ldots,N\,, \tag{2.11c}$$

$$0 \leq q_{j0} \leq 1\,, \quad j=1,\ldots,N\,, \tag{2.11d}$$

$$0 \leq q_{j1} \leq 1\,, \quad j=1,\ldots,N\,, \tag{2.11e}$$

$$p_j(\alpha_j q_{j0}+(1-\alpha_j)q_{j1}) \leq Z_j\,,\ j=1,\ldots,N\,, \tag{2.11f}$$

where

$$Z_j := \begin{cases} 1\,, & \text{if } \epsilon_j \geq \theta_j\,, \\ 1-\sqrt[M]{1-\frac{\epsilon_j}{\theta_j}}\,, & \text{if } \epsilon_j < \theta_j\,. \end{cases} \tag{2.12}$$

We obtain the optimal solution of $P3$ specified by the following theorem in a

similar fashion to the proof of Theorem 2.3.1. First, let us define

$$\beta_{j+} := \beta_j \mathbf{1}_{\beta_j \geq \alpha_j} + (1-\beta_j)\mathbf{1}_{\beta_j < \alpha_j}\,, \tag{2.13}$$

$$\beta_{j-} := \beta_j \mathbf{1}_{\beta_j < \alpha_j} + (1-\beta_j)\mathbf{1}_{\beta_j \geq \alpha_j}\,, \tag{2.14}$$

$$\alpha_{j+} := \alpha_j \mathbf{1}_{\beta_j \geq \alpha_j} + (1-\alpha_j)\mathbf{1}_{\beta_j < \alpha_j}\,, \tag{2.15}$$

$$\alpha_{j-} := \alpha_j \mathbf{1}_{\beta_j < \alpha_j} + (1-\alpha_j)\mathbf{1}_{\beta_j \geq \alpha_j}\,, \tag{2.16}$$

$$q_{j+} := q_{j0} \mathbf{1}_{\beta_j \geq \alpha_j} + q_{j1}\mathbf{1}_{\beta_j < \alpha_j}\,, \tag{2.17}$$

$$q_{j-} := q_{j0} \mathbf{1}_{\beta_j < \alpha_j} + q_{j1}\mathbf{1}_{\beta_j \geq \alpha_j}\,, \tag{2.18}$$

$$x_{j+} := p_j q_{j+}\,, \tag{2.19}$$

$$x_{j-} := p_j q_{j-}\,, \tag{2.20}$$

$$t_j := \beta_{j+} x_{j+} + \beta_{j-} x_{j-}\,, \tag{2.21}$$

where $\mathbf{1}$ is the indicator function.

Theorem 2.4.1. *Assume secondary users can sense and access a single channel, and are equipped with erroneous spectrum sensors with mis-detection and false-alarm probabilities α_j and $1-\beta_j$, receptively, for $j = 1, \ldots, N$. The optimal random sensing and access scheme that maximizes the expected total secondary network throughput is*

$$(q^*_{j+}, q^*_{j-}, p^*_j) = \begin{cases} (N \min\{\frac{\beta_{j+}}{\alpha_{j+}} Z_j, \frac{1}{M}\}^+, 0, \frac{1}{N}) & \text{if } \sum_{j=1}^N \min\{\frac{\beta_{j+}}{\alpha_{j+}} Z_j, \frac{1}{M}\} \leq 1 \\ (1, 0, \min\{\frac{\beta_{j+}}{\alpha_{j+}} Z_j, g^{-1}(\frac{\nu^*}{MC_j\bar{\theta}_j})^+\}^+)\,, & \text{otherwise} \end{cases} \tag{2.22}$$

for $j = 1, \ldots, N$, where $g(t) := (1-Mt)(1-t)^{M-2}$ and $\nu > 0$ is chosen such that $\sum_{j=1}^N p^*_j = 1$.

Proof. Using (2.13)–(2.21), we can rewrite

$$\begin{aligned}
p_j(\beta_j q_{j0} + (1-\beta_j)q_{j1}) &= p_j[\beta_j(q_{j+}\mathbf{1}_{\beta_j \geq \alpha_j} + q_{j-}\mathbf{1}_{\beta_j < \alpha_j}) + (1-\beta_j)(q_{j+}\mathbf{1}_{\beta_j < \alpha_j} + q_{j-}\mathbf{1}_{\beta_j \geq \alpha_j})] \\
&= p_j[q_{j+}(\beta_j \mathbf{1}_{\beta_j \geq \alpha_j} + (1-\beta_j)\mathbf{1}_{\beta_j < \alpha_j}) + q_{j-}(\beta_j \mathbf{1}_{\beta_j < \alpha_j} + (1-\beta_j)\mathbf{1}_{\beta_j \geq \alpha_j})] \\
&= p_j\left[q_{j+}\beta_{j+} + q_{j-}\beta_{j-}\right] \\
&= \beta_{j+}x_{j+} + \beta_{j-}x_{j-} \\
&=: t_j\,,
\end{aligned}$$

and since we assume $\Pr(H_{j0}) > 0$, α_j and β_j cannot be both zero (please refer to the definitions of α_j and β_j). As such, we have $\beta_{j+} > 0$ for all j and similarly as before, we can rewrite

$$\begin{aligned}
p_j(\alpha_j q_{j0} + (1-\alpha_j)q_{j1}) &= p_j[\alpha_j(q_{j+}\mathbf{1}_{\beta_j \geq \alpha_j} + q_{j-}\mathbf{1}_{\beta_j < \alpha_j}) \\
&\quad + (1-\alpha_j)(q_{j+}\mathbf{1}_{\beta_j < \alpha_j} + q_{j-}\mathbf{1}_{\beta_j \geq \alpha_j})] \\
&= p_j[q_{j+}(\alpha_j \mathbf{1}_{\beta_j \geq \alpha_j} + (1-\alpha_j)\mathbf{1}_{\beta_j < \alpha_j}) \\
&\quad + q_{j-}(\alpha_j \mathbf{1}_{\beta_j < \alpha_j} + (1-\alpha_j)\mathbf{1}_{\beta_j \geq \alpha_j})] \\
&= p_j\left[q_{j+}\beta_{j+} + q_{j-}\beta_{j-}\right] \\
&= \alpha_{j+}x_{j+} + \alpha_{j-}x_{j-} \\
&= \frac{\alpha_{j+}}{\beta_{j+}}\left(t_j - \beta_{j-}x_{j-}\right) + \alpha_{j-}x_{j-} \\
&= \frac{\alpha_{j+}t_j + [\beta_{j+}\alpha_{j-} - \beta_{j-}\alpha_{j+}]x_{j-}}{\beta_{j+}}\,.
\end{aligned}$$

Now, we can reformulate the optimization problem $P3$ as $\widetilde{P3}$ with a (possibly)

larger feasible set:

$$\text{maximize} \qquad \sum_{j=1}^{N} MC_j\overline{\theta}_j t_j(1-t_j)^{M-1}\,, \tag{2.23a}$$

$$\text{such that} \qquad \sum_{j=1}^{N} t_j \leq 1\,, \tag{2.23b}$$

$$\sum_{j=1}^{N} x_{j-} \leq 1\,, \tag{2.23c}$$

$$t_j \geq 0\,, \qquad j=1,\ldots,N\,, \tag{2.23d}$$

$$x_{j-} \geq 0\,, \qquad j=1,\ldots,N\,, \tag{2.23e}$$

$$\alpha_{j+}t_j + (\beta_{j+}\alpha_{j-} - \beta_{j-}\alpha_{j+})x_{j-} \leq \beta_{j+}Z_j\,,\ j=1,\ldots,N\,. \tag{2.23f}$$

It is easy to verify that $\beta_{j+} \geq \alpha_{j+}$ and $\beta_{j-} \leq \alpha_{j-}$ for all j. Therefore, we have $(\beta_{j+}\alpha_{j-} - \beta_{j-}\alpha_{j+})x_{j-} \geq 0$ for all j, and the objective function in (2.23a) is independent of x_{j-}'s. Therefore, we can simply put $x_{j-} = 0$ for $j = 1,\ldots,N$, while satisfying the feasibility conditions. As such we can omit conditions (2.23c) and (2.23e), and simplify (2.23f) to $\alpha_{j+}t_j \leq \beta_{j+}Z_j$ for $j = 1,\ldots,N$. Now, similar to the proof of Theorem 2.3.1, we can prove that if $P3$ has an optimal solution, it must lie in $t_j \leq \frac{1}{M}$, $j = 1,\ldots,N$, where in this region, (2.23a) and consequently $P3$ are convex. Hence, we can obtain the optimal solution using the following KKT conditions:

$$g(t_j^*) \leq \frac{\nu^*}{MC_j\overline{\theta}_j}\,,$$

$$(g(t_j^*) - \frac{\nu^*}{MC_j\overline{\theta}_j})\left(\alpha_{j+}t_j^* - \beta_{j+}Z_j\right) = 0\,,$$

$t_j^* \geq 0$, for $j = 1, \ldots, N$, and

$$\nu^*(\sum_{j=1}^{N} t_j^* - 1) = 0\,,$$
$$\sum_{j=1}^{N} t_j^* \leq 1\,,$$
$$\nu^* \geq 0\,,$$

where ν is the Lagrangian multiplier associated with (2.23b). After some algebraic calculation we obtain that

$$t_j^* = \min\left\{\frac{\beta_{j+}}{\alpha_{j+}} Z_j, \frac{1}{M}\right\}^+ ,$$

if $\sum_{j=1}^{N} \min\{\frac{\beta_{j+}}{\alpha_{j+}} Z_j, \frac{1}{M}\} \leq 1$, and

$$t_j^* = \min\left\{\frac{\beta_{j+}}{\alpha_{j+}} Z_j, g^{-1}\left(\frac{\nu^*}{MC_j\overline{\theta}_j}\right)^+\right\}^+ ,$$

otherwise, with ν^* is chosen such that $\sum_{j=1}^{N} t_j^* = 1$. Together with (2.19)–(2.21), we can obtain (2.22). □

Remark 2.4.2. *Note the similarity between* (2.3) *and* (2.22)*:* 1) *If the inter-network interference constraint and the secondary spectrum detector ROC operate in a way such that* $\frac{\beta_{j+}}{\alpha_{j+}} Z_j \geq \frac{1}{M}$ *in all channels, the optimal sensing and access scheme and the secondary network expected throughput for error-free and erroneous scenarios will be equal.* 2) *Similar to the error-free scenario, if the inter-network interference constraint and the secondary spectrum detector ROC operate in a way such that* $\sum_{j=1}^{N} \min\{\frac{\beta_{j+}}{\alpha_{j+}} Z_j, \frac{1}{M}\} \leq 1$*, the secondary optimal sensing and access scheme is independent of the channel bandwidths and usage statistics.* 3) *Note the binary behavior*

of the optimal access scheme with respect to the primary signal mis-detection probability α_j and spectrum opportunity-detection probability β_j: On average, we gain no throughput enhancement by transmitting in a channel detected as busy when the probability of opportunity-detection is larger than the probability of mis-detection in that channel, or by transmitting in a channel detected as idle when the probability of opportunity-detection is smaller than the probability of mis-detection in that channel.

2.5 Summary

In this section we considered an overlaid network scenario, where N licensed frequency bands are made available to a secondary network, contingent upon adherence to certain inter-network interference constraints. To limit the interference to the primary network, secondary nodes are equipped with spectrum sensors and are capable of sensing and accessing a limited number of channels simultaneously. We considered both the error-free and the erroneous spectrum detection scenarios and established the jointly optimal random sensing and access scheme, which maximizes the secondary network expected sum throughput while abiding by the primary interference constraint. We have shown that in the case of error-free spectrum detection, when the number of secondary users times the number of channels that they can access is larger than the number of primary frequency bands, the optimal sensing and access scheme is independent of the channel bandwidths and usage statistics; otherwise they follow water-filling-like strategies. In the case of erroneous spectrum detection, we have shown similar characteristics for the optimal sensing and access scheme under slightly different conditions. Moreover, we derived the optimal number of secondary users that can co-exist with the primary network, and demonstrated a binary behavior for the optimal access scheme at each channel depending on whether the opportunity-detection probability or the mis-detection probability is larger in that

channel.

3. LARGE OVERLAID COGNITIVE RADIO NETWORKS: FROM THROUGHPUT SCALING TO ASYMPTOTIC MULTIPLEXING GAIN

3.1 Introduction

In this section we study the asymptotic performance of multi-hop overlaid networks in which a primary ad-hoc network and a cognitive secondary ad-hoc network coexist over the same spatial, temporal, and spectral dimensions. In order to limit the secondary interference to the primary network, we adopt the *dynamic spectrum access* [38] approach, where secondary users opportunistically explore the white spaces detected using spectrum sensors. In [39], Vu *et al.* considered the throughput scaling law for single-hop overlaid cognitive radio networks, where a linear scaling law is obtained for the secondary network with an outage constraint considered for the primary network. In [40], Jeon *et al.* considered a multi-hop cognitive network coexisting with a primary network and assumed that the secondary nodes know the locations of all primary nodes (both primary transmitters and receivers). They showed that by defining a preservation region around each primary node and following time-slotted deterministic transmission protocols, both networks can achieve the same throughput scaling law as a stand-alone wireless network, while a vanishing fraction of the secondary nodes may suffer from a finite outage probability (as the number of the nodes tends to infinity). In [41], the authors studied the throughput scaling and throughput-delay trade-off with the same system model as in [40], except that the secondary users only know the locations of the primary transmitters. By establishing preservation regions around primary transmitters, they showed that both networks could achieve the throughput scaling derived by Gupta and Kumar in [42] without outage.

In all the previously mentioned papers, centralized deterministic schemes are used to achieve the feasible rates for both primary and secondary networks. Moreover, results are provided only when the secondary nodes are more densely distributed than the primary nodes. On the other hand, the desired autonomous feature of large wireless systems makes the use of a central authority to coordinate the primary/secondary users less appealing. In addition, in many practical situations, as the secondary users are opportunistic (or sporadic) spectrum utilizers, it is more likely that the secondary nodes are less densely distributed.

In the literature, the asymptotic performance of traditional single-tier networks with distributed random access schemes has been studied, e.g., [43]–[46]. In [43], the performance of the slotted ALOHA protocol in a multi-hop environment was studied and the optimum transmission radius is derived to maximize the throughput for a random planar network. The spatial capacity of a slotted multi-hop network with capture was studied in [44]. In [45], Weber *et al.* derived the transmission capacity of wireless ad-hoc networks, where the transmission capacity is defined as the product between the maximum density of successful transmissions and their data rate, given an outage constraint. Baccelli *et al.* [46] proposed an ALOHA-based protocol for multi-hop wireless networks in which nodes are randomly located in an infinite plane according to a Poisson point process and are mobile according to a waypoint mobility model. They derived the optimum multiple access probability that achieves the maximum *mean density of progress*.

In [47], the achievable spatial throughput of a multi-antenna underlay cognitive radio network is considered, where the primary network model follows the bipolar network model introduced in [46]. Secondary users concurrently access the channel along the primary users according to a Slotted-ALOHA protocol, while satisfying the primary minimum success probability constraint. Authors derived the maximum

permissible secondary density together with the optimal secondary medium access probability that maximizes the secondary spatial throughput. They showed that this is possible due to employing multiple antennas at the primary user. In [48], authors considered an overlay cognitive radio network where both primary and secondary networks follow the bipolar network model introduced in [46]. The cognitive users follow the policy that a cognitive transmitter is active only when it is outside the primary user exclusion regions. Authors derived bounds for the inter- and intra-network interferences and show that the spatial distribution of the secondary users can be approximated by the Poisson hole process.

In this section we consider decentralized ALOHA-based scheduling schemes for both primary and secondary networks in an overlaid scenario, where secondary users can only make use of localized information obtained via spectrum sensing to control their actions and limit their interferences to primary users. The distributed nature of ad-hoc networks and the passive property of primary receivers lead to uncertainties about the primary system state even with perfect spectrum sensing. As such, we focus on the case where the secondary users are able to *perfectly detect* the primary user signals when the primary transmitters are within a certain range. In particular, we study the asymptotic performance of the two overlaid networks, where we start with the throughput scaling laws, and then introduce a new metric called *asymptotic multiplexing gain* that further quantifies the performance trade-off between the two networks. We do so under two scenarios, i.e., the secondary network is denser vs. sparser than the primary network, and identify their key differences.

The rest of this section is organized as follows. Section 3.2 introduces the mathematical model, notations, and definitions. In Section 3.3 we consider the *spatial throughput* of the single-tier network. Section 3.4 studies the cognitive overlaid scenario and addresses the trade-off between the primary and secondary networks by

introducing the notion of asymptotic multiplexing gain (AMG). In particular, we show that both networks can achieve their corresponding single-tier throughput scaling regardless of the setting for the spectrum sensing range. However, for the case with a denser secondary network, spectrum sensing can improve the overlaid networks performances; whereas, for the case with a sparser secondary network, the spectrum sensing turns out to be redundant and the primary network AMG cannot be enhanced by employing spectrum sensors. Section 3.5 concludes this study.

3.2 System Model and Definitions

Consider a circular region A in which a network of primary nodes and a network of secondary nodes share the same temporal, spectral, and spatial resources. Both primary and secondary nodes are distributed according to Poisson point processes with densities $\lambda^{(p)}$ and $\lambda^{(s)} = (\lambda^{(p)})^{\beta}$ $(\beta > 0, \beta \neq 1)$, respectively. Let $\phi^{(p)} = \{X_i^{(p)}\}$ and $\phi^{(s)} = \{X_i^{(s)}\}$ denote the (Cartesian) coordinates of a realization of the primary and secondary nodes. As mentioned earlier, the primary users are legacy users, and thus have a higher priority to access the spectrum; the secondary users can access the spectrum opportunistically (based on the spectrum sensing outcome) as long as they abide by the primary "interference constraints", i.e., maximum permissible primary throughput degradation.

Throughout this section we denote the parameters associated with the primary and the secondary users with superscripts (p) and (s), respectively. Each primary receiver tries to decode the signal from its intended transmitter located within $R_r^{(p)}$ radius and is prone to interference from other primary and secondary transmitters within $R_I^{(p)}$ and $R_I^{(sp)}$ radii, respectively. Likewise, a secondary receiver tries to decode the signal from its intended transmitter located within $R_r^{(s)}$ radius and is prone to interference from other secondary and primary transmitters within $R_I^{(s)}$ and $R_I^{(ps)}$

radii, respectively. Considering the primary and secondary users' transmission powers, it is reasonable to assume that the inter- and intra-network interference ranges are of the same order and the interference ranges are no less than the transmission ranges in both networks. In other words, $R_I^{(ps)} = O(R_I^{(p)})$, $R_I^{(sp)} = O(R_I^{(s)})$, $R_I^{(p)} = \sqrt{1+l^{(p)}}R_r^{(p)}$ and $R_I^{(s)} = \sqrt{1+l^{(s)}}R_r^{(s)}$ for some constants $l^{(p)}, l^{(s)} \geq 0$. This is similar to the protocol model introduced in [42]. Further, secondary nodes are equipped with perfect spectrum sensors that can reliably detect the primary user signals (i.e., the existence of transmitting primary users) within R_D radius. In this section we only consider perfect spectrum sensors for secondary users to focus on the effect of spectrum availability uncertainties, caused by the distributed nature of ad-hoc networks and the passive property of primary receivers, on the cognitive network performance. We leave the effect of spectrum sensing errors to a future work.

Intuitively, we expect the throughput scaling results presented in this section to still hold even when considering erroneous spectrum sensors; in the worst case scenario, the information gathered by the spectrum sensors is completely unreliable and secondary users might as well access the channel ignoring the spectrum sensors' outcome. In this case, as shown later, both networks can still achieve their stand-alone throughput scalings. A detailed analysis of overlaid networks with spectrum sensing errors is non-trivial due to the complex spatial correlation among primary and secondary users caused by non-perfect sensing.

Let $|A|$ denote the area of region A and $B_R(\cdot)$ denote a full disk with radius R centered at $(\cdot)$, which could be either the polar coordinates in the form of (r, φ) or the location of a node X in the form of (X). We interpret $B_{R_1}(r_1, \varphi_1) - B_{R_2}(r_2, \varphi_2)$ as the remaining region of a disk with radius R_1 centered at polar coordinates (r_1, φ_1) excluding the overlapping region with another disk with radius R_2 centered at (r_2, φ_2). Furthermore, given measurable sets (or events) σ_1 and σ_2 we denote by $\overline{\sigma}_1$ the com-

plement of event σ_1 and denote by $\sigma_1\sigma_2 := \sigma_1 \cap \sigma_2$ their intersection.

In addition, $f(\lambda) = o\left(g(\lambda)\right)$ means that $\lim f(\lambda)/g(\lambda) \to 0$ as $\lambda \to \infty$, $f(\lambda) = O\left(g(\lambda)\right)$ means that there exist positive constants c and M such that $f(\lambda)/g(\lambda) \leq c$ whenever $\lambda \geq M$, $f(\lambda) = \omega(g(\lambda))$ means that $\lim f(\lambda)/g(\lambda) \to \infty$ as $\lambda \to \infty$, $f(\lambda) = \Theta\left(g(\lambda)\right)$ means that both $f(\lambda) = O\left(g(\lambda)\right)$ and $g(\lambda) = O\left(f(\lambda)\right)$, $f(\lambda) \sim g(\lambda)$ means that $\lim f(\lambda)/g(\lambda) \to 1$ as $\lambda \to \infty$.

For the transmission protocols in both networks, the time axis is slotted and both networks are synchronized. The slot duration is defined as the time required to transmit a packet in the system, where all packets are assumed to be of the same size. We do not make any explicit assumptions regarding the frame structure of the networks, since we are comparing the performance of the overlaid networks against their stand-alone counterparts. The assumptions on the frame structures and their effects on the network throughput will be the same in both overlaid and stand-alone scenarios, and consequently immaterial for the comparison. In the following, we outline the primary and secondary network protocols, both based on the slotted ALOHA structure.

3.2.1 Primary Network Protocol

Each primary node picks a destination uniformly at random among all other nodes in the primary network. Communication occurs between a primary source-destination (S-D) pair through a single-hop transmission if they are close enough, or through multi-hop transmissions over intermediate relaying nodes if they are far apart. In this manner, each primary node might act as a source, destination or a relay, and always has a packet to transmit (which is either its own packet or a packet being relayed). We assume that each node has an infinite queue for packets where the first packet in the queue is transmitted with probability $q^{(p)}$ (the ALOHA parameter).

The selection of relaying nodes along the (multi-hop) routing path is governed by a variant of geometric routing schemes [43, 49, 50, 51], namely *the random* $\frac{1}{2}$*disk routing scheme*, as discussed in Section 3.2.3.

We choose the random $\frac{1}{2}$disk routing scheme mainly for tractability and simplicity in mathematical characterization as discussed in Section 4. However, the solution techniques developed in this section can be used (with some modifications) to study other variants of geographical routing schemes, such as MFR, NFP, DIR, etc.

3.2.2 Secondary Network Protocol

Similar to the primary network, each secondary node picks a destination uniformly at random among all other nodes in the secondary network. Each secondary node has an infinite queue for packets with the first one in the queue transmitted with probability $q^{(s)}$, *whenever* the channel is deemed idle: In particular, each secondary user senses the channel for primary activities prior to a transmission initiation and commences the transmission of the first packet in the queue with probability $q^{(s)}$ whenever there are no primary transmitters detected within R_D radius. Setting $R_D = 0$ implies that secondary nodes always initiate transmissions with probability $q^{(s)}$ regardless of the primary channel occupancy status. The secondary network utilizes the same routing scheme as the primary network.

3.2.3 Random $\frac{1}{2}$*Disk Routing Scheme*

Since both primary and secondary networks utilize the same routing scheme, in this section we introduce our routing scheme for a generic wireless ad-hoc network (omitting the superscripts (p) and (s)). Consider an arbitrary packet b for a source-destination pair that is h-distance apart. We set the destination node at the origin and assume that the routing path starts from the source node at $X_0 = (-h, 0)$, where X_n is the (Cartesian) coordinate of the n^{th} relay node along the routing path and

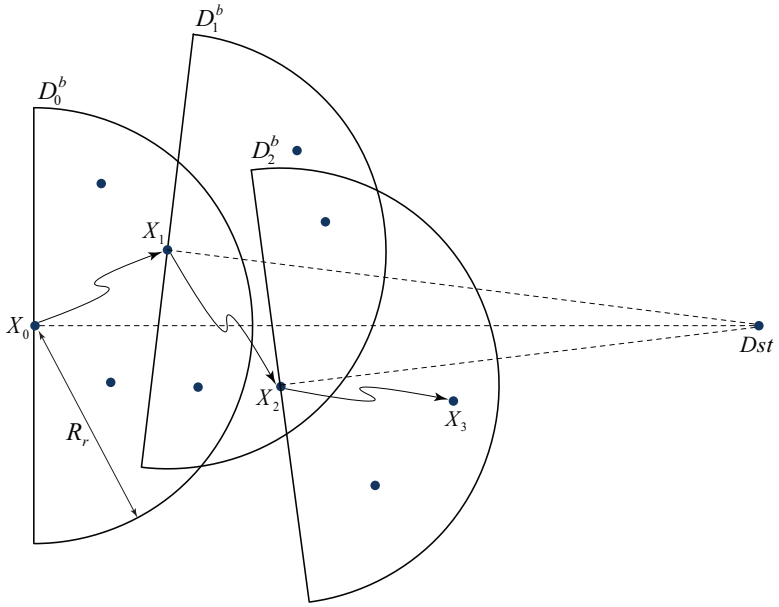

Figure 3.1: Evolution of the random $\frac{1}{2}$disk routing path.

$r_n := \|X_n\|$ is the (Euclidean) distance of the n^{th} relay node from the destination. More specifically, the routing path starts at the source node $X_0 = (-h, 0)$ with its transmission $\frac{1}{2}$disk D_0^b that is a $\frac{1}{2}$disk with radius R_r centered at X_0 and oriented towards the destination at $(0, 0)$. The next relay X_1 is selected at random from nodes contained in D_0^b. This induces a new $\frac{1}{2}$disk D_1^b, centered at X_1 and oriented towards the destination. Relay X_2 is selected randomly among the nodes in D_1^b, and the process continues in the same manner until the destination is within the transmission range.[1] Note that at any hop n if D_n^b does not contain any nodes then the route terminates and the packet is dropped. We claim that the routing path converges (or is established) in finitely many hops whenever it enters the transmission/reception

[1]For the operation of the random $\frac{1}{2}$disk routing scheme, each node needs to be aware of the location of itself and its neighbors. Due to the static network configuration, the location information can be obtained once during the network initialization phase. Furthermore, each packet should contain the location of its destination. In [52], the authors showed that the performance of the geometric routing schemes will remain order-wise the same even with imprecise location information at network nodes.

range of the final destination, i.e., $r_\nu \leq R_r$, for some $\nu < \infty$. In Fig. 3.1, we illustrate the progress of a packet towards its destination. We define the *progress* at the n^{th} hop of the routing path as $Y_n^b := \|X_n\| - \|X_{n+1}\| = r_n - r_{n+1}$ if there is at least one node in D_n^b and $Y_n^b = -\infty$ otherwise, which amounts to $\nu = \infty$.

In Theorem 4.2.1, we showed that the routing paths generated by the random $\frac{1}{2}$disk routing scheme connect any source to its destination in finitely many hops if the transmission region D of every node in the network looking in any direction contains at least one relaying node; this condition can be guaranteed asymptotically almost surely if $R_r = K\sqrt{\log \lambda/\lambda}$ for a large enough constant K. In this section we assume that K and λ are sufficiently large and $R_r = K\sqrt{\log \lambda/\lambda}$. Consequently, we can assume that the transmission region D of every node in the network looking in any direction contains at least one relaying node, $Y_n^b = r_n - r_{n+1} > -\infty$ for all n and any possible b, and $\nu < \infty$ with high probability.

3.2.4 Spatial Throughput

In this section we adopt a notion of throughput similar to *mean spatial density of progress* in [46].

Definition 3.2.1. *We define the spatial throughput of the network as the mean total progress of all successfully transmitted packets in the whole network over a single hop. More specifically, let b be the packet at the head of queue of node $X \in \phi$, Y_X^b be the progress of packet b at node X, and Λ_X^b be the event of successful transmission of packet b at node X. Then the spatial throughput of the network is defined as*

$$C(\lambda) := \lambda |A| \mathrm{E}\left(Y_X^b \mathbf{1}_{\Lambda_X^b}\right), \tag{3.1}$$

where $\mathbf{1}$ *is the indicator function and* $\mathrm{E}()$ *is the expectation operator taken over*

all realizations of the network nodes, S-D pair assignments, and the routing paths between S-D pairs.[2]

There are two key differences between our notion of throughput and the mean spatial density of progress. The first difference lies in the fact that in the mean spatial density of progress only a typical snapshot of the network is considered and the progress is computed only for the typical realization of the local neighborhood of a transmitting node. However, in our notion of throughput we consider the whole routing path of a packet and compute the mean progress of the packet over a single hop along that path. In other words, we are computing the expected progress of packets over both time and space. The second difference between our notion of throughput and the mean spatial density of progress stems from the definition of the progress, where in [46] the progress is defined to be the decrement in the distance of the packet's position projected on the line connecting the transmitting node and the destination, whereas in this dissertation we define the progress to be the decrement in the radial distance of a packet to its destination, as shown in Fig. 3.2. In order to highlight the difference between these two definitions, consider the following exaggerated example.

Assume a (very unfortunate) realization of the routing path where at each hop a node in the upper/lower corner of the transmission $\frac{1}{2}$disk is chosen as the next relay (e.g., $\tilde{X}$ in Fig. 3.2). Over this path, the packet gets farther away from the destination at each hop and should never reach the destination; this is an intuitive result that our definition of progress complies with. However, according to the projected distance progress definition in [46], at each hop, the packet has made a positive drift

[2]In this section we ignore the edge effects, i.e., we assume that the location of network nodes in $B_R(X)$ is uniformly distributed irrespective of the location of X. Essentially, we are ignoring the fact that the portion of disks around edge nodes that fall outside of the network region do not contain any other nodes.

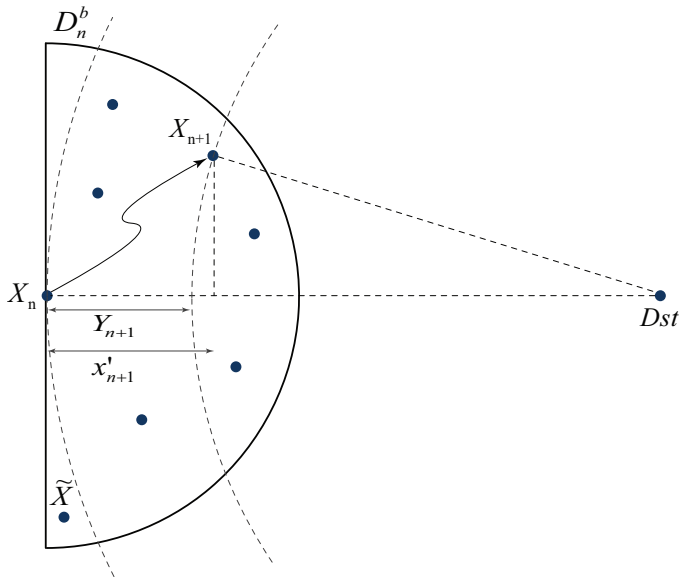

Figure 3.2: Progress of the packet at the n^{th} hop. Y_{n+1} is the decrement in the radial distance of a packet to its destination and x'_{n+1} is the decrement in the distance of the projection of the packets position on the line connecting the transmitting node and the destination.

towards the destination and should eventually reach the destination. Furthermore, based on the projected distance progress, the progress of a packet towards its destination is i.i.d. over all relay nodes. This means that the packet progress is independent of the distance from the transmitting node to the destination. However, as we show later, the packet distance from the destination decreases more (on average), when it is farther away from the destination, and decreases less as the packet gets closer to the destination (cf. Eq. (3.7)). This suggests that the packet progress is a function of its relative position to its destination and the current distance from the packet to the destination should be considered in evaluating the progress at each hop. In the next section, we determine the spatial throughput for the stand-alone primary and secondary networks and provide some interpretations for this metric.

3.3 Single Network Throughput Scalings

In this section we consider the spatial throughput of a single-tier network when no other networks are overlaid. This serves as a performance benchmark for the overlaid case discussed in the next section. The following lemma provides us with an equivalent definition and a method of computing the spatial throughput for our system.

Lemma 3.3.1 (Separation Principle)**.** *Consider the single-tier version of the wireless ad-hoc network defined in Section 3.2. The spatial throughput of such a network equals the product between the expected number of simultaneously successful transmissions in the whole network and the average progress of a typical packet over a single-hop transmission. Specifically, the spatial throughput of the network can be obtained as*

$$C(\lambda) = \lambda |A| \mathrm{E}\left(Y_X^b\right) \Pr\left(\Lambda_X^b\right) , \tag{3.2}$$

where Λ_X^b and Y_X^b are defined in Definition 3.2.1 and the expectation is taken over all realizations of the network nodes, S-D assignments, and the routing paths between S-D pairs.

Proof. Let b be the packet at the head of node X's queue at an arbitrary time slot. Note that b and Y_X^b are random variables which dependent on the specific realization of the network nodes, the S-D assignments, and the routing path establishment with the random $\frac{1}{2}$disk routing scheme. Assume that X_0 and X_{ν^b+1} are the source and destination of packet b respectively, where $\nu^b + 1$ is total number of hops that b

traverses over. Let $\{X_1, X_2, \ldots X_{\nu^b}\}$ be the nodes that b hops over. We have

$$\begin{aligned}\mathrm{E}_{\nu^b}\left(Y_X^b \mathbf{1}_{\Lambda_X^b}\right) &= \mathrm{E}\left(Y_X^b \mathbf{1}_{\Lambda_X^b} \mathbf{1}_{\{X=X_n : n=0,\ldots,\nu^b\}}\right) \\ &= \frac{1}{\nu^b+1}\sum_{n=0}^{\nu^b} \mathrm{E}\left(Y_{X_n}^b \mathbf{1}_{\Lambda_{X_n}^b}\right),\end{aligned}$$

where we define $\mathrm{E}_X(Y) := \mathrm{E}(Y \mid X)$. Therefore, we can reformulate (3.1) as

$$\begin{aligned}C &= \lambda|A|\mathrm{E}\left(\mathrm{E}_{\nu^b}\left(Y_X^b \mathbf{1}_{\Lambda_X^b}\right)\right) \\ &= \lambda|A|\mathrm{E}\left(\frac{1}{\nu^b+1}\sum_{n=0}^{\nu^b} \mathrm{E}\left(Y_{X_n}^b \mathbf{1}_{\Lambda_{X_n}^b}\right)\right). \end{aligned} \tag{3.3}$$

Now, consider the transmission of packet b from node X_n to X_{n+1}. Recall that we assume λ and R_r as large enough such that there exist at least one relay node for every transmitting node with high probability. Packet b is successfully transmitted/relayed if:

I) Node X_n initiates a transmission according to the ALOHA protocol with probability q (denoted by event Λ_{1,X_n}^b).

II) For any node X_{n+1} that is selected as the next relay for b according to the random $\frac{1}{2}$disk routing scheme, we have that neither X_{n+1} nor any other nodes contained in its interference range $B_{R_I}(X_{n+1})$, except for X_n, initiate a transmission (denoted by event $\Lambda_{2,X_{n+1}}^b$).

In other words, $\Lambda_{X_n}^b = \Lambda_{1,X_n}^b \Lambda_{2,X_{n+1}}^b$ as defined above. Note that since we assumed $R_I \geq R_r$, $\Lambda_{2,X_{n+1}}^b$ also implies that in the event of successful transmission no two nodes transmit packets to X_{n+1} at the same time. Moreover, $\Lambda_{X_n}^b$ only depends on the multiple access decisions of X_n, X_{n+1}, and the nodes that are contained in

the interference range of X_{n+1}. All these nodes initiate transmissions independent of each other and independent of all previous transmission attempts. Together with the fact that all network nodes always have a packet to transmit, we conclude that $\Pr(\Lambda^b_{X_n})$ only depends on the number of nodes contained in the interference range of the next relay node. Hence, due to the homogeneity of the underlying Poisson point process of the network nodes, $\Pr(\Lambda^b_{X_n})$ is only a function of the area of $B_{R_I}(X_{n+1})$, and is independent of the realization of X_{n+1}. In other words, $\{\Lambda^b_{X_n}\}_{b,n}$ are identically distributed (but possibly correlated) collection of random variables, and are independent of X_n, X_{n+1}, and consequently $Y^b_{X_n}$. From (3.3) we get

$$\begin{aligned} C &= \lambda|A|\mathrm{E}\left(\frac{1}{\nu^b+1}\sum_{n=0}^{\nu^b}\mathrm{E}\left(Y^b_{X_n}\right)\right)\Pr\left(\Lambda^b_{X_n}\right) \\ &= \lambda|A|\mathrm{E}\left(Y^b_X\right)\Pr\left(\Lambda^b_X\right)\ . \end{aligned}$$

□

As a consequence of Lemma 3.3.1, we can derive the spatial throughput of the network by separately determining the probability of a successful one-hop transmission and the average progress for a typical packet b at a typical node X. Based on the proof of Lemma 3.3.1 we have

$$\begin{aligned} \Pr\left(\Lambda^b_X\right) &= \mathrm{E}\left(\sum_{X_j\in D^b_X}\frac{q(1-q)^{n_{X_j}+1}}{n'_X}\right) \\ &= q(1-q)e^{-\lambda q|B_{R_I}|} \\ &= q(1-q)e^{-\lambda q\pi R_I^2}\,, \end{aligned} \tag{3.4}$$

where $n'_X \sim \mathrm{Pois}(\lambda|D^b_X|)$ is the number of nodes in D^b_X and $n_{X_j} \sim \mathrm{Pois}(\lambda|B_{R_I}|)$ is

the number of nodes in the interference range of X_j (excluding X_j and X).

In order to derive the average packet progress we need some more nomenclature and intermediate results. Consider a packet b. To simplify the notation we drop the superscripts associated with this packet. According to Theorem 4.2.1, we can (approximately) model the distance $\{r_n\}$ of packet b to its destination as a Markov process solely characterized by its progress $\{Y_n\}$. Let $\{X_n\}$ be the set of nodes that b hops over, and let (x'_{n+1}, y'_{n+1}) be the projection of $X_{n+1} - X_n$ onto the *local* Cartesian coordinates with node X_n as the origin and the x-axis pointing from X_n to the destination node as shown in Fig. 3.3. Hence, we have

$$r_{n+1} = \sqrt{(r_n - x'_{n+1})^2 + y'^2_{n+1}}\,. \tag{3.5}$$

Based on this Markov approximation model (cf. Section 4.4.1), X_{n+1} is uniformly distributed on D_n for a large enough λ; hence $\{(x'_n, y'_n)\}$ is an i.i.d. sequence of random variables with ranges $x'_n \in [0, R_r]$ and $y'_n \in [-R_r, R_r]$ for all n, whenever λ is large enough.

Define $\nu_r^{(h)} := \inf\{n : r_n \le r,\, r_0 = h\}$, $R_r \le r \le h$, to be the index of the first relay node closer than r to the destination when the source and destination nodes are h-distance apart. Hence, $\nu_{R_r}^{(h)} + 1$ represents the length (or hop-count) of the routing path. In Section 4, we prove that $\nu_{R_r}^{(h)}$ is finite asymptotically almost surely if $R_r = K\sqrt{\log\lambda/\lambda}$ for large enough K. Note that $\nu_r^{(h)}$ is a stopping time [53] and

$$r - R_r \le r_{\nu_r^{(h)}} \le r\,. \tag{3.6}$$

Furthermore, define $g(r, x', y') := \sqrt{(r - x')^2 + y'^2} - r$. Observe that g is a non-decreasing function over $r > R_r$, for fixed (x', y'), and $-x' \le g(r, x', y') \le -x' + \frac{R_r^2}{2r}$

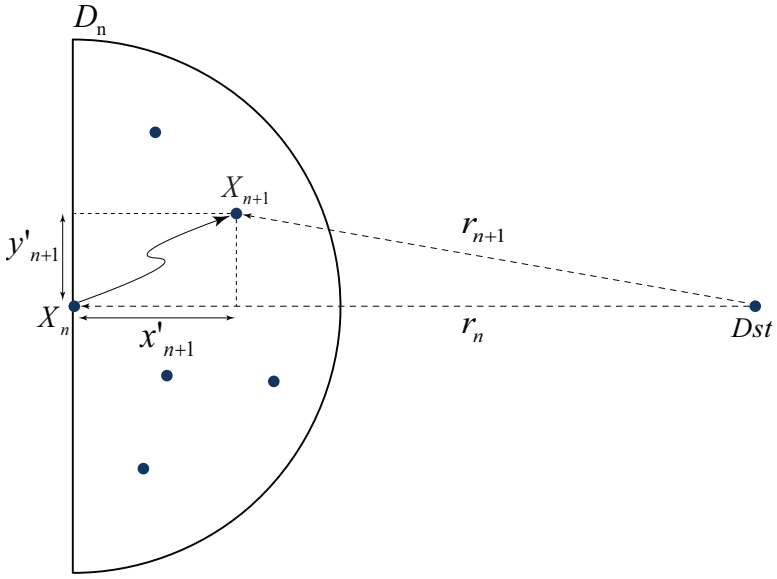

Figure 3.3: Distance between the next relay and the current node projected onto to the local coordinates at the current node.

for $r > R_r$, $|x'| \leq R_r$, and $|y'| \leq R_r$. Thus, for $n < \nu_r^{(h)}$, we have $r_n > r$ and

$$\begin{aligned} -x'_{n+1} &\leq r_{n+1} - r_n \\ &= g(r_n, x'_{n+1}, y'_{n+1}) \\ &\leq g(r, x'_{n+1}, y'_{n+1}) \\ &\leq -x'_{n+1} + \frac{R_r^2}{2r}\,. \end{aligned} \tag{3.7}$$

Applying telescopic sum to (3.7) and using (3.6) we have that for a source-destination pair that is h-distance apart ($r_0 = h$)

$$r - R_r \leq r_{\nu_r^{(h)}} \leq h + \sum_{n=0}^{\nu_r^{(h)}} g(r, x'_{n+1}, y'_{n+1})\,, \tag{3.8a}$$

$$h + \sum_{n=0}^{\nu_r^{(h)}} (-x'_{n+1}) \leq r_{\nu_r^{(h)}} \leq r\,. \tag{3.8b}$$

Together with (3.7) and the fact that $Y_n = -g(r_n, x'_{n+1}, y'_{n+1})$, we have

$$\begin{aligned}
\mathrm{E}\left(\frac{h-r}{\nu_r^{(h)}+1} - \frac{R_r^2}{2r}\right) &\le \mathrm{E}\left(Y_X^b\right) \\
&= \mathrm{E}\left(\frac{1}{\nu_r^{(h)}+1}\sum_{n=0}^{\nu_r^{(h)}} Y_n\right) \\
&= \mathrm{E}\left(\frac{1}{\nu_r^{(h)}+1}\sum_{n=0}^{\nu_r^{(h)}} -g(r_n, x'_{n+1}, y'_{n+1})\right) \le \mathrm{E}\left(\frac{h-r+R_r}{\nu_r^{(h)}+1}\right),
\end{aligned}$$

where the expectation is taken over all network, S-D assignment, and routing path realizations. Now let $S_m := \sum_{n=1}^{m} x'_n$ with $S_0 = 0$, and $\eta(z) := \mathrm{E}(e^{zx'_n})$. We know that $\exp(zS_m - m\log(\eta(z)))$ is a positive martingale, with value 1 at $m = 0$, [53, Section 10.14]. Hence, recalling (4.9b), we have

$$\mathrm{E}\left(e^{z(h-r)-(\nu_r^{(h)}+1)\log(\eta(z))}\right) \le \mathrm{E}\left(e^{zS_{\nu_r^{(h)}+1}-(\nu_r^{(h)}+1)\log(\eta(z))}\right) \le 1\,.$$

This implies

$$\mathrm{E}\left(e^{-(\nu_r^{(h)}+1)\log(\eta(z))}\right) \le e^{-z(h-r)}\,. \tag{3.9}$$

Using Jensen's inequality and the monotone convergence theorem [53], it is easy

to show that

$$\begin{aligned}\frac{1}{\mathrm{E}\left(\nu_{R_r}^{(h)}+1 \mid h\right)} \leq \mathrm{E}\left(\frac{1}{\nu_{R_r}^{(h)}+1}\middle| h\right) &= \int_0^\infty \mathrm{E}\left(e^{-t(\nu_{R_r}^{(h)}+1)}\right)\mathrm{d}t \\ &\leq \int_0^\infty e^{-z(h-r)}\mathrm{d}(\log(\eta(z))) \\ &= \int_0^\infty \frac{\eta'(u)}{\eta(u)}e^{-u(h-r)}\mathrm{d}u \\ &= \int_0^\infty \frac{\mathrm{E}\left(x_n' e^{zx_n'}\right)}{e^{zx_n'}}e^{-z(h-r)}\mathrm{d}z \\ &\leq \int_0^\infty \mathrm{E}\left(x_n'\right)e^{-z(h-r-R_r)}\mathrm{d}z \\ &= \frac{\mathrm{E}\left(x_n'\right)}{h-r-R_r}\,. \end{aligned} \tag{3.10}$$

Finally, choosing $r = R_r(1+\sqrt{\frac{h}{R_r}})$, we can determine the average progress of a typical packet at a typical node X by

$$\mathrm{E}\left(Y_X^b\right) = \frac{4R_r}{3\pi} + O\left(R_r^{3/2}\right) \sim \frac{4R_r}{3\pi}\,, \tag{3.11}$$

where we have used the facts that $\mathrm{E}(\nu_{R_r}^{(h)} \mid h) \sim \frac{h}{\mathrm{E}(x_n')}$ (cf. [54, Section IV.B]) and $\mathrm{E}\left(x_n'\right) = \frac{4R_r}{3\pi}$ (cf. [54, Appendix B]). Substituting (3.4) and (3.11) into (3.2), we obtain the spatial throughput of the single-tier network as

$$\begin{aligned} C(\lambda) &\sim \lambda|A|\mathrm{E}\left(\frac{h}{\nu_{R_r}^{(h)}+1}\right)\Pr\left(\Lambda_X^b\right) \\ &= \frac{4|A|}{3\pi}\lambda R_r q(1-q)e^{-\lambda q\pi R_I^2}\,. \end{aligned} \tag{3.12}$$

Observe that based on (3.12), one can show that $q = (\lambda\pi R_I^2)^{-1}$ maximizes the spatial throughput of the network (when λ is large) and $q = O\left(1/\log(\lambda)\right)$ is a *necessary* condition for C to be asymptotically nontrivial given that $R_r = O\left(\sqrt{\log(\lambda)/\lambda}\right)$.

Recall that R_r is chosen as such to ensure network connectivity. Consequently, for $q = O\left(1/\log(\lambda)\right)$ we we obtain that

$$C(\lambda) = \Theta\left(\sqrt{\frac{\lambda}{\log(\lambda)}}\right). \tag{3.13}$$

Remark 3.3.2. *Observe that if the network is* stable*, the spatial throughput of the network equals the expected number of packet-meters that the network delivers to the destinations at each time slot, which is equivalent to the transport capacity defined in [42]. The network is stable if the rate at which new packets are generated is equal to the rate at which packets are delivered to their respective destinations. In other words, the queue length of all network nodes is almost surely finite and packets are not being stored indefinitely in some nodes in the network. Intuitively, when the network is stable, there are* $\lambda|A|\Pr\left(\Lambda_X\right)$ *successful one-hop transmissions occurring in the whole network in each time slot; however, due to relaying, only* $\mathrm{E}(1/\nu_{R_r} + 1)$ *of these successful transmissions (on average) contribute to the throughput and the rest are only the retransmissions of relayed packets.*[3]

We denote the spatial throughput of stand-alone primary and secondary networks by $C^{(p)}(\lambda)$ and $C^{(s)}(\lambda)$ respectively; i.e., $C^{(p)}(\lambda)$ (or $C^{(s)}(\lambda)$) equals the single-tier spatial throughput expression in (3.12) with primary (or secondary) network parameters substituted. We will show in Section 3.4 that even when we have two networks sharing the same resources and the secondary network accesses the spectrum without sensing (as if the primary tier is not present), both networks can still achieve the above throughput scaling. This suggests that throughput scaling alone is not adequate to evaluate the performance of large-scale overlaid networks, as it masks

[3]The temporal analysis of the system is beyond the scope of this dissertation and is left for a future work.

the effect of mutual interference between the two networks. It turns out that the augmented interference from secondary users only causes a constant penalty to the primary throughput in the asymptotic sense such that the scaling law by itself cannot reflect this effect.

To quantify the effect of mutual interference between the two networks, we define a new measure, *asymptotic multiplexing gain (AMG)*, to characterize the protection vs. competition trade-off between the two networks. Note that AMG should be a function of spectrum sensing range and the medium access policy of the secondary users.

Definition 3.3.3. *Assume that the throughput $C(\lambda)$ of a network scales as $\Theta(f(\lambda))$; we define the Asymptotic Multiplexing Gain (AMG) of the network as the constant* $\lim_{\lambda\to\infty}\frac{C(\lambda)}{f(\lambda)}$.

Note that the exact AMG value may not be always computable, but its bounds always are. As such, we can define a *partial ordering* [55] on the set of all network throughputs. Specifically, consider two networks N_1 and N_2 with throughputs C_{N_1} and C_{N_2}, and asymptotic multiplexing gains $x_1 \leq AMG_{N_1} \leq y_1$ and $x_2 \leq AMG_{N_2} \leq y_2$. We say $C_{N_1} \preceq C_{N_2}$ if and only if $C_{N_1}/C_{N_2} = o(1)$, or $y_1 \leq x_2$ when $C_{N_1}/C_{N_2} = O(1)$. From a different perspective, if we plot $C(\lambda)$ over $f(\lambda)$ for asymptotically large λ, AMG is nothing but the slope of the throughout scaling curve, hence the connotation "multiplexing gain"; and it is intuitive to always desire a large AMG.

Accordingly, we can determine the single-tier network AMG in the absence of the other network as:

$$G = \frac{4|A|e^{-1}}{3\pi^2\sqrt{1+l}}, \tag{3.14}$$

when $q = (\lambda\pi R_I^2)^{-1}$ and $R_I/R_r = \sqrt{1+l}$.

3.4 Overlaid Cognitive Network Spatial Throughput

In this section we consider the case where both primary and secondary networks are present in the overlaid fashion under two distinct scenarios: one with the secondary network being denser than the primary network ($\beta > 1$) and the other with the primary network being denser ($\beta < 1$). As shown later, the impact of each tier on the spatial throughput of the other tier is materialized in the reduction of expected number of successful one-hop transmissions.

The distinctive feature of the overlaid cognitive network is that the secondary users are allowed to transmit only if they detect no primary transmitters within an R_D radius. The possible overlap between the detection ranges of secondary users correlates their medium access decisions, which consequently, correlates the successes of one-hop transmissions with the Euclidean hop-lengths in both primary and secondary networks. Therefore, in the overlaid scenario, the separation principle (Lemma 3.3.1) is no longer directly applicable; this makes the characterization of the primary and secondary network spatial throughputs challenging.

In the following two subsections we derive the spatial throughputs of the overlaid cognitive radio networks. The analysis closely follows that in the previous section, however, with proper modifications that take into account the opportunistic access mechanism adopted by secondary users and the extra inter-network interferences.

3.4.1 Throughput Analysis for the Primary Network

Let $\Lambda_{X_n^{(p)}}$ be the event of successful transmission for primary packet b from a primary node $X_n^{(p)}$ to the next relay $X_{n+1}^{(p)}$ in the presence of the secondary network. Henceforth, we drop the superscript b for brevity. We have that $\Lambda_{X_n^{(p)}}$ happens if events $\Lambda_{1,X_n^{(p)}}$, $\Lambda_{2,X_{n+1}^{(p)}}$, and $\Lambda_{3,X_{n+1}^{(p)}}$ all happen. As in the proof of Lemma 3.3.1, $\Lambda_{1,X_n^{(p)}}$ denotes the event that $X_n^{(p)}$ initiates a transmission, $\Lambda_{2,X_{n+1}^{(p)}}$ denotes the event

that neither $X_{n+1}^{(p)}$ nor any primary nodes contained in $B_{R_I^{(p)}}(X_{n+1}^{(p)})$, except $X_n^{(p)}$, initiate a transmission, and $\Lambda_{3,X_{n+1}^{(p)}}$ denotes the event that there are no secondary transmitters within inter-network interference range $R_I^{(sp)}$ of $X_{n+1}^{(p)}$.

Recall that we require the secondary network to be transparent to the primary network. Hence, we assume that primary users utilize the same medium access probability as if the secondary tier was not present, i.e., $q^{(p)} = (\lambda^{(p)}\pi(R_I^{(p)})^2)^{-1}$. On the other hand, each secondary transmitter initiates transmission with probability $q^{(s)}$ only if it detects the channel as *idle*, i.e., when there are no primary transmitters within R_D radius. Therefore, if $X_n^{(p)}$ initiates a transmission, all secondary users in $B_{R_D}(X_n^{(p)})$ would refrain from transmission. As such, to compute the probability of successful transmission for the primary network, we only need to consider the possible inter-network interference from the secondary nodes in $B_{R_I^{(sp)}}(X_{n+1}^{(p)}) - B_{R_D}(X_n^{(p)})$. From this we observe the following two facts:

i) The likelihood of a secondary user interfering with the transmission from $X_n^{(p)}$ to $X_{n+1}^{(p)}$ decreases as R_D increases. Thus, the probability of successful transmission for a primary user is an increasing function of R_D. Setting $R_D = R_I^{(sp)} + R_r^{(p)}$ guarantees zero interference from the secondary network to the primary network since all the secondary nodes in $B_{R_I^{(sp)}}$ of a primary receiver will detect the corresponding primary transmitter and refrain from transmission. However, as shown in Section 3.4.2, increasing R_D deteriorates the secondary network throughput and if R_D is too large, i.e., $R_D = \omega(R_r^{(p)})$, then the secondary network throughput diminishes to zero asymptotically (cf. Lemma 3.4.4). Therefore, in what follows, we assume $R_D = O(R_r^{(p)})$ and $R_D \leq R_I^{(sp)} + R_r^{(p)}$.

ii) For a given $R_D \leq R_I^{(sp)} + R_r^{(p)}$, the closer $X_n^{(p)}$ is to $X_{n+1}^{(p)}$, the lower is the

likelihood of interference from secondary nodes to $X_{n+1}^{(p)}$. Hence, in the overlaid scenario, $\Lambda_{X_n^{(p)}}$ and $Y_{X_n^{(p)}}$ are no longer independent and the separation principle does not apply.

In the following, we derive the asymptotic spatial throughput of the primary network in the presence of a secondary tier. We first consider the $\beta > 1$ scenario. In this case we have $R_r^{(p)} = \omega(R_r^{(s)})$. In Propositions 3.4.1 and 3.4.2 given below, we establish that regardless of the secondary spectrum sensing settings (i.e., $R_D = o(R_r^{(p)})$ or $R_D = O(R_r^{(p)})$), the primary network can still achieve its stand-alone sum spatial throughput scaling when $\beta > 1$. Furthermore, we derive the primary network AMG and identify its relation with secondary medium access and spectrum sensing strategies.

Proposition 3.4.1. *Assuming $\beta > 1$ and $R_D = o(R_r^{(p)})$, the primary network throughput is asymptotically independent of the secondary network spectrum sensing and can be obtained as*

$$C_{\beta>1}^{(p)}(\lambda) \sim G_{\beta>1}^{(p)} \sqrt{\frac{\lambda^{(p)}}{\log(\lambda^{(p)})}}\,, \tag{3.15}$$

where the primary network AMG in the presence of a secondary network equals

$$G_{\beta>1}^{(p)} = \gamma^{\alpha_1} G\,, \tag{3.16}$$

when the secondary medium access probability equals $q^{(s)} = \alpha_1(\lambda^{(s)}\pi(R_I^{(s)})^2)^{-1}$, with $\alpha_1 > 0$, and $\gamma := \exp(-(R_I^{(sp)}/R_I^{(s)})^2) < 1$.

Proof. Refer to Appendix A. □

From Proposition 3.4.1, we observe that spectrum sensing cannot improve the

primary network AMG if $R_D = o(R_r^{(p)})$. However, secondary users can still satisfy the primary AMG requirement by decreasing their access probability via decreasing α_1 at the cost of reducing their sum throughput significantly. Note that as shown in the next section, the secondary access probability should be chosen as $q^{(s)} = \alpha_1(\lambda^{(s)}\pi(R_I^{(s)})^2)^{-1}$ to ensure an asymptotically nontrivial throughput for the secondary network. Next, we consider the case where $R_D = O(R_r^{(p)})$, and in particular assume that $R_D = \alpha_2 R_r^{(p)}$, for $0 < \alpha_2 \leq 1$.

Proposition 3.4.2. *Assume $\beta > 1$ and $R_D = \alpha_2 R_r^{(p)}$ with $0 < \alpha_2 \leq 1$. Then, the primary network spatial throughput can be obtained as*

$$C_{\beta>1}^{(p)}(\lambda) \sim G_{\beta>1}^{(p)} \sqrt{\frac{\lambda^{(p)}}{\log(\lambda^{(p)})}}\,, \tag{3.17}$$

where the primary network AMG in the presence of a secondary network equals

$$G_{\beta>1}^{(p)} = \left(\alpha_2^3 + (1-\alpha_2^3)\gamma^{\alpha_1}\right) G\,, \tag{3.18}$$

when the secondary medium access probability equals $q^{(s)} = \alpha_1(\lambda^{(s)}\pi(R_I^{(s)})^2)^{-1}$, with $\alpha_1 > 0$, and $\gamma := \exp(-(R_I^{(sp)}/R_I^{(s)})^2) < 1$.

Proof. Refer to Appendix B. □

Observe that based on (3.18), the primary network AMG loss due to secondary activity can be recovered arbitrarily by decreasing the secondary medium access probability (through decreasing α_1) or increasing the secondary detection range (by increasing α_2). As shown in the next section, one can numerically obtain optimal α_1 and α_2 values that maximize the secondary network AMG while satisfying the primary AMG constraint.

Next, we consider primary network spatial throughput when $\beta < 1$, where we have much fewer secondary nodes with much larger interference ranges (than primary nodes) and $R_r^{(p)} = o(R_r^{(s)})$.

Proposition 3.4.3. *Assuming $\beta < 1$, the primary network spatial throughput can be obtained as*

$$C_{\beta<1}^{(p)}(\lambda) \sim G_{\beta<1}^{(p)} \sqrt{\frac{\lambda^{(p)}}{\log(\lambda^{(p)})}}, \tag{3.19}$$

where the primary network AMG in the presence of secondary network only depends on the effective medium access probability $\tilde{q}^{(s)} := q^{(s)} \exp(-\lambda^{(p)} q^{(p)} \pi R_D^2)$ of secondary users:

$$G_{\beta<1}^{(p)} = e^{-\lambda^{(s)} \tilde{q}^{(s)} \pi (R_I^{(sp)})^2} G\,. \tag{3.20}$$

Proof. Refer to Appendix C. □

3.4.2 Throughput Analysis for the Secondary Network

In this section we derive the spatial throughput for the secondary network when secondary users try to access the channel opportunistically in the presence of primary users. The throughput analysis closely follows the methods in Section 3.3 but with proper modifications to the calculation of successful transmission probability, which now should take into account the opportunistic access mechanism adopted by secondary users and the extra inter-network interference from primary users.

Let $\tilde{\Lambda}_{X_n^{(s)}}$ be the event of successful transmission of a packet b from a secondary node $X_n^{(s)}$ to the next relay $X_{n+1}^{(s)}$ in the presence of the primary network. Similar to Section 3.4.1, we have that $\tilde{\Lambda}_{X_n^{(s)}}$ happens if events $\tilde{\Lambda}_{1,X_n^{(s)}}$, $\tilde{\Lambda}_{2,X_{n+1}^{(s)}}$, and $\Lambda_{3,X_{n+1}^{(s)}}$ all happen. Here, $\Lambda_{3,X_{n+1}^{(s)}}$ denotes the event that there are no primary transmitters within inter-network interference range $R_I^{(ps)}$ of $X_{n+1}^{(s)}$. $\tilde{\Lambda}_{1,X_n^{(s)}}$ and $\tilde{\Lambda}_{2,X_{n+1}^{(s)}}$ are similar

to the events in the proof of Lemma 3.3.1, except that unlike the single-tier network case, the secondary users initiate transmissions with probability $q^{(s)}$ only when they detect no primary transmitters within R_D radius.

We define the effective access probability $\tilde{q}^{(s)} := q^{(s)} \exp(-\lambda^{(p)} q^{(p)} \pi R_D^2)$ and denote by $\Lambda_{X_n^{(s)}} := \Lambda_{1,X_n^{(s)}} \Lambda_{2,X_{n+1}^{(s)}} \Lambda_{3,X_{n+1}^{(s)}}$ the event of successful transmission if all secondary users initiate transmissions with probability $q^{(s)}$ regardless of the spectrum sensing outcome. The distinctive feature in the secondary network is that the transmission initiation is contingent upon the detection of idle spectrum. Thus, the larger R_D is, the smaller the likelihood of secondary transmission initiation is. On the other hand, the larger R_D is, the smaller the likelihood of intra-network interference among secondary users is. Therefore, there exists a trade-off between $\Pr(\tilde{\Lambda}_{1,X_n^{(s)}})$ and $\Pr(\tilde{\Lambda}_{2,X_{n+1}^{(s)}})$ via the choice of R_D.

We show in Lemma 3.4.4 that the secondary network sum throughput is asymptotically zero regardless of the relative density of the two networks when the secondary detection range is "too" big.

Lemma 3.4.4. *The secondary network sum throughput is asymptotically zero when $R_D = \omega(R_r^{(p)})$. Therefore, in order to satisfy the primary network AMG constraint while achieving asymptotically non-trivial sum throughput for the secondary network, the detection range should satisfy $R_D = \alpha_2 R_r^{(p)}$, with constant $0 < \alpha_2 \leq 1$ when $\beta > 1$ and $R_D = \alpha_2 R_r^{(p)}$, with constant $\alpha_2 > 0$ when $\beta < 1$.*

Proof. Using (3.3) we have

$$\begin{aligned} C_{\beta>1}^{(s)} &= \lambda^{(s)}|A|\mathrm{E}\left(\frac{1}{\nu+1}\sum_{n=0}^{\nu}\mathrm{E}\left(Y_{X_n^{(s)}}\mathbf{1}_{\tilde{\Lambda}_{X_n^{(s)}}}\right)\right) \\ &\leq \lambda^{(s)}|A|R_r^{(s)}\Pr\left(\tilde{\Lambda}_{1,X_n^{(s)}}\right) \\ &\leq \lambda^{(s)}|A|R_r^{(s)}\Pr\left(\tilde{\Lambda}_{X_n^{(s)}} \mid \tilde{\Lambda}_{1,X_n^{(s)}}\right)\Pr\left(\tilde{\Lambda}_{1,X_n^{(s)}}\right) \\ &\leq \lambda^{(s)}|A|R_r^{(s)}e^{-\left(\frac{R_D}{R_I^{(p)}}\right)^2} \to 0\,, \end{aligned}$$

as $\lambda^{(p)} \to \infty$. Together with the result in Proposition 3.4.1, the proof of the lemma is complete. □

In the following, we derive the asymptotic spatial throughput of the secondary network in the presence of a primary tier when the secondary spectrum sensing range is $R_D = \alpha_2 R_r^{(p)}$, with constant $0 < \alpha_2 \leq 1$ when $\beta > 1$ and $R_D = \alpha_2 R_r^{(p)}$, with constant $\alpha_2 > 0$ when $\beta < 1$. We first consider the $\beta > 1$ scenario. In this case we have $R_r^{(p)} = \omega(R_r^{(s)})$. As mentioned before, the medium access decisions of secondary users are correlated due to their overlapping spectrum sensing regions. For example, if $X_n^{(s)}$ initiates a transmission, the probability that the secondary users located inside $B_{R_I^{(s)}}(X_{n+1}^{(s)})$ initiate transmissions increases, which in turn decreases the probability of successful transmissions between $X_n^{(s)}$ and $X_{n+1}^{(s)}$. Furthermore, as $X_n^{(s)}$ gets closer to $X_{n+1}^{(s)}$, the probability of intra-network interference to $X_{n+1}^{(s)}$ increases, knowing $X_n^{(s)}$ initiates transmission.

In general, the probability that a secondary node $X_i^{(s)}$ initiates a transmission is a non-increasing function of $|X_j^{(s)} - X_i^{(s)}|$ if $X_j^{(s)}$ is transmitting and a non-decreasing function of $|X_j^{(s)} - X_i^{(s)}|$ if $X_j^{(s)}$ is idling. Similarly, the probability that a secondary node $X_i^{(s)}$ idles is a non-decreasing function of $|X_j^{(s)} - X_i^{(s)}|$ if $X_j^{(s)}$ is transmitting

and a non-increasing function of $|X_j^{(s)} - X_i^{(s)}|$ if $X_j^{(s)}$ is idling.

In Propositions 3.4.5, we establish that the secondary network can still achieve its stand-alone sum spatial throughput scaling when $\beta > 1$. Furthermore, we derive the secondary network AMG and identify its relation with the secondary medium access and spectrum sensing strategies.

Proposition 3.4.5. *Assume $\beta > 1$. The secondary network sum spatial throughput can be obtained as*

$$C_{\beta>1}^{(s)}(\lambda) \sim G_{\beta>1}^{(s)} \sqrt{\frac{\lambda^{(s)}}{\log(\lambda^{(s)})}}\,, \tag{3.21}$$

where the secondary network AMG in the presence of primary network equals

$$G_{\beta>1}^{(s)} = e^{-\left(\frac{\max\{\alpha_2 R_r^{(p)}, R_I^{(ps)}\}}{R_I^{(p)}}\right)^2} \alpha_1 e^{1-\alpha_1} G\,, \tag{3.22}$$

when the secondary medium access probability equals $q^{(s)} = \alpha_1(\lambda^{(s)}\pi(R_I^{(s)})^2)^{-1}$ and $R_D = \alpha_2 R_r^{(p)}$, with $\alpha_1 > 0$ and $0 < \alpha_2 \leq 1$.

Proof. Refer to Appendix D. □

From (3.22) we have that $q^{(s)} = O\left(1/\log(\lambda^{(s)})\right)$ is still a necessary condition to ensure an asymptotically nontrivial throughput for the secondary network. Similar to the single-tier network case, setting $q^{(s)} = (\lambda^{(s)}\pi(R_I^{(s)})^2)^{-1}$ is still the optimal access probability for the secondary nodes. Observe that setting $\alpha_1 \neq 1$ or $\alpha_2 > R_I^{(ps)}/R_r^{(p)}$ degrades the secondary network AMG. However, the secondary network AMG remains unaffected for $\alpha_2 < R_I^{(ps)}/R_r^{(p)}$.

In Fig. 3.4, we compare the optimal secondary sensing radius α_2, access probability α_1, and AMG $G_{\beta>1}^{(s)}$ as a function of primary AMG requirement $G_{\beta>1}^{(p)}$ for

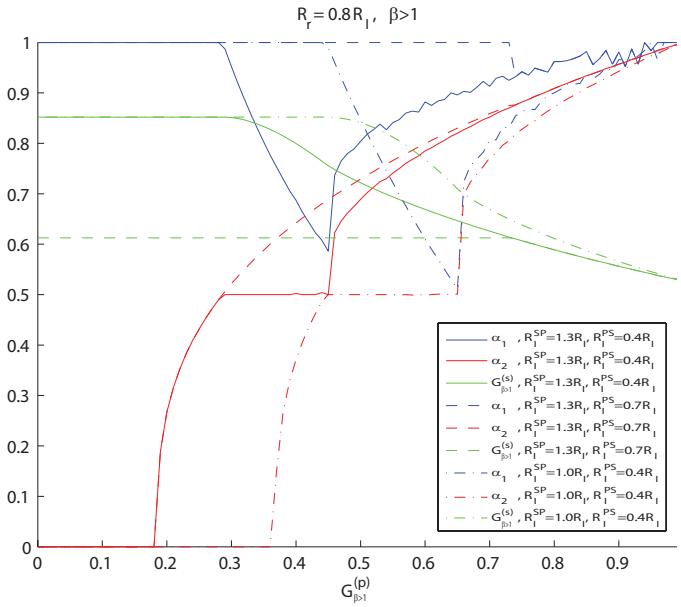

Figure 3.4: Optimal secondary sensing radius α_2, access probability α_1, and AMG $G^{(s)}_{\beta>1}$ as a function of primary AMG loss requirement $G^{(p)}_{\beta>1}$ for different inter-network interference parameters.

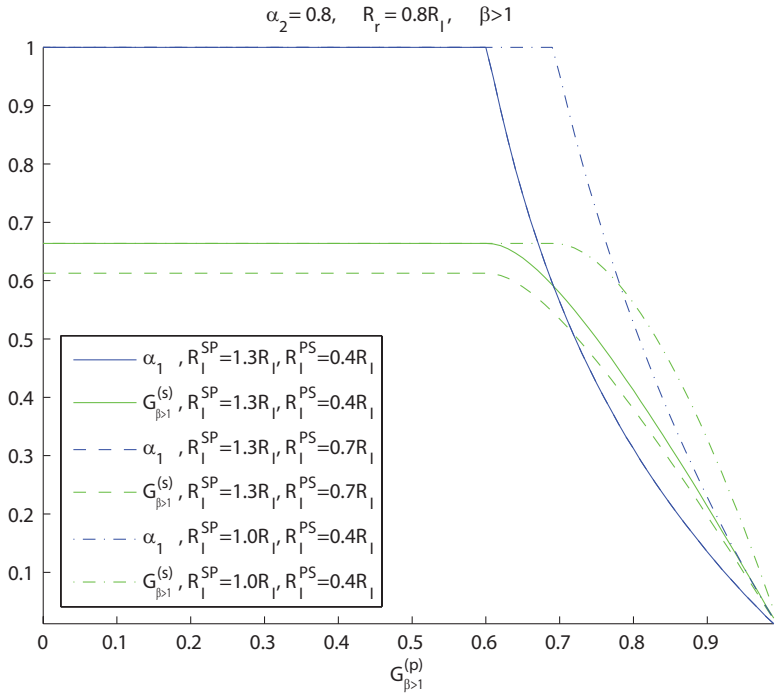

Figure 3.5: Optimal secondary access probability α_1 and achievable AMG $G^{(s)}_{\beta>1}$ as a function of primary AMG loss requirement $G^{(p)}_{\beta>1}$ for different inter-network interference parameters.

different inter-network interference parameters. In Fig. 3.5, we repeat the same analysis but with the detection range fixed ($\alpha_2 = 0.8$). Observe that the secondary throughput performance degrades significantly as the primary AMG requirement increases, when the secondary detection range is fixed. Therefore, to achieve an acceptable secondary throughput performance when primary AMG requirements is stringent, high-performance spectrum detectors are crucial. Also it is worth noting the disproportional effect of $R_I^{(ps)}/R_I^{(p)}$ and $R_I^{(sp)}/R_I^{(s)}$ on the optimal secondary AMG performance; For any fixed primary AMG requirement, the secondary AMG improved more by decreasing $R_I^{(ps)}/R_I^{(p)}$ rather than $R_I^{(sp)}/R_I^{(s)}$, cf. (3.18) and (3.22).[4]

Next, we determine the secondary network throughput scaling and AMG when $\beta < 1$. In this case we have $R_r^{(p)} = o(R_r^{(s)})$. In the next proposition, we derive the secondary network spatial throughput and show that the secondary network can still achieve its stand-alone sum spatial throughput scaling when $\beta < 1$.

Proposition 3.4.6. *When $\beta < 1$, the secondary network throughput performance in the presence of primary users resembles the stand-alone secondary network but with a reduced medium access probability $\tilde{q}^{(s)}$. In other words,*

$$C^{(s)}_{\{\beta<1\}}(\lambda) = e^{-(\frac{R_I^{(ps)}}{R_I^{(p)}})^2} \tilde{C}^{(s)}(\lambda)\,, \tag{3.23}$$

where $\tilde{C}^{(s)}$ equals the single-tier spatial throughput expression in (3.12) *with the secondary network parameters and the effective medium access probability $\tilde{q}^{(s)}$ substituted. The secondary network can achieve a throughput scaling of $\Theta\left(\sqrt{\lambda^{(s)}/\log(\lambda^{(s)})}\right)$ with the effective ALOHA access probability $\tilde{q}^{(s)} = O\left(1/\log(\lambda^{(s)})\right)$ even when the sec-*

[4]Reducing $R_I^{(ps)}/R_I^{(p)}$ and $R_I^{(sp)}/R_I^{(s)}$ can be achieved by employing certain cognitive features, e.g., by acquiring knowledge about primary messages and utilizing joint encoding techniques to partially mitigate primary interference or employing interference alignment techniques at the primary receivers.

ondary nodes are much more sparsely distributed than the primary nodes.

Proof. Refer to Appendix E. □

Observe that according to (3.20) and (3.23), the primary and secondary network throughput performance (i.e., AMGs) depends only on $\tilde{q}^{(s)} \in [0, 1]$ when $\beta < 1$. Therefore, the desired network performances can be achieved by setting $q^{(s)}$ appropriately while $R_D = 0$. Hence, the spectrum sensing turns out to be redundant and secondary user should blindly access the channel according to the traditional ALOHA medium access scheme without resorting to spectrum sensing when they are much sparser than the primary users. However, as shown in Fig. 3.6, in this case the secondary network throughput performance degrades significantly for high primary AMG requirements and employing spectrum detectors cannot improve the secondary performance degradation neither.

3.5 Conclusion

In this section, we studied the interaction between two overlaid ad-hoc networks: one with legacy primary users who are licensed to access the spectrum and the other with cognitive secondary users who opportunistically access the spectrum. We showed that regardless of the spectrum sensing settings, both networks can achieve their stand-alone throughput scalings. Furthermore, with the newly defined performance metric, the asymptotic multiplexing gain (AMG), we quantified how the asymptotic network performances is affected by the mutual interference between the two networks. In addition, we derived the spatial throughput of an ad-hoc overlaid cognitive network with exact expressions for the pre-constant multipliers. We showed that employing the proper spectrum sensing and medium access probability settings, secondary users can achieve a reasonable throughout performance while satisfying the primary AMG requirement when the secondary network is denser; However, when

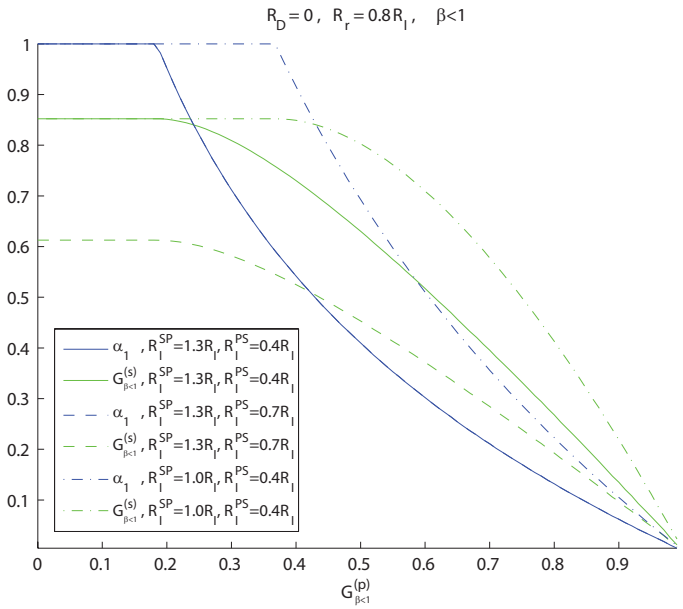

Figure 3.6: Optimal secondary sensing radius α_2, access probability α_1, and achievable AMG as a function of primary AMG loss requirement $G_{\beta<1}^{(p)}$ for different internetwork interference parameters.

the secondary network is sparser, the spectrum sensing cannot improve the throughput performance of the secondary users. As such, secondary users should satisfy the primary AMG requirement by appropriate selection of medium access probability, which results in a significant secondary throughput degradation.

4. ASYMPTOTIC STATISTICS FOR GEOMETRIC ROUTING SCHEMES IN WIRELESS AD-HOC NETWORKS

4.1 Introduction

A wireless ad-hoc network consists of autonomous wireless nodes that collaborate on communicating information in the absence of a fixed infrastructure. Each of the nodes might act as a source/destination node or as a relay. Communication occurs between a source-destination pair through a single-hop transmission if they are close enough, or through multi-hop transmissions over intermediate relaying nodes if they are far apart. The selection of relaying nodes along the multi-hop path is governed by the adopted routing scheme.

The conventional method to establish a routing path between a given source-destination pair is through exchanges of control packets containing the complete network topology information [56], which creates scalability issues when the network size becomes large. One way to reduce the overhead for global topology inquiries is to build routes on demand via flooding techniques [57]. However, such routing protocols essentially suffer from a similar issue of large signaling overheads. To deal with the above issues, Takagi and Kleinrock [43] introduced the first geographical (or position-based) routing scheme, coined as Most Forward within Radius (MFR), based on the notion of progress:[1] Given a transmitting node S and a destination node Dst, the progress at relay node V is defined as the projection of the line segment SV onto the line connecting S and Dst. In MFR, each node forwards the packet to the neighbor with the largest progress (e.g., node V_2 in Fig. 4.1), or discards the packet if none of its neighbors are closer to the destination than itself. There are some

[1]It should be noted that the reduction in complexity comes at the cost of knowing the location of the neighboring nodes in addition to that of the destination.

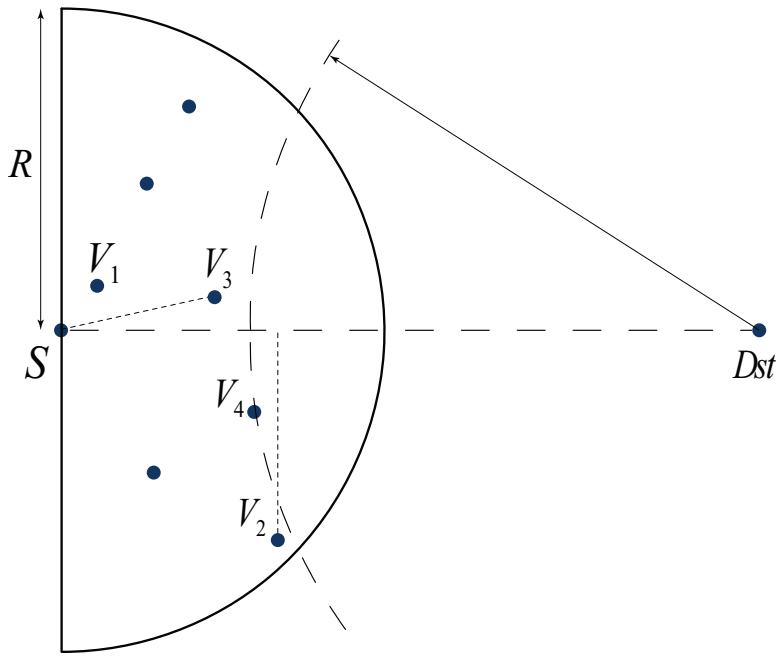

Figure 4.1: Some variants of geometric routing schemes: The source node S has different choices to find a relay node for further forwarding a message to the destination Dst. V_1 = nearest forward progress (NFP), V_2 = most forward within radius (MFR), V_3 = compass routing (DIR), V_4 = shortest remaining distance (SRD).

other variants of the geographical routing scheme in the literature [49][50][51], which are similar to MFR. In [49], the authors introduced the Nearest Forward Progress (NFP) method that selects the nearest neighbor of the transmitter with forward (positive) progress (e.g., node V_1 in Fig. 4.1); in [50], the Compass Routing (also referred to as the DIR method) was proposed, where the neighbor closest to the line connecting the sender and the destination is chosen (e.g., node V_3 in Fig. 4.1); in [51], the authors considered the Shortest Remaining Distance (SRD) method, where the neighbor closet to the destination is selected as the relay (e.g., node V_4 in Fig. 4.1).

Geographical routing protocols might fail for some network configurations due to dead-ends or routing loops. In these cases, alternative routing strategies, such

as route discovery based on flooding [58] and face routing [59] can be deployed. However, it has been shown in [42] that for dense wireless networks, the MFR-like routing strategies will succeed with high probability and there is no need to resort to recovery methods such as face routing. In this section we study the network layer performance of geographical routing schemes in such dense or large wireless networks; and we expect to observe a similar high-probability successful routing performance (the proof of this claim is presented in Section 4.4.2).

Below we present a methodology employing statistical analysis and stochastic geometry to study geometric routing schemes in wireless ad-hoc networks. We consider a wireless ad-hoc network consisting of wireless nodes that are distributed according to a Poisson point process over a circular area, where nodes are randomly grouped in source-destination pairs and can establish direct communication links with other nodes that are within a certain range. We determine the conditions under which, in such a network, all source-destination node pairs are connected via the adopted geographical routing scheme with high probability and quantify the asymptotic statistics (mean and variance) for the length of the generated routing paths. In particular, we focus on a variant of the geographical routing schemes, namely the random $\frac{1}{2}$disk routing scheme, as an example, where each node chooses the next relay uniformly at random among the nodes in its transmission range over a $\frac{1}{2}$disk with radius R oriented towards the destination. This scheme is similar to the geometric routing scheme discussed in [43], in which one of the nodes with forward progress is chosen as a relay at random, arguing that there is a trade-off between progress and transmission success.

We chose the random $\frac{1}{2}$disk routing scheme mainly for tractability and simplicity in mathematical characterization. However, the solution techniques developed in this section can be used (with some modifications) to study other variants of geographical

routing schemes, such as MFR, NFP, DIR, etc, which will be further discussed in Section 4.6. Moreover, the random $\frac{1}{2}$disk routing scheme can be used to model situations where nodes have partial or imprecise routing information and the locally optimal selection criterion of greedy forwarding schemes fails [52], e.g., when nodes have perfect knowledge about their destination locations but imprecise information about their own locations, or when nodes only know the half-plane over which the final destination lies such that randomly forwarding the packet to a node in the general direction of the destination is a plausible choice.

There has been a considerable interest regarding the network connectivity and the average length of the route generated by geographical routing schemes under different network settings [52][60]–[63]. The authors in [60] considered a wireless network that consists of n nodes uniformly distributed over a disc of unit area with each node transmission covering an area of $r(n) = (\log n + c(n))/n$. They show that this network is connected asymptotically with probability one *if and only if* $c(n) \to \infty$ as $n \to \infty$. Although the asymptotic expression that they derived for the sufficient transmission range is similar to ours, their notion of connectivity is quite different from ours. In [60], the network is connected as long as it is percolated, i.e., the network contains an infinite-order component, where no constraints are considered for the paths connecting source-destination pairs. However, the routing paths that we consider in this work have more structure such that we need a different proof technique to prove the asymptotic connectivity of the network. Xing *et al.* showed in [61] that the route establishment can be guaranteed between any source-destination pair using greedy forwarding schemes if the transmission radius is larger than twice the sensing radius in a fully covered homogeneous wireless sensor network. In [51] the authors derived the critical transmission radius to be $\sqrt{\frac{\beta_0 \log n}{n}}$ which ensures network connectivity asymptotically almost surely (a.a.s.) based on the SRD routing method,

where $\beta_0 = 1/(2\pi/3 - \sqrt{3}/2)$.

In [62], Bordenave considered the maximal progress navigation for small world networks and showed that small world navigation is regenerative.[2] It is shown furthermore in [62] that as the cardinality of the navigation (or routing) path grows, the expected number of hops converges, without providing an explicit value for the limit. Baccelli *et al.* [46] introduced a time-space opportunistic routing scheme for wireless ad-hoc networks which utilizes a self-selection procedure at the receivers. They show through simulations that such opportunistic schemes can significantly outperform traditional routing schemes when properly optimized. Furthermore, they analytically proved the asymptotic convergence of such schemes. In [52], Subramanian and Shakkottai studied the routing delay (measured by the expected length of the routing path) of geographic routing schemes when the information available to network nodes is limited or imprecise. They showed that one can still achieve the same delay scaling even with limited information. Note that the asymptotic delay expression derived in [52] is similar to the one we derive in this section; however, our proof technique is more constructive and enables us to derive tight bounds for the mean and the variance of the routing-path lengths in a network of arbitrary size, together with the exact expressions for their asymptotes. Moreover, in [52] the authors presumes that the progress (as defined in [43] and described earlier) at nodes along the routing path form a sequence of i.i.d. random variables. However, as we show later (cf. Proposition 4.4.1), this assumption may not hold for Poisson distributed networks of arbitrary finite sizes as the distribution of nodes contained in the transmission range of a given node along a routing path depends on the history of the routing path up to this node, i.e., the progress at each hop is history dependent. Hence, it is neither independent nor identically distributed; but we show that, as the size of the network

[2]This routing scheme, unlike ours, assumes nonnegative progress in each hop.

(either density or area) goes to infinity, the conditional distribution of the progresses along the routing path given the two previous hops, in fact, depends asymptotically only on the last hop.

The remainder of this section is organized as follows. In Section 4.2 we introduce the system model and describe the random $\frac{1}{2}$disk routing scheme. Then we define the notion of connectivity based on generic geometric routing schemes and state the main results of the section in a theorem regarding the connectivity and the statistical performance of the random $\frac{1}{2}$disk routing scheme. In Sections 4.3 and 4.4 we prove the claims made in this theorem. In Section 4.3, we establish sufficient conditions on the transmission range that ensure the existence of a relaying node in every direction of a transmitting node for both dense and large-scale networks. In Section 4.4, we study the stochastic properties of the paths generated by the random $\frac{1}{2}$disk routing scheme. Specifically, in Section 4.4.1, we prove that the routing path progress conditioned on the previous two hops can be approximated with a Markov process. In Section 4.4.2, using the Markovian approximation, we derive the asymptotic expression for the expected length, and in Section 4.4.3 we derive the asymptotic expression for the variance of the length of the random $\frac{1}{2}$disk routing paths. In Section 4.5, we present some simulation results to validate our analytical results. In Section 4.6, we present some guidelines on how to generalize the results derived for the random $\frac{1}{2}$disk routing scheme to other variants of the geometric routing schemes. We conclude the section in Section 4.7.

4.2 System Model

Consider a circular area A over which a network of wireless nodes resides.[3] Nodes are distributed according to a homogeneous Poisson point process with density λ.

[3]The results will carry over, with some minor considerations, to any convex region with bounded curvature.

In this work we adopt a continuum model for the network where each node is a zero-dimensional point in a unit-area disk.[4] As such, network nodes can be located at any geometric locations $(x, y) \in \mathbb{R}^2$ such that $x^2 + y^2 \leq \frac{|A|}{\pi}$, where $|A|$ denotes the area of region A.

Each node picks a destination node uniformly at random among all other nodes in the network, and operates with a fixed transmission power that can cover a disk of radius $R = R(\lambda, |A|)$.[5]

For a generic geometric routing scheme, when the targeted destination node is out of the one-hop transmission range R of a given transmitting node, the next relay is selected (based on some rules) among the nodes contained in the *relay selection region* (RSR) of the transmitting node, where the RSR, in general, can be any subset of a full disk of radius R centered at the transmitting node. For example, the RSR for all the geometric routing schemes cited in the introduction section is a $\frac{1}{2}$*disk* of radius R centered at the transmitting node and oriented towards the destination (denoted by $\frac{1}{2}$RSR). We define the rule that governs the selection of the next relay in each node's RSR as the *relay selection rule* (RSL). For example, the RSL for MFR is to choose the node with the largest "progress" towards the destination among the nodes contained in its $\frac{1}{2}$RSR. We define the progress x'_V at a relay node V as in [43], and described in the introduction section.

We define the network to be *connected* if for any source-destination node pair in the network, there exists a path constructed by a *finite sequence of relay nodes*

[4]This is due to the asymptotic nature of the results presented in this work. Furthermore, a Poisson point process model for the node locations can be considered on a discrete space of countably infinite isolated points (for instance, lattices). Adapting such a model does not change the nature of the results presented.

[5]As mentioned earlier, we are only interested in the network layer performance of the network; as such, we do not consider physical layer related issues such as interference. However, as a rule of thumb (cf. [42]), to minimize the interference among wireless nodes we are interested in the smallest transmission radius that ensures network connectivity in this section.

complying with the RSL, with *high probability*;[6] henceforth, we call such a relay sequence a *routing path*. Note that a node can potentially act as a *relay* only if it is contained in the RSR of the current transmitting node. For the sake of definition, we claim that the network is connected if the set of network nodes is empty.

In this section we study a special case of localized geometric routing schemes, namely the *random* $\frac{1}{2}$*disk routing scheme*, where for each transmitting node S in the network, the next relay V is selected *uniformly at random* among the nodes contained in the $\frac{1}{2}$RSR of S. We denote the relay selection rule of the random $\frac{1}{2}$disk routing scheme by rRSL. Observe that according to our routing scheme, the next chosen relay might be farther away from the destination than the current transmitting node.

In the following, we present a theorem that summarizes the main results of this section on the random $\frac{1}{2}$disk routing scheme, regarding i) the sufficient conditions on $R(\lambda, |A|)$, which ensure the existence of a relaying node in any direction of a particular transmitting node based on a generalized version of $\frac{1}{2}$RSR; ii) the mathematical model describing the routing path; iii) the mean asymptotes of the path-lengths established by the random $\frac{1}{2}$disk routing scheme; iv) the corresponding variance asymptotes; and v) the asymptotic network connectivity with the random $\frac{1}{2}$disk routing scheme. For the generalized version of the $\frac{1}{2}$RSR, we assume that the RSR of a node is a wedge of angle $2\pi\eta$ with radius R, where $0 < \eta \leq 1$ (hereafter called ηdisk or ηRSR, interchangeably). Hence, the $\frac{1}{2}$RSR is a special case of the ηRSR with $\eta = 1/2$.

Note that in this section we define the *length* of a routing path as the number of hops traversed over the routing path between a source and its destination. For notational convenience, we let $N := \lambda|A|$ designate the expected number of nodes

[6]According to this definition, the network is connected if starting from any source and choosing relays based on the routing scheme, the destination is reachable with high probability.

in the network region of area $|A|$ and $d = d(N) := \frac{\pi R^2}{|A|}$ denote the normalized area of a full disk with radius R relative to the area of the whole region, such that dN is the expected number of nodes in such a disk. The *asymptotic* nature of the results presented in this section is due to $N \to \infty$, which can represent results for either large-scale networks (i.e., when $|A| \to \infty$ with a fixed λ) or dense networks (i.e., when $\lambda \to \infty$ with a fixed $|A|$).

Also, $f(n) = O(g(n))$ means that there exist positive constants c and M such that $f(n)/g(n) \leq c$ whenever $n \geq M$, $f(n) = o(g(n))$ means that $\lim f(n)/g(n) \to 0$ as $n \to \infty$, $f(n) \sim g(n)$ means that $\lim f(n)/g(n) \to 1$ as $n \to \infty$, and $f(n) = \Theta(g(n))$ means that both $f(n) = O(g(n))$ and $g(n) = O(f(n))$.

Theorem 4.2.1. *Consider a Poisson distributed wireless network with an average node population N deployed over a circular area A. Each node picks a destination node uniformly at random among all other nodes in the network. Assume all nodes have the same transmission range $R(N)$ that covers a normalized area $d = d(N)$ and let x' be the progress at each node. Choosing $R(N)$ such that $\eta dN + \log d \to +\infty$ as $N \to \infty$, we have*

i) the ηdisk of each node in the network pointing at any direction in which its targeted destinations may lie contains at least one relaying node asymptotically almost surely (a.a.s.);

ii) the routing path progress can be approximated to a "second-order" with a Markov process; more specifically, the conditional distribution of the next hop given the previous two hops, asymptotically depends only on the last hop.

iii) Using the Markovian approximation, we have that the length ν of the random $\frac{1}{2}$disk routing path is asymptotically finite with the asymptotic expected

value $\mathrm{E}(\nu) \sim \frac{32}{15}\frac{1}{\sqrt{d}}$*; specifically, the expected length of the random* $\frac{1}{2}$*disk routing path connecting a source-destination pair that is* h*-distance apart satisfies* $\mathrm{E}(\nu \mid h) \sim \frac{h}{\mathrm{E}(x')} = \frac{3\pi}{4}\frac{h}{R}$ *as* $N \to \infty$*;*

iv) the variance-to-mean ratio of the routing path length satisfies $\frac{\mathrm{Var}(\nu)}{\mathrm{E}(\nu)} \sim \frac{\mathrm{Var}(x')}{\mathrm{E}(x')^2} = \frac{9\pi^2}{61} - 1$ *as* $N \to \infty$*;*

v) the network is asymptotically connected with the random $\frac{1}{2}$*disk routing scheme with high probability,*

where the expectation is taken over all realizations of the network nodes, source-destination pair assignments, and the routing paths between source-destination pairs.

Proof. Here we only sketch the outline of the proof and present the respective details in the following sections. In Section 4.3, we show that for random networks, choosing $R(N)$ such that $\eta d N + \log d \to +\infty$ as $N \to \infty$ guarantees the existence of at least one relaying node in the ηdisk of each network node pointing at any directions in which their targeted destinations may lie a.a.s..[7] To this end, we first derive an upper bound on the probability $\sigma(N)$ that the ηdisk of some nodes in the network pointing at some directions is empty. Then we show that choosing $d(N)$ as mentioned before ensures the asymptotic convergence of $\sigma(N)$ to zero as $N \to \infty$. This ensures the existence of a relaying node in every direction of a particular transmitting node and ascertains the possibility of packet delivery to a particular destination from any direction a.a.s..

In Section 4.4, assuming $R(N)$ satisfies the above condition and N is large enough such that there exists a relaying node in every direction of a particular transmitting node with high probability, we prove that the routing path progress conditioned

[7] A specific node might act as a relay for multiple source-destination pairs.

on the previous two hops can be approximated with a Markov process. Using the Markovian approximation, we then derive the asymptotic expressions for the mean and variance of the routing path length generated by the random $\frac{1}{2}$disk routing scheme between a source-destination pair that is h-distance apart and show that they are asymptotic to $\frac{h}{\mathrm{E}(x')} = \frac{3\pi}{4}\frac{h}{R}$ and $\frac{\mathrm{Var}(x')}{\mathrm{E}(x')^2}\mathrm{E}(\nu) = \left(\frac{9\pi^2}{61} - 1\right)\mathrm{E}(\nu)$, respectively. Furthermore, we show that the length of the random $\frac{1}{2}$disk routing path connecting a source to its destination is finite asymptotically. This shows that starting from a source and following the random $\frac{1}{2}$disk routing scheme we can reach the destination in finitely many hops with high probability; hence the network is asymptotically *connected* with the random $\frac{1}{2}$disk routing scheme. □

4.3 Theorem 4.2.1.*i* Proof: Uniform Relaying Capability

In this section we derive the sufficient conditions on $R(N)$ that ensures, for any node in the network, its ηdisks pointing at any directions over which its targeted destinations may lie contain at least one potential relaying node. To this end, we first characterize the upper bound on the probability $\sigma(N)$ that, for some network nodes, there are certain directions at which their ηdisks are empty; we then choose R such that this bound is vanishingly small. In this process, we can distinguish between two types of network nodes based on their distances to the edge of the network: Nodes that are farther than R away from the edge of the network, which we call *interior nodes*, and nodes that are closer than R to the edge of the network, which we call *edge nodes*. For the sake of definition, we assume $\sigma(N) = 0$ when $N = 0$.

For interior nodes, it is clear that the node distribution in their ηdisks, pointing at any direction, is the same. Therefore, the existence probability of an empty ηdisk for an interior node is independent of its targeted destination direction. However,

due to the proximity of edge nodes to the boundary of the network, the existence probability of an empty ηdisk for an edge node highly depends on its destination orientation. For example, the ηdisks that fall partly outside the network region are more likely to be empty than the ones that are fully contained in the network region. Hence, we derive the probabilities of a node having an empty ηdisk in some direction separately for the interior nodes and the edge nodes, denoted by $\sigma'(N)$ and $\sigma''(N)$, respectively.

Recall that a ηdisk is a wedge of angle $2\pi\eta$ and radius R, with $0 < \eta \leq 1$. Each ηdisk has an expected number of nodes ηdN. As shown in Section 4.3.3, the existence probability of an empty ηdisk increases as η decreases. However, we can show that the expected length of the routing path connecting a source to its destination will decrease as η decreases. Hence, there exist a trade-off between the existence probability of an empty ηdisk (i.e., a disconnected node) and the expected length of the routing path between a source-destination pair parameterized by η. We leave the study of this trade-off to a future work and only derive (in Section 4.4) the mean and variance of the path length connecting a source-destination pair when $\eta = 1/2$.

4.3.1 Calculation of $\sigma'(N)$

Consider an interior node x, fixed for now. Given $i \geq 1$ nodes are in the transmission range of x, their directions in reference to x are independent and uniformly distributed on $[0, 2\pi]$. The probability that x has an empty ηdisk in some direction equals the probability $U_i(\eta)$ that the angle of the widest wedge containing none of these i nodes is at least $2\eta\pi$. It is not difficult to give a simple upper bound on $U_i(\eta)$: Of the i nodes, without loss of generality (W.L.O.G.), we can assume that (at least) one is at one edge of an empty wedge with angle of $2\eta\pi$, while the other $i - 1$ are

distributed independently and uniformly in the remainder of the full transmission disk, as shown in Fig. 4.2. Hence, we obtain $U_i(\eta) \leq i(1-\eta)^{i-1}$, for $i \geq 1$. Of course, if $i = 0$ the probability is $U_0(\eta) = 1$.

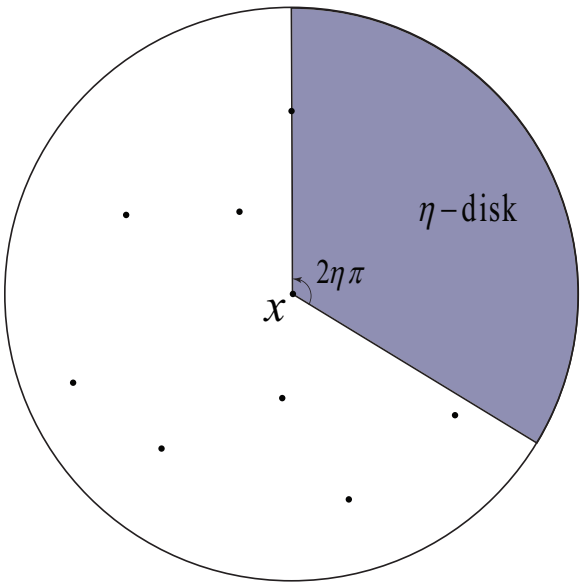

Figure 4.2: A realization for which the widest wedge between the nodes is of an angle at least $2\eta\pi$.

One can obtain a more precise expression for $U_i(\eta)$ using results in [64, p. 188]:

$$U_i(\eta) = \sum_{k=1}^{\min\{\lfloor 1/\eta \rfloor, i\}} (-1)^{k-1} \binom{i}{k} (1-k\eta)^{i-1} \leq i(1-\eta)^{i-1} \,,$$

for $i \geq 1$, where $\lfloor a \rfloor$ is the largest integer smaller than a. This expression is based on the inclusion-exclusion principle for the probability of the union of events, for which the first term in the sum provides an upper bound and the first two terms provide a lower bound.

Averaging over i (number of the nodes in the transmission range of x) and over

the number of network nodes, we have:

$$\begin{aligned}
\sigma'(N) &\leq \sum_{k=1}^{\infty} e^{-N} \frac{N^k}{k!} k \sum_{i=0}^{k-1} \binom{k-1}{i} d^i (1-d)^{k-1-i} U_i(\eta) \\
&\leq \sum_{k=1}^{\infty} e^{-N} \frac{N^k}{(k-1)!} \left[(1-d)^{k-1} + d(k-1) \sum_{i=0}^{k-1} \binom{k-2}{i} (d(1-\eta))^{i-1} (1-d)^{k-1-i} \right] \\
&= e^{-N} \left[N \sum_{k=1}^{\infty} \frac{(N(1-d))^{k-1}}{(k-1)!} + dN^2 \sum_{k=2}^{\infty} \frac{(N(1-\eta d))^{k-2}}{(k-2)!} \right] \\
&= dN^2 e^{-\eta dN} \left(1 + \frac{1}{dN} e^{-(1-\eta)dN} \right) . \qquad (4.1)
\end{aligned}$$

4.3.2 Calculation of $\sigma''(N)$

So far we have considered the interior nodes that are at least R-distance away from the boundary of the network region. Now, we consider edge nodes that are within R of the network edge. Some ηdisks of an edge node may fall partially (up to half) outside the region, which increases the chance that they are empty. We refer to this phenomenon as the *edge effect*. Since the network region is circular, the number of such edge nodes equals $(2 - \sqrt{d})\sqrt{d}N$, which is of order $\Theta\left(\sqrt{d}N\right)$. We need to determine how their contribution to $\sigma(N)$ differs from the interior nodes.

Consider an edge node e, $(\delta' R)$-distance away from the network edge, with $0 < \delta' < 1$. As shown in Fig. 4.3, we take node e as the pole and the ray eu (perpendicular to the network edge) as the polar axis of the *local* (polar) coordinates at node e. We argued at the beginning of this section that, for edge node e, the probability of an ηdisk being empty, depends highly on its orientation. Let us consider this claim more closely. Let $\varphi := \cos^{-1}(\delta)$, as shown in Fig. 4.3, where δR is the distance between

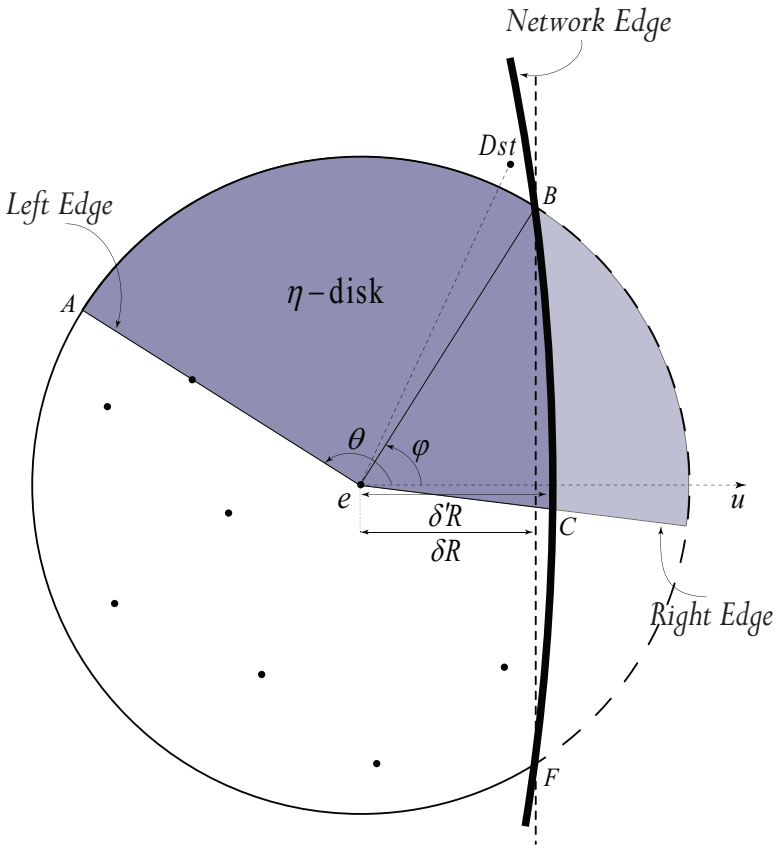

Figure 4.3: Intersection of the ηdisk with the network region.

node e and the line passing through the intersection points B and F in Fig. 4.3 with

$$\delta = \delta' - \frac{R}{L}\frac{1-\delta'^2}{2(1-\delta'\frac{R}{L})},$$

and $L := \sqrt{|A|/\pi} = R/\sqrt{d}$ being the network region radius.

Note that all the ηdisks are oriented towards the destination node. Hence, for all ηdisks that are oriented towards an angle in the range $(-\varphi, \varphi)$, we must have that the destination is within node e's transmission range. Therefore, we only need to be concerned with empty ηdisks oriented towards an angle in the range $(\varphi, 2\pi - \varphi)$. The ηdisks oriented to an angle in the range $(-\varphi - \eta\pi, -\varphi) \cup (\varphi, \varphi + \eta\pi)$ are partially

outside the network region, as illustrated in Fig. 4.3, and those oriented to any angle in $(\varphi+\eta\pi, 2\pi-\varphi-\eta\pi)$ are fully contained inside the network region. Note that here, all the angles are measured relative to the polar axis eu. In both aforementioned cases, the area of the ηdisk inside the network region is at least $\eta\pi R^2/2$. Hence, we can compute a simple upper bound on $\sigma''(N)$ as follows. Let $a_2 := \pi(L^2-(L-R)^2)/|A| = \sqrt{d}(2-\sqrt{d})$ and $a_1 := \pi(L^2-(L-2R)^2)/|A| = 4\sqrt{d}(1-\sqrt{d})$ be the normalized areas of the network edge region and the network extended edge region[8] respectively. We have

$$\begin{aligned}\sigma''(N) &\leq \sum_{l=1}^{\infty} e^{-a_1 N}\frac{(a_1N)^l}{l!}\, l\, \frac{a_2}{a_1}\sum_{i=0}^{l-1}\binom{l-1}{i}(\frac{d}{2a_1})^i(1-\frac{d}{2a_1})^{l-1-i}U_i(\frac{\eta}{2}) \\ &\leq (2-\sqrt{d})\sqrt{d}Ne^{-\frac{1}{2}dN} + (1-\frac{\sqrt{d}}{2})d^{3/2}N^2e^{-\frac{\eta}{4}dN}\,. \end{aligned} \tag{4.2}$$

A much tighter upper bound on $\sigma''(N)$ can be obtained as follows. First, suppose that there are *no* nodes within the transmission range of node e; this event occurs with probability no greater than

$$\begin{aligned}\sigma''(N) &\leq \sum_{l=1}^{\infty} e^{-a_1 N}\frac{(a_1N)^l}{l!}\, l\, \frac{a_2}{a_1}(1-\frac{d}{2a_2})^{l-1} \\ &= a_2Ne^{-a_1N}\sum_{l=1}^{\infty}\frac{(a_1N(1-\frac{d}{2a_2}))^{l-1}}{(l-1)!} \\ &\leq (2-\sqrt{d})\sqrt{d}Ne^{-\frac{1}{2}dN}\,. \end{aligned} \tag{4.3}$$

Second, suppose that there are $i \geq 1$ nodes in the intersection of node e's transmission range with the network region. If an empty ηdisk exists and it is completely contained within the network region, W.L.O.G., there should be a node on its left edge at some angle $\theta \in (\varphi + 2\eta\pi, 2\pi - \varphi)$. However, for an empty ηdisk that is

[8]The extended edge region is the area of the network that is within $2R$ of the network edge.

partially contained within the network region there should be, again W.L.O.G., a node at an angle $\theta \in (\varphi + \eta\pi, \varphi + 2\eta\pi)$ or $\theta \in (-\varphi, -\varphi + \eta\pi)$ on the left edge of the ηdisk (note that, as discussed earlier, no ηdisks can be oriented towards an angle in $(-\varphi, \varphi)$). Clearly, the existence probability of such empty ηdisks (that is partially contained in the region A) increases as either δ or $|\theta|$ decreases. The area of the intersection between such an ηdisk (that is partially contained in the region A) and the network region A is that of a wedge with angle $|\theta| - \varphi$ (wedge AeB in Fig. 4.3) plus at least a triangle abutting the right edge of the wedge (triangle BeC in Fig. 4.3). In fact for an arbitrary small ϵ, if either $\delta \geq \sin(3\epsilon\pi)$ or $\theta \geq \varphi + \eta\pi + 2\epsilon\pi$, the area of the intersection between the ηdisk and the network region is at least $(\eta/2 + \epsilon)\pi R^2$. Otherwise, it is at least $\eta\pi R^2/2$. Thus, averaging over δ, θ and the number of edge nodes, the probability that some edge nodes have empty ηdisks in some directions, $\sigma''(N)$, is derived to be no more than

$$
\begin{aligned}
&\sum_{l=1}^{\infty} e^{-a_2 N} \frac{(a_2 N)^l}{l!}\, l\, \frac{a_2}{a_1} \sum_{i=1}^{l-1} \binom{l-1}{i} (\frac{d}{2a_1})^i (1 - \frac{d}{2a_1})^{l-1-i} i \\
&\cdot \Bigg\{ \Pr\left(\delta < \sin(3\pi\epsilon)\right) \Pr\left(\exists \text{ empty } \eta\text{disk} \;\middle|\; i, \delta < \sin(3\pi\epsilon)\right) \\
&+ \Pr\left(\delta > \sin(3\pi\epsilon)\right) \Pr\left(\exists \text{ empty } \eta\text{disk} \;\middle|\; i, \delta > \sin(3\pi\epsilon)\right) \Bigg\} \\
&\leq \sum_{l=1}^{\infty} e^{-a_2 N} \frac{(a_2 N)^l}{(l-1)!}\, \frac{a_2}{a_1} \sum_{i=1}^{l-1} \binom{l-1}{i} (\frac{d}{2a_1})^i (1 - \frac{d}{2a_1})^{l-1-i} i \\
&\cdot \Bigg\{ \frac{3\pi\epsilon}{1 - \frac{\sqrt{d}}{2}} \left[4\epsilon (1 - \frac{\eta}{1+8\epsilon})^{i-1} + 2\eta (1 - \frac{\eta + 2\epsilon}{1+8\epsilon})^{i-1} + (1-2\eta)(1 - \frac{2\eta}{1+8\epsilon})^{i-1} \right] \\
&+ \left[2\eta (1 - (\eta/2 + \epsilon))^{i-1} + (1-2\eta)(1-\eta)^{i-1} \right] \Bigg\} \\
&\leq \frac{d^{3/2} N^2}{2 - \sqrt{d}} \Bigg\{ 12\pi\epsilon^2 e^{-\frac{\eta d N}{1+8\epsilon}} + 6\pi\epsilon e^{-\frac{(\eta+2\epsilon) d N}{1+8\epsilon}} + 3\pi\epsilon e^{-\frac{2\eta d N}{1+8\epsilon}} + 2e^{-\frac{(\eta+2\epsilon) d N}{2}} + e^{-\eta d N} \Bigg\},
\end{aligned}
\tag{4.4}
$$

for arbitrary $\epsilon \geq 0$. Choosing $\epsilon = \frac{2 \log dN}{dN}$, together with (4.3), yields a tighter upper bound for the probability that some edge nodes has an empty ηdisk oriented in some direction:

$$\sigma''(N) \leq \frac{400\pi \left(\log dN\right)^2}{\sqrt{d}} e^{-\frac{\eta}{2} dN} + \frac{16(dN)^2}{\sqrt{d}} e^{-\eta dN} + 4\sqrt{d} N e^{-\frac{1}{2} dN}, \tag{4.5}$$

for large enough dN where the last summand is the probability that some edge nodes have no other nodes within their transmission ranges, derived in (4.3).

4.3.3 Calculation of $\sigma(N)$

Finally, summing (4.1) and (4.5), we obtain the bound $\sigma(N)$ on the probability that some nodes in the network have empty ηdisks looking in some directions as:

$$\sigma(N) \leq \frac{400\pi \left(\log dN\right)^2}{\sqrt{d}} e^{-\frac{\eta}{2} dN} + \frac{16(dN)^2}{\sqrt{d}} e^{-\eta dN} + 4\sqrt{d} N e^{-\frac{1}{2} dN} + 4dN^2 e^{-\eta dN}. \tag{4.6}$$

This bound on $\sigma(N)$ is asymptotic to $\frac{400\pi (\log dN)^2}{\sqrt{d}} e^{-\frac{\eta}{2} dN}$, which goes to zero if $\eta dN + \log d \to \infty$ as $N \to \infty$. Hence, setting $d = \frac{c \log N}{N}$ with $c > 1/\eta$, we obtain that every node in the network have at least one relaying node in every direction over which their targeted destinations may lie with probability approaching one as $N \to \infty$, which shows the consistency between our result and the ones derived in [60], [65] and [41] for $\eta = 1$.

Remark 4.3.1. *Setting $d = \frac{c \log N}{N}$ is equivalent to setting $R(\lambda, |A|) = \sqrt{\frac{c}{\pi} \frac{\log \lambda + \log |A|}{\lambda}}$ for $c > 1/\eta$. In particular, for the case of dense networks (i.e., $\lambda \to \infty$ with a finite $|A|$) and for the case of large-scale networks (i.e., $|A| \to \infty$ with a finite*

λ), setting $R(\lambda) = K\sqrt{\log \lambda/\lambda}$ and $R(|A|) = K\sqrt{\log |A|}$ respectively, with a large enough constant K, guarantees the existence of relaying nodes in a "uniform" manner around each node in the network.

4.4 Theorem 4.2.1.*ii–v* Proof: Path Length Statistics and Connectivity

Assume $R(N)$ is chosen such that $\eta d N + \log d \to +\infty$ as $N \to \infty$ and N is large enough such that each node in the network has at least one relaying node in every direction with high probability. We now investigate the question of how long the path generated by the random ηdisk routing scheme is, where we focus on the $\eta = 1/2$ case in this section. To answer this question, we need to characterize the process of path establishment from a given source to its destination by the random $\frac{1}{2}$disk routing scheme.

In the following, we ignore the edge effect for the sake of simplicity in mathematical characterization. In other words, we assume that the $\frac{1}{2}$disks of *all* network nodes looking in any direction is completely contained in the network region. Later, we show (through simulation) in Section 4.5 that the asymptotic results derived in this section still holds even when considering the routing next to the boundary for source-destination pairs that are located near the network boundary.

Now consider an arbitrary source-destination pair that is h-distance apart. We set the destination node at the origin and assume that the routing path starts from the source node at $X_0 = (-h, 0)$, where X_n is the Cartesian coordinate of the n^{th} relay node along the routing path and $r_n := \|X_n\|$ is the Euclidean distance of the n^{th} relay node from the destination.

More specifically, the routing path starts at the source node $X_0 = (-h, 0)$ with its $\frac{1}{2}$RSR D_0 that is a $\frac{1}{2}$disk with radius R centered at X_0 and oriented towards the destination at $(0, 0)$. The next relay X_1 is selected at random from those contained in

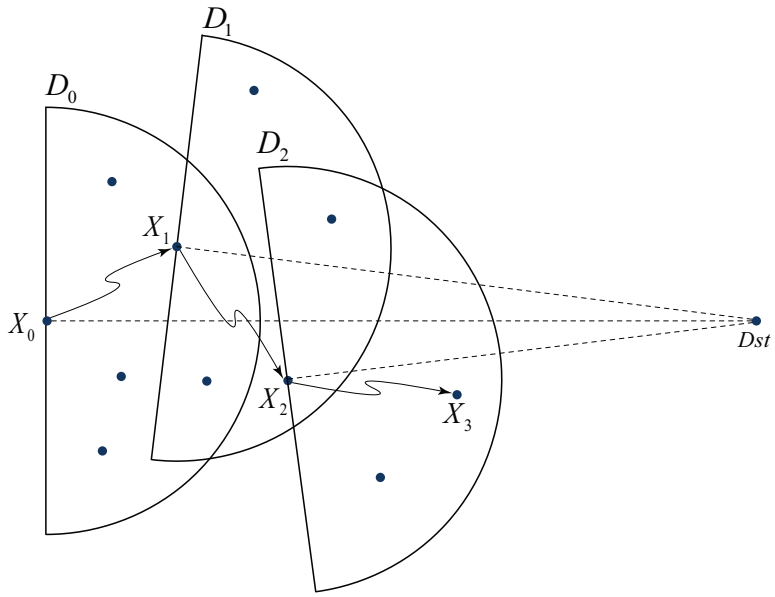

Figure 4.4: Evolution of the random $\frac{1}{2}$disk routing path.

D_0 (the rRSL rule). This induces a new $\frac{1}{2}$RSR D_1, also a $\frac{1}{2}$disk but centered at X_1 and oriented towards the destination. Relay X_2 is selected randomly among the nodes in D_1, and the process continues in the same manner until the destination is within the transmission range. Note that D_n solely depends on X_n. We claim that the routing path has converged (or is established) whenever it enters the transmission/reception range of the final destination, i.e., $r_\nu \leq R$, for some $\nu \in \{1, 2, \cdots\}$. In Fig. 4.4, we illustrate the progress of routing towards the destination.

Define $S_n := h - r_n$ and the routing increment as $Y_n := S_n - S_{n-1} = r_{n-1} - r_n$. Let $\phi(D_n)$ be the number of nodes in D_n. For the sake of definition, we set $Y_i = 0$ for $i > n$ if $\phi(D_{n-1}) = 0$. In the next subsection we investigate how similar $\{S_n\}$ and consequently $\{r_n\}$ are to a Markov process.[9]

[9]For an alternative treatment of the problem refer to [66], Section 4.1.

4.4.1 Theorem 4.2.1.ii Proof: Markov Approximation

In this subsection we investigate how close our Markov approximation model for $\{r_n\}$ is to the actual process of route establishment by the random $\frac{1}{2}$disk routing scheme. Observe that even though the underlying distribution of the network nodes is Poisson and the new relays are chosen uniformly at random within each $\frac{1}{2}$RSR, the increments $Y_1, Y_2, \ldots$ are neither independent nor identically distributed. This is due to the fact that the orientations of all $\frac{1}{2}$RSRs are pointing to a common node (destination) and might overlap, as shown in Fig. 4.4.

More specifically, let k_n be the number of previous relaying nodes whose RSRs intersect with D_n. Assuming $\phi(D_n) > 0$, $S_{n+1} = S_n + Y_{n+1}$ is a Markov process if the conditional distribution of Y_{n+1} given S_i, $n - k_n \leq i \leq n$, only depends on S_n. Equivalently, $r_{n+1} = h - S_{n+1}$ is a Markov process if the conditional distribution of X_{n+1} given X_i, $n - k_n \leq i \leq n$, only depends on X_n. However, the overlap of D_n with D_j, $n - k_n \leq j < n$, correlates the spatial distribution of nodes in D_n (and consequently X_{n+1} and Y_{n+1}), not only with X_n, but also possibly with X_j, $n - k_n \leq j < n$.[10] In fact, given X_i, $n - k_n \leq i \leq n$, the nodes contained in D_n are no longer uniformly distributed over D_n as one would expect for a Poisson distributed network due to the overlap of D_n with D_j, $n - k_n \leq j < n$ (cf. Proposition 4.4.1). As such, the process of path establishment by the random $\frac{1}{2}$disk routing scheme, $\{r_n\}$, is *not* a Markov process. What is less clear, however, is how close $\{r_n\}$ is to a Markov process.

Tracking the dependence of X_{n+1} on all X_j, $n - k_n \leq j \leq n$, is extremely tedious.

[10]This dependence increases as the packet gets closer to the destination due to the fact that the overlapping area between D_n and D_{n-1}, D_{n-2}, ... increases (stochastically) as the packet gets closer to the destination. In [66] and its companion papers [67]–[70], the authors looked at hop length distributions in ad hoc sensor networks with geometric routing schemes, and reported similar dependencies between hop increments $Y_1, Y_2, \ldots$.

As such, in this work we only show how close the routing path progress conditioned on the previous two hops is to a Markov process, i.e., we show in Proposition 4.4.1 that the conditional distribution of X_{n+1} given (X_n, X_{n-1}) is close to that of X_{n+1} given X_n for large N. We show that the error resulted from considering only X_n and neglecting the effect of X_{n-1} on the distribution of X_{n+1} is at most $1/(dN)$, which goes to zero as $N \to \infty$.[11]

Note that, by a method similar to the proof of Proposition 4.4.1, we might show that the incurred errors in modeling $\{r_n\}$ due to higher-order dependencies should be at most $k_n/(dN)$, which is relatively negligible *if* $k_n = o\left(\sqrt{dN}\right)$ for large N. Simulations indicate that k_n should in fact remain in the order of $o\left(\sqrt{dN}\right)$; however, we could not establish an explicit proof for this claim, which will be left for our future study.

We emphasize that, in what follows, conditioning on $\phi(D_n) > 0$ means we only know that there is at least one node in D_n; however, conditioning on $\phi(D_n)$ means we know the exact number of nodes in D_n. Furthermore, Let $C^c := A - C$ denote the complement of C with respect to network region A and $\mathbf{1}_{\cdot}$ represent the indicator function, i.e., $\mathbf{1}_{\cdot} = 1$ if the event in the subscript happens and $\mathbf{1}_{\cdot} = 0$ otherwise.

Now we investigate how similar the distribution of X_{n+1} over D_n is to a uniform distribution given (X_n, X_{n-1}). Note that given only X_n, X_{n+1} is uniformly distributed over D_n. Given X_n, X_{n-1}, $\phi(D_{n-1})$, and $\phi(D_n) > 0$, the number of nodes in $D_{n-1}D_n := D_{n-1} \cap D_n$ is $\phi(D_{n-1}D_n) \sim \text{Binomial}\left(\phi(D_{n-1}) - 1, \frac{|D_{n-1}D_n|}{|D_{n-1}|}\right) + \mathbf{1}_{X_{n-1} \in D_n}$ and is independent of the number of nodes in $D_{n-1}^c D_n$, which is $\phi(D_{n-1}^c D_n) \sim \text{Poisson}(\lambda |D_{n-1}^c D_n|)$. Moreover, conditioned additionally on the two random variables $\phi(D_{n-1}D_n)$ and $\phi(D_{n-1}^c D_n)$, each collection of nodes (located in $D_{n-1}D_n$ and

[11] Note that by Theorem 4.2.1, R is chosen such that $\eta dN + \log d \to +\infty$ as $N \to \infty$, which implies that $dN \to \infty$ and $d \to 0$ for smallest transmission radius [42].

$D_{n-1}^c D_n$) is uniformly distributed over the respective areas. This does not, however, imply that the combined collection of nodes is uniformly distributed over D_n as shown in the following proposition. The combined points are uniformly distributed over D_n *only if* the (conditional) expected proportion of points in $D_{n-1}D_n$ is $\mathrm{E}(\frac{\phi(D_{n-1}D_n)}{\phi(D_n)} \mid \phi(D_n) > 0, \phi(D_{n-1}) > 0, X_n, X_{n-1}) = \frac{|D_{n-1}D_n|}{|D_n|}$.

Proposition 4.4.1. *Assume the locations of current and previous relay nodes* (X_n, X_{n-1}) *are given and* $\phi(D_{n-1}) > 0$. *Given* $\phi(D_n) > 0$, *the distribution of the nodes located inside* D_n *converges to a uniform distribution over* D_n *as* $N \to \infty$. *In particular, the conditional probability of selecting the next node* X_{n+1} *from* $D_{n-1}D_n$, *i.e.,* $\rho(X_{n-1}, X_n) := \mathrm{E}(\ \frac{\phi(D_{n-1}D_n)}{\phi(D_n)} \ \Big|\ \phi(D_n) > 0, \phi(D_{n-1}) > 0, X_n, X_{n-1})$ *satisfies*

$$\left(1 - \frac{2}{dN} - \alpha_1(n) e^{-\alpha_2(n) dN}\right) \frac{|D_{n-1}D_n|}{|D_n|} < \rho(X_{n-1}, X_n) < \frac{|D_{n-1}D_n|}{|D_n|}, \tag{4.7}$$

where $\alpha_1(n) > 2$ *and* $0 < \alpha_2(n) < 1$ *are independent of* N.

Proof. Refer to Appendix F. □

Observe that according to (4.7), given the locations of two previous relay nodes (X_{n-1}, X_n), it is less likely that the next relay X_{n+1} is selected from $D_{n-1}D_n$ as opposed to the case where the nodes were actually uniformly distributed over D_n. Hence, X_{n+1} is *not* uniformly distributed over D_n given (X_{n-1}, X_n). However, we have $\rho(X_{n-1}, X_n) \to \rho(X_n) = |D_n D_{n-1}|/|D_n|$ as $N \to \infty$. Hence, the routing path progress given the second-order history of the routing path converges asymptotically to a Markov process. Nevertheless, the routing increments $Y_1, Y_2, \ldots$ are not identically distributed and as shown in the next subsection, Y_{n+1} is in fact a function of r_n. As such, in the following, we proceed *as if* the process that governs the path

establishment by the random $\frac{1}{2}$disk routing scheme is a *non-homogeneous Markov process* for large N.

4.4.2 Theorem 4.2.1.iii and v Proof: Expected Length of the Random $\frac{1}{2}$Disk Routing Path and Network Connectivity

Using the Markovian approximation model for the routing path evolution $\{r_n\}$, we now derive the asymptotic statistics for the length of the random $\frac{1}{2}$disk routing paths. Let X_n be the n^{th} hop of the routing path and (x'_{n+1}, y'_{n+1}) be the projection of $X_{n+1} - X_n$ onto the *local* Cartesian coordinates with node X_n as the origin and the x-axis pointing from X_n to the destination node as shown in Fig. 4.5. Hence,

$$r_{n+1} = \sqrt{(r_n - x'_{n+1})^2 + y'^2_{n+1}}\,, \tag{4.8}$$

characterizes the distance evolution of the routing path at the n^{th} hop. Based on the Markov approximation model, X_{n+1} is uniformly distributed over D_n; hence $\{(x'_n, y'_n)\}$ is an i.i.d. sequence of random variables with ranges $x'_n \in [0, R]$ and $y'_n \in [-R, R]$ for all n.

Define $\nu_r^{(h)} := \inf\{n : r_n \leq r,\, r_0 = h\}$, $r \geq R$, to be the index of the first relay node (along the routing path) that gets closer than r to the destination when the source and destination nodes are h-distance apart. Hence, $\nu_R^{(h)}$ represents the first time the routing path enters the reception range of the destination and $\nu_R^{(h)} + 1$ quantifies the length of the routing path, where $\nu_R^{(h)} \sim \nu_R^{(h)} + 1$. Recall that in this section we define the length of a routing path as the number of hops traversed over the routing path. It is easy to show that $\nu_r^{(h)}$ is a stopping time [71] and

$$r - R \leq r_{\nu_r^{(h)}} \leq r\,.$$

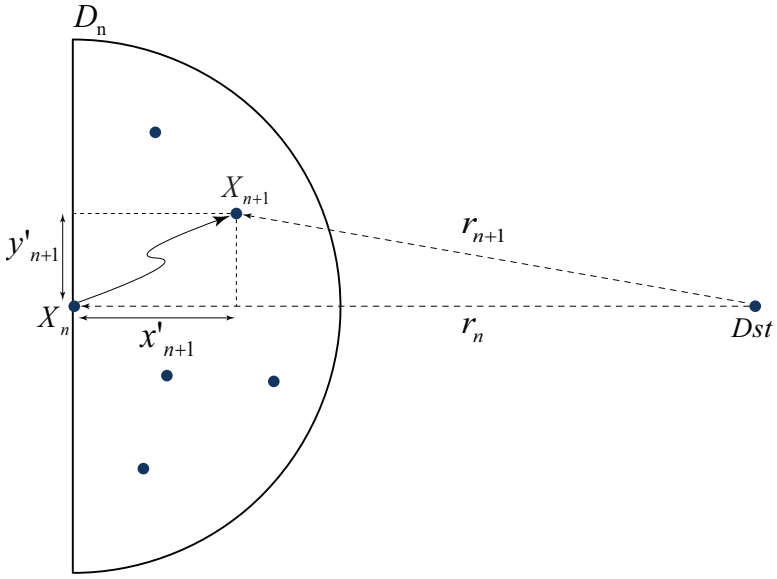

Figure 4.5: Distance between the next relay and the current node projected onto to the local coordinates at the current node.

Furthermore, let $g(r, x', y') := \sqrt{(r - x')^2 + y'^2} - r$. Observe that g is a nonincreasing function over $r \geq R$, for fixed (x', y'), and $g(r_n, x'_{n+1}, y'_{n+1}) = -Y_{n+1}$. Thus, for $n < \nu_r^{(h)}$, we have $r_n > r$ and

$$-x'_{n+1} \leq r_{n+1} - r_n = g(r_n, x'_{n+1}, y'_{n+1}) \leq g(r, x'_{n+1}, y'_{n+1})\,.$$

Hence, for a source-destination pair that is h-distance apart ($r_0 = h$), we have

$$r - R \leq r_{\nu_r^{(h)}} \leq h + \sum_{n=1}^{\nu_r^{(h)}} g(r, x'_n, y'_n)\,, \tag{4.9a}$$

$$h + \sum_{n=1}^{\nu_r^{(h)}} (-x'_n) \leq r_{\nu_r^{(h)}} \leq r\,. \tag{4.9b}$$

Note, as well, that (refer to Appendix G)

$$-\frac{4R}{3\pi} = \mathrm{E}\left(-x'_n\right) \leq \mathrm{E}\left(g(r, x'_n, y'_n)\right) \leq \mathrm{E}\left(g(R, x'_n, y'_n)\right) < -\frac{R}{4} < 0\,. \tag{4.10}$$

Now, applying Wald's equality [53] to (4.9a) and (4.9b) and rearranging, we obtain a bound on the expected value of the stopping time $\nu_r^{(h)}$:

$$\frac{3\pi(h-r)}{4R} \leq \mathrm{E}\left(\nu_r^{(h)} \mid h\right) \leq \frac{h-r+R}{-\mathrm{E}\left(g(r, x'_n, y'_n)\right)} \leq \frac{h}{-\mathrm{E}\left(g(r, x'_n, y'_n)\right)} \leq \frac{4h}{R}\,. \tag{4.11}$$

Substituting r with R we obtain a general bound for the expected length of routing path (minus one) between a source-destination pair that is h distance apart as

$$\frac{3\pi}{4}\left(\frac{h}{R} - 1\right) \leq \mathrm{E}\left(\nu_R^{(h)} \mid h\right) \leq \frac{4h}{R}\,.$$

This implies that the length of the random $\frac{1}{2}$disk routing path is almost surely (a.s.) finite when each network node has at least one node in its $\frac{1}{2}$RSR looking in any direction, which happens with probability no less than $1-\sigma(N)$ as obtained in (4.6). In other words, when $dN/2+\log d \to \infty$ as $N \to \infty$, we obtain that $\Pr(\nu_R^{(h)} < \infty) \to 1$ as $N \to \infty$. This in turn shows that given $dN/2+\log d \to \infty$ as $N \to \infty$, every path starting from any source will reach its destination in finitely many hops a.a.s., which proves that the network is connected employing the random $\frac{1}{2}$disk routing scheme, according to the connectivity definition in Section 4.2.

When the ratio h/R (i.e., the ratio between the source-destination distance and the transmission range) is large, we can obtain a tighter bound on the expected

length of the routing path between a source-destination pair with h separation. For the following, we assume $h \geq 2R$. Since $r_{\nu_r^{(h)}} \leq r$, we must have $\mathrm{E}(\nu_R^{(h)} \mid h) \leq \mathrm{E}(\nu_r^{(h)} \mid h) + \mathrm{E}(\nu_R^{(r)} \mid r)$. Thus, by (4.11) and proper substitutions, we have

$$\frac{3\pi}{4}\left(1-\frac{R}{h}\right) \leq \frac{\mathrm{E}\left(\nu_R^{(h)} \mid h\right)}{h/R} \leq \frac{R}{-\mathrm{E}\left(g(r, x_n', y_n')\right)} + \frac{4r}{h}\,,$$

for all $R \leq r \leq h$. Using

$$-x_n' \leq g(r, x_n', y_n') \leq -x_n' + \frac{(y_n')^2}{2(r-R)}\,, \tag{4.12}$$

and (G.1b) we get $\mathrm{E}(g(r, x_n', y_n')) \leq -\frac{4R}{3\pi} + \frac{R^2}{8(r-R)}$. Choose r such that

$$\frac{8(r-R)}{R} = \frac{3\pi}{4}(\sqrt{\frac{h}{2R}}+1)\,.$$

We may do so using the intermediate value theorem and the fact that $\frac{3\pi}{4}(\sqrt{\frac{h}{2R}}+1) \leq \frac{8(h-R)}{R}$ for $R \leq r \leq h$, $h \geq 2R$; this can be easily observed by the following inequalities:

$$\begin{aligned}
\frac{3\pi}{4}\left(\sqrt{\frac{h}{2R}}+1\right) \leq \frac{3\pi}{2}\sqrt{\frac{h}{2R}} &\leq^{?} \frac{8(h-R)}{R}\,,\\
\frac{3\pi}{16}\sqrt{\frac{h}{2R}}+1 &\leq^{?} \frac{h}{R}\,,\\
\frac{3\pi}{16}\sqrt{\frac{h}{2R}}+1 \leq (\frac{3\pi}{16}+1)\sqrt{\frac{h}{2R}} &\leq^{?} \frac{h}{R}\,,\\
\frac{\frac{3\pi}{16}+1}{\sqrt{2}} &\leq^{\checkmark} \sqrt{\frac{h}{R}}\,.
\end{aligned}$$

Hence, we may determine that

$$\frac{3\pi}{4}\left(1-\frac{R}{h}\right) \leq \frac{\mathrm{E}\left(\nu_R^{(h)} \mid h\right)}{h/R} \leq \frac{3\pi}{4}\frac{1}{1-\left(\sqrt{\frac{h}{2R}}+1\right)^{-1}} + \frac{4R}{h}\left(\frac{3\pi}{32}\left(\sqrt{\frac{h}{2R}}+1\right)+1\right)$$
$$= \frac{3\pi}{4}\left(1+\frac{5}{2}\sqrt{\frac{R}{2h}}+\frac{R}{2h}\right)+\frac{4R}{h}\,. \tag{4.13}$$

This implies

$$\frac{R}{h}\mathrm{E}\left(\nu_R^{(h)} \mid h\right) \to \frac{R}{\mathrm{E}\left(x_n'\right)} = \frac{3\pi}{4}\,, \tag{4.14}$$

or

$$\mathrm{E}\left(\nu_R^{(h)} \mid h\right) \sim \frac{h}{\mathrm{E}\left(x_n'\right)} = \frac{3\pi}{4}\frac{h}{R}\,, \tag{4.15}$$

as $\frac{h}{R} \to \infty$ given that $r_0 = h$.

Remark 4.4.2. *Recall that* $L = \sqrt{|A|/\pi}$ *and observe that* $\Pr\left(h \leq \alpha\right) \leq \frac{\pi\alpha^2}{|A|}$. *Therefore, we can obtain that* $\Pr\left(h \leq \alpha(N)\right) \to 0$ *for* $\alpha(N) = o\left(L\right)$ *as* $N \to \infty$, *which in return implies that* $\Pr\left(h/R \to \infty \mid \eta d N + \log d \to \infty \text{ as } N \to \infty\right) = 1$. *Hence, assuming that the conditions in Theorem 4.2.1.i hold, we have* $h/R \to \infty$ *a.s. as* $N \to \infty$.

Remark 4.4.3. *The asymptotic expected length of the routing path established by the random* $\frac{1}{2}$*disk routing scheme is* $\frac{3\pi}{4} = R/\mathrm{E}\left(x_n'\right) \approx 2.36$ *times greater compared to the length of the routing path generated by the ideal direct-line routing scheme; in the ideal direct-line routing scheme we assume that there are relays located on the line connecting the source and destination with the maximal separation* R.

By averaging over all the possible source-destination pair distances h, we can determine the expected length of a typical random $\frac{1}{2}$disk routing path. Again using

$\Pr(h \leq \alpha R) \leq \frac{\pi}{|A|}(\alpha R)^2$ and (4.13) we have that

$$\begin{aligned}\mathrm{E}(\nu_R) &= \mathrm{E}\left(\mathrm{E}\left(\nu_R^{(h)} \mid h\right)\mathbf{1}_{h\leq\alpha R} + \mathrm{E}\left(\nu_R^{(h)} \mid h\right)\mathbf{1}_{h>\alpha R}\right) \\ &\leq \frac{\pi\alpha^3 R^2}{|A|}\left[\frac{3\pi}{4}\left(1+\frac{5}{\sqrt{8\alpha}}+\frac{1}{2\alpha}\right)+\frac{4}{\alpha}\right] + \frac{3\pi}{4}\frac{\mathrm{E}(h\mathbf{1}_{h>\alpha R})}{R}\left(1+\frac{5}{\sqrt{8\alpha}}+\frac{1}{2\alpha}\right)+4\,,\end{aligned}$$

and

$$\begin{aligned}\mathrm{E}(\nu_R) &= \mathrm{E}\left(\mathrm{E}\left(\nu_R^{(h)} \mid h\right)\right) \\ &\geq \frac{3\pi}{4}\left(\frac{\mathrm{E}(h)}{R}-1\right).\end{aligned}$$

The problem of quantifying $\mathrm{E}(h)$ is well studied in the literature [69], with the following known results for two network regions specifically: If the region is a planar disc with diameter $2L$, we have $\mathrm{E}(h) = 128L/(45\pi) \approx 0.9054L$; and if it is a square with side length L, we have $\mathrm{E}(h) = \left(2+\sqrt{2}+5\log(\sqrt{2}+1)\right)L/15 \approx 0.5214L$. Recalling Remark 4.4.2, we have that $h = O(L) = O\left(d^{-1/2}R\right)$, then for any $\alpha = o\left(d^{-1/2}\right)$ we obtain that $\Pr(h > \alpha R) \to 1$ as $N \to \infty$. Hence, choosing $\alpha = o\left(d^{-1/6}\right)$, we observe that $\mathrm{E}(h\mathbf{1}_{h>\alpha R}) \to \mathrm{E}(h)$ as $N \to \infty$ and

$$\mathrm{E}(\nu_R) \sim \frac{32}{15}\frac{1}{\sqrt{d}}\,, \tag{4.16}$$

as $N \to \infty$.

4.4.3 Theorem 4.2.1.iv Proof: Variance of the Random $\frac{1}{2}$Disk Routing Path Length

So far we have characterized the expected length of the routing paths generated by the random $\frac{1}{2}$disk routing scheme. However, the expected value alone is not descriptive enough regarding the *individual realizations* of the routing path length.

We need to determine how much the individual realization deviates from the expected value. Therefore, in this section, we consider the variance of the path lengths generated by the random $\frac{1}{2}$disk routing scheme. We first show that the variance is finite almost surely and then we show that asymptotically it grows linearly with the expected path length:

$$\frac{\mathrm{Var}\left(\nu_R^{(h)} \mid h\right)}{\mathrm{E}\left(\nu_R^{(h)} \mid h\right)} \to \frac{\mathrm{Var}\left(x'_n\right)}{\left(\mathrm{E}\left(x'_n\right)\right)^2} = \frac{9\pi^2}{64} - 1, \tag{4.17}$$

as $N \to \infty$. We will frequently use the following well known inequalities

$$\left|\sqrt{\mathrm{E}\left(X^2\right)} - \sqrt{\mathrm{E}\left(Y^2\right)}\right| \leq \sqrt{\mathrm{E}\left((X-Y)^2\right)},$$

and

$$\left|\sqrt{\mathrm{Var}\left(X\right)} - \sqrt{\mathrm{Var}\left(Y\right)}\right| \leq \sqrt{\mathrm{Var}\left(X-Y\right)}.$$

Consider the i.i.d. sequence $\{(x'_n, y'_n)\}$ as defined in Section 4.4.2, and define the generalized stopping time $\nu_a^{(b)}$ to be $\nu_a^{(b)} := \inf\{n : r_n \leq a,\, r_0 = b\}$ for $R \leq a < b \leq h$. Observe that $\{\nu_a^{(b)} \geq N\}$ and $\{x'_n\}_{n<N}$ are independent, and $\mathrm{E}(\nu_a^{(b)}) < \infty$ and $\mathrm{E}\left((x'_n)^2\right) < \infty$ as shown in Section 4.4.2 and Appendix G.

Note first that, by definition,

$$\mathrm{E}\left(\sum_{i=1}^{\nu_R^{(h)} \wedge n} \left(-g(r_{i-1}, x'_i, y'_i)\right)\right) = \mathrm{E}\left(r_0 - r_{\nu_R^{(h)} \wedge n}\right) \leq h,$$

for any n, where $\nu_R^{(h)} \wedge n := \min\{\nu_R^{(h)}, n\}$. Define $U_n := \sum_{i=1}^{n}(-g(R, x'_i, y'_i))$. From Wald's equation, Eq. (4.10), and the fact that

$g(r, x', y')$ is a nonincreasing function over $r \geq R$, we have

$$\begin{aligned}\frac{R}{4}\mathrm{E}\left(\nu_R^{(h)} \wedge n \;\middle|\; h\right) &\leq \mathrm{E}\left(-g(R, x_i', y_i')\right)\mathrm{E}\left(\nu_R^{(h)} \wedge n \;\middle|\; h\right) \\ &= \mathrm{E}\left(U_{\nu_R^{(h)} \wedge n} \;\middle|\; h\right) \\ &\leq \mathrm{E}\left(\sum_{i=1}^{\nu_R^{(h)} \wedge n} \left(-g(r_{i-1}, x_i', y_i')\right) \;\middle|\; h\right) \leq h\,,\end{aligned}$$

for all n. As shown in the previous section, it follows that

$$\mathrm{E}(\nu_R^{(h)} \mid h) = \lim_{n\to\infty} \mathrm{E}(\nu_R^{(h)} \wedge n \mid h) \leq \frac{4h}{R} < \infty\,.$$

Similarly,

$$\begin{aligned}&\left(\mathrm{E}\left(-g(R, x_i', y_i')\right)\right)^2 \mathrm{Var}\left(\nu_R^{(h)} \wedge n \;\middle|\; h\right) \leq 2\Bigg[\mathrm{Var}\left(U_{\nu_R^{(h)} \wedge n} \;\middle|\; h\right) \\ &+ \mathrm{Var}\left((\nu_R^{(h)} \wedge n)\mathrm{E}\left(-g(R, x_i', y_i')\right) - U_{\nu_R^{(h)} \wedge n} \;\middle|\; h\right)\Bigg] \\ &\leq 2\left[\mathrm{Var}\left(U_{\nu_R^{(h)} \wedge n} \;\middle|\; h\right) + \mathrm{E}\left(\nu_R^{(h)} \wedge n \;\middle|\; h\right)\mathrm{Var}\left(-g(R, x_i', y_i')\right)\right] \\ &\leq 2\left[h^2 + \frac{4h}{R}\frac{R^2}{4}\right]\,,\end{aligned}$$

for all n, where the second inequality is due to Wald's identity ([53, p. 398]). Thus,

$$\begin{aligned}\mathrm{Var}\left(\nu_R^{(h)} \;\middle|\; h\right) &= \lim_{n\to\infty} \mathrm{Var}\left(\nu_R^{(h)} \wedge n \;\middle|\; h\right) \\ &\leq \frac{32h(h+R)}{R^2} < \infty\,. \qquad (4.18)\end{aligned}$$

This proves that the variance of path length generated by the random $\frac{1}{2}$disk routing scheme is finite almost surely. Next we will find some asymptotically tight bounds on the variance of the routing path lengths.

Let $S_\nu := \sum_{n=1}^{\nu} x'_n$ for a stopping time ν such that $\{\nu \geq N\}$ and $\{x'_n\}_{n<N}$ are independent and $\mathrm{E}(\nu) < \infty$. Then by Wald's identity ([53, p. 398]) we have $\mathrm{E}(S_\nu) = \mathrm{E}(x'_n)\,\mathrm{E}(\nu)$ and

$$\mathrm{Var}(\nu \mathrm{E}(x'_n) - S_\nu) = \mathrm{E}\left((S_\nu - \nu \mathrm{E}(x'_n))^2\right) = \mathrm{E}(\nu)\,\mathrm{Var}(x'_n)\,.$$

As such, we have

$$\begin{aligned}\left|\sqrt{\mathrm{Var}(\nu)}\mathrm{E}(x'_n) - \sqrt{\mathrm{E}(\nu)\,\mathrm{Var}(x'_n)}\right| &= \left|\sqrt{\mathrm{Var}(\nu \mathrm{E}(x'_n))} - \sqrt{\mathrm{Var}(\nu \mathrm{E}(x'_n) - S_\nu)}\right| \\ &\leq \sqrt{\mathrm{Var}(S_\nu)}.\end{aligned}$$

In particular, for $\nu = \nu_R^{(h)}$, we have

$$\left|\sqrt{\frac{\mathrm{Var}\left(\nu_R^{(h)} \mid h\right)}{\mathrm{E}\left(\nu_R^{(h)} \mid h\right)}} - \sqrt{\frac{\mathrm{Var}(x'_n)}{(\mathrm{E}(x'_n))^2}}\right| \leq \sqrt{\frac{\mathrm{Var}\left(S_{\nu_R^{(h)}} \mid h\right)}{\mathrm{E}\left(\nu_R^{(h)} \mid h\right)(\mathrm{E}(x'_n))^2}}\,. \tag{4.19}$$

Hence, in order to prove the limit in (4.17), we need to show that

$$\frac{\mathrm{Var}\left(S_{\nu_R^{(h)}} \mid h\right)}{\mathrm{E}\left(\nu_R^{(h)} \mid h\right)(\mathrm{E}(x'_n))^2} \sim \frac{\mathrm{Var}\left(S_{\nu_R^{(h)}} \mid h\right)}{\frac{3\pi}{16}Rh} \to 0\,,$$

as $N \to \infty$. Suppose $R \leq a < b \leq h$ and note that

$$-g(r_{n-1}, x'_n, y'_n) \leq x'_n \leq -g(r_{n-1}, x'_n, y'_n) + \frac{R^2}{2r_{n-1}}\,;$$

then together with (4.9a), we obtain

$$\begin{aligned} b-a &\leq \sum_{n=1+\nu_R^{(a)}}^{\nu_R^{(b)}} \left(-g(r_{n-1}, x'_n, y'_n)\right) \\ &\leq \sum_{n=1+\nu_R^{(a)}}^{\nu_R^{(b)}} x'_n \\ &= S_{\nu_R^{(b)}} - S_{\nu_R^{(a)}} \\ &\leq \sum_{n=1+\nu_R^{(a)}}^{\nu_R^{(b)}} \left(-g(r_{n-1}, x'_n, y'_n)\right) + \sum_{n=1+\nu_R^{(a)}}^{\nu_R^{(b)}} \frac{R^2}{2r_{n-1}} \\ &\leq b-a+R+\frac{R^2}{2a}\nu_R^{(b)}\,, \end{aligned}$$

where the last inequality is due to the fact that $r_n \geq a$ for $\nu_R^{(a)} \leq n \leq \nu_R^{(b)}$. Therefore, we obtain

$$\begin{aligned} \sqrt{\mathrm{Var}\left(S_{\nu_R^{(b)}} - S_{\nu_R^{(a)}} \;\middle|\; a, b\right)} &= \sqrt{\mathrm{E}\left(\left[S_{\nu_R^{(b)}} - S_{\nu_R^{(a)}} - \mathrm{E}\left(S_{\nu_R^{(b)}} - S_{\nu_R^{(a)}}\right)\right]^2 \;\middle|\; a, b\right)} \\ &\leq \sqrt{\mathrm{E}\left(\left[S_{\nu_R^{(b)}} - S_{\nu_R^{(a)}} - b + a\right]^2 \;\middle|\; a, b\right)} \\ &\leq \sqrt{\mathrm{E}\left(\left[R + \frac{R^2}{2a}\nu_R^{(b)}\right]^2 \;\middle|\; a, b\right)} \\ &\leq R + \frac{R^2}{2a}\mathrm{E}\left(\nu_R^{(b)} \mid b\right) + \frac{R^2}{2a}\sqrt{\mathrm{Var}\left(\nu_R^{(b)} \mid b\right)} \\ &\leq R + \frac{2Rb}{a} + \frac{R}{2a}\sqrt{32b(b+R)} \\ &\leq 6R + \frac{5Rb}{a}\,, \end{aligned}$$

using (4.18) and the fact that $\mathrm{E}(\nu_R^{(b)} \mid b) \leq \frac{4b}{R}$ and $\mathrm{Var}(\nu_R^{(b)} \mid b) \leq \frac{32b(b+R)}{R^2}$. Finally, we let $a_i = R\left(\frac{h}{R}\right)^{i/k}$, for $k = \lceil \log \frac{h}{R} \rceil$ and $i = 0, 1, 2, \ldots, k$, where $\lceil \log \frac{h}{R} \rceil$ is the smallest

integer larger than $\log \frac{h}{R}$. Then we have

$$\begin{aligned}
\sqrt{\mathrm{Var}\left(S_{\nu_R^{(h)}} \mid h\right)} &\le \sum_{i=1}^{k} \sqrt{\mathrm{Var}\left(S_{\nu_R^{(a_i)}} - S_{\nu_R^{(a_{i-1})}} \;\middle|\; h\right)} \\
&\le 6kR + 5R \sum_{i=1}^{k} \frac{a_i}{a_{i-1}} \\
&= 6kR + 5kR \left(\frac{h}{R}\right)^{1/k} \\
&\le (6+5e)(1+\log \frac{h}{R})R. \qquad (4.20)
\end{aligned}$$

From this, it follows that

$$\sqrt{\frac{\mathrm{Var}\left(S_{\nu_R^{(h)}} \mid h\right)}{Rh}} \le (6+5e)(1+\log \frac{h}{R})\sqrt{\frac{R}{h}} \to 0$$

as $N \to \infty$, which concludes the proof for the limit in Eq. (4.17).

Remark 4.4.4. *It is worth noting that the path-stretch statistics can be easily derived from the hop-count statistics: Let $\mathcal{L}_{\nu_R^{(h)}}$ denote the path-stretch of a routing path with length $\nu_R^{(h)}$ connecting a source-destination pair that is h-distance apart, i.e.,*

$$\mathcal{L}_{\nu_R^{(h)}} := \|X_1 - X_0\| + \|X_2 - X_1\| + \cdots + \|X_{\nu_R^{(h)}+1} - X_{\nu_R^{(h)}}\|.$$

Then, it is easy to show that

$$\begin{aligned}
\mathrm{E}\left(\mathcal{L}_{\nu_R^{(h)}} \mid h\right) &\sim \frac{\pi}{2} h\,, \\
\mathrm{Var}\left(\mathcal{L}_{\nu_R^{(h)}} \mid h\right) &\sim \frac{\pi}{12} Rh\,,
\end{aligned}$$

as $N \to \infty$. *Therefore, in the case of a dense network,* $\mathcal{L}_{\nu_R^{(h)}} \to \frac{\pi}{2}h$ *a.a.s. since* $Var(\mathcal{L}_{\nu_R^{(h)}}) \to 0$ *as* $N \to \infty$.

4.5 Simulation Results

In this section we compare our analytical results with some empirical results derived through simulation. In Fig. 4.6, we depict some realizations for the routing paths generated by the random $\frac{1}{2}$disk routing scheme for an arbitrary source located at $(-1/4, -1/4)$ and its destination at $(1/4, 1/4)$ with the following network specifications: $|A| = 1$, $\lambda = 10^6$, and $R = \sqrt{\frac{2\log\lambda}{\lambda}} \approx 5.2 \times 10^{-3}$. As illustrated in this figure, the path realizations do not closely follow the direct line connecting the source-destination nodes. The lengths of the routing paths are 328, 314, 343 for the realizations depicted in Fig. 4.6 (a), (b), and (c) respectively. Fig. 4.6 (d) depicts an ensemble of thirty realizations of the random $\frac{1}{2}$disk routing scheme. Based on (4.13) we obtain the lower and upper bounds of 314, 370 for the expected path length with the asymptotic value of 317. (Note that the bounds derived in (4.13) are for the expected path length; therefore, individual realizations for the path length might violate these bounds.)

The following empirical path length statistics are obtained by generating 100 realizations of the network via placing $N \sim \text{Poisson}(\lambda)$ nodes uniformly over a circular disk with unit area. For each network realization we constructed 100 realizations for the random $\frac{1}{2}$disk routing path: starting from a fixed source node, we find the subsequent relaying nodes according to the rRSL scheme until (possibly) reaching the fixed destination node. Source and destination are set $h = \sqrt{2}/2$ distance apart and the transmission ranges are chosen as $R = \sqrt{\frac{2\log\lambda}{\lambda}}$. In Fig. 4.7, we compare the (normalized) empirical mean, $\frac{R}{h}\text{E}(\nu_R^{(h)})$, of the path lengths generated by the random $\frac{1}{2}$disk routing scheme with the analytical bounds derived in Eq. (4.13) for different

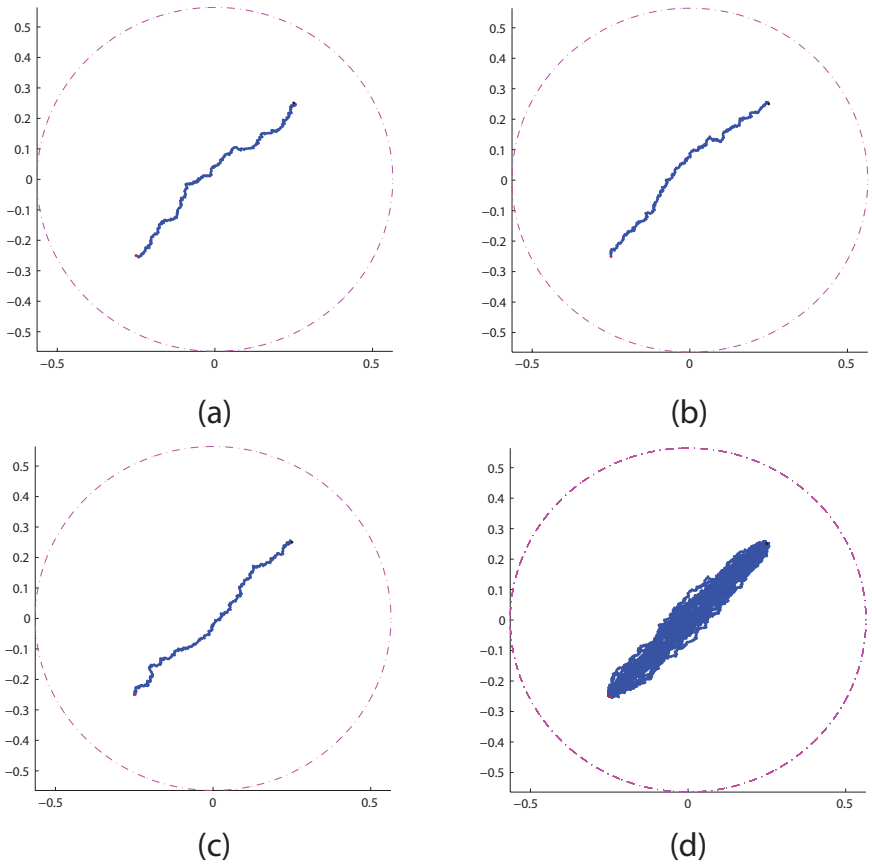

Figure 4.6: Random $\frac{1}{2}$disk routing realizations for $\lambda = 10^6$, $|A| = 1$, and $R = \sqrt{\frac{2\log\lambda}{\lambda}}$, when the source is located at $(-1/4, -1/4)$ and its destination is located at $(1/4, 1/4)$. The lengths of the routing paths depicted in (a), (b), and (c) are 328, 314, 343, respectively, while (d) depicts an ensemble of thirty realizations of the random $\frac{1}{2}$disk routing scheme. The dashed circle demonstrates the network boundary.

values of network node density. As shown in this figure, the normalized empirical mean converges to $3\pi/4 \approx 2.3562$, and is always bounded by the expressions derived in Eq. (4.13).

In Fig. 4.8, we compare the empirical variance-to-mean ratio of the random $\frac{1}{2}$disk routing scheme, $\sqrt{\mathrm{Var}(\nu_R^{(h)})/\mathrm{E}(\nu_R^{(h)})}$, with the analytical bounds derived in Eq. (4.20) for different values of network node density. As shown in this figure, the normalized empirical standard deviation converges to $\sqrt{9\pi^2/64 - 1} \approx 0.6228$,

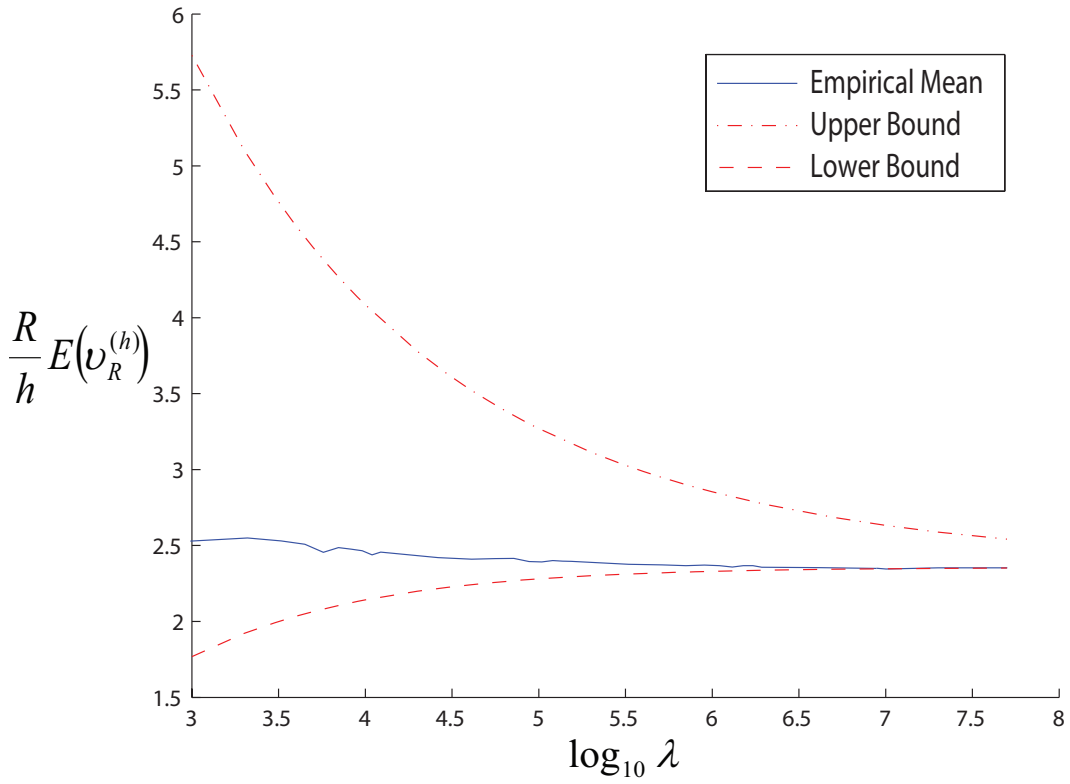

Figure 4.7: Numerical comparison between analytical bounds derived in Eq. (4.13) and the (normalized) empirical mean of the path length generated by the random $\frac{1}{2}$disk routing scheme when $h = \sqrt{2}/2$, $|A| = 1$, and $R = \sqrt{\frac{2\log\lambda}{\lambda}}$.

and is always bounded by the expressions derived in Eq. (4.20). Furthermore, it can be seen that although the bounds in (4.20) are quite loose for small values of λ, the asymptotic standard deviation derived in (4.17) is very close to the empirical standard deviation even for small values of λ.

In Fig. 4.9, we demonstrate the deviation of the path length realizations from its asymptotic expected value for different values of network node density. As shown in this figure, the deviation of the path length realizations increases as the network density and consequently the expected length of the routing path increases. However, all realizations stay relatively close to the value predicted by Eq. (4.15).

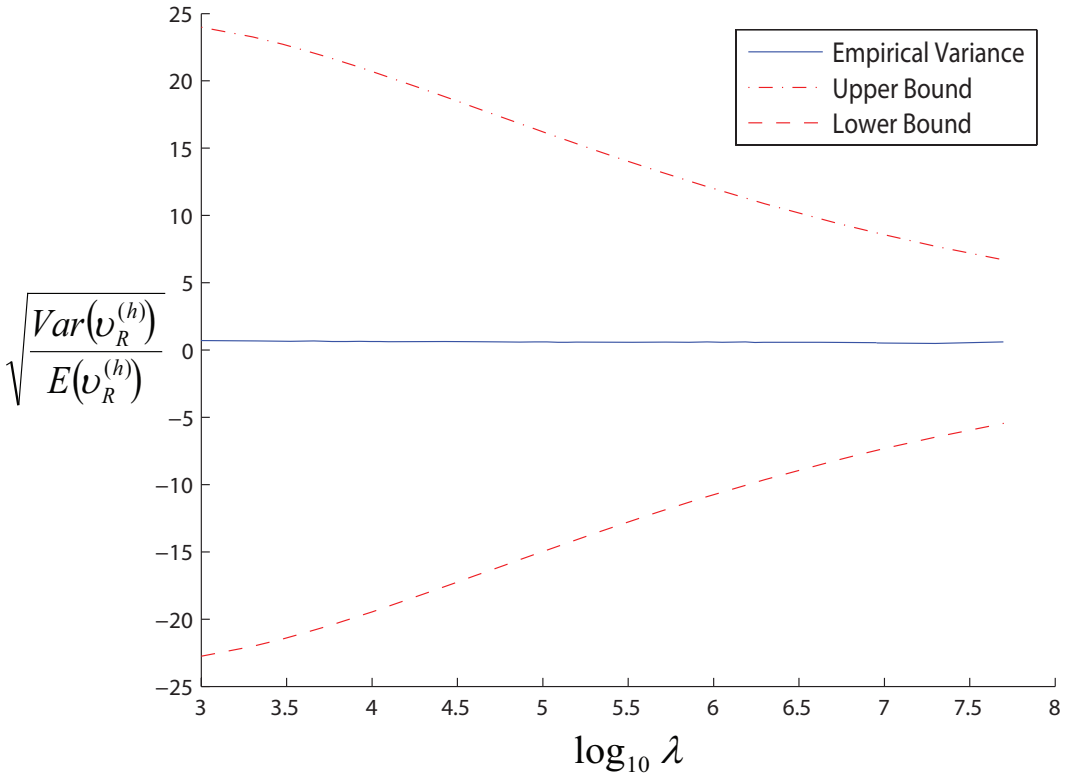

Figure 4.8: Numerical comparison between analytical bounds derived in Eq. (4.19) and the (normalized) empirical standard deviation of the path length generated by the random $\frac{1}{2}$disk routing scheme, when $h = \sqrt{2}/2$, $|A| = 1$, and $R = \sqrt{\frac{2\log\lambda}{\lambda}}$.

As mentioned earlier, we ignored the edge effect when computing the asymptotic path length statistics of the random $\frac{1}{2}$disk routing scheme. In Figs. 4.10 and 4.11, we consider two source-destination pairs that are close to the network edge with different distances and investigate whether routing "next to the boundary" has a considerable impact on the length of the routing paths. We consider a source node S at $(-0.379, -0.379)$ and two destination nodes Dst_1 at $(0.3267, -0.4234)$ and Dst_2 at $(-0.315, -0.4336)$ such that $h_1 = \|S - Dst_1\| = \sqrt{2}/2$ and $h_2 = \|S - Dst_2\| = \sqrt{2}/33$. Note that $\|S\| = 0.95L$, $\|Dst_1\| = 0.948L$, and $\|Dst_2\| = 0.95L$. Fig. 4.10 depicts the empirical mean and Fig. 4.11 depicts the empirical variance-to-mean ratio of

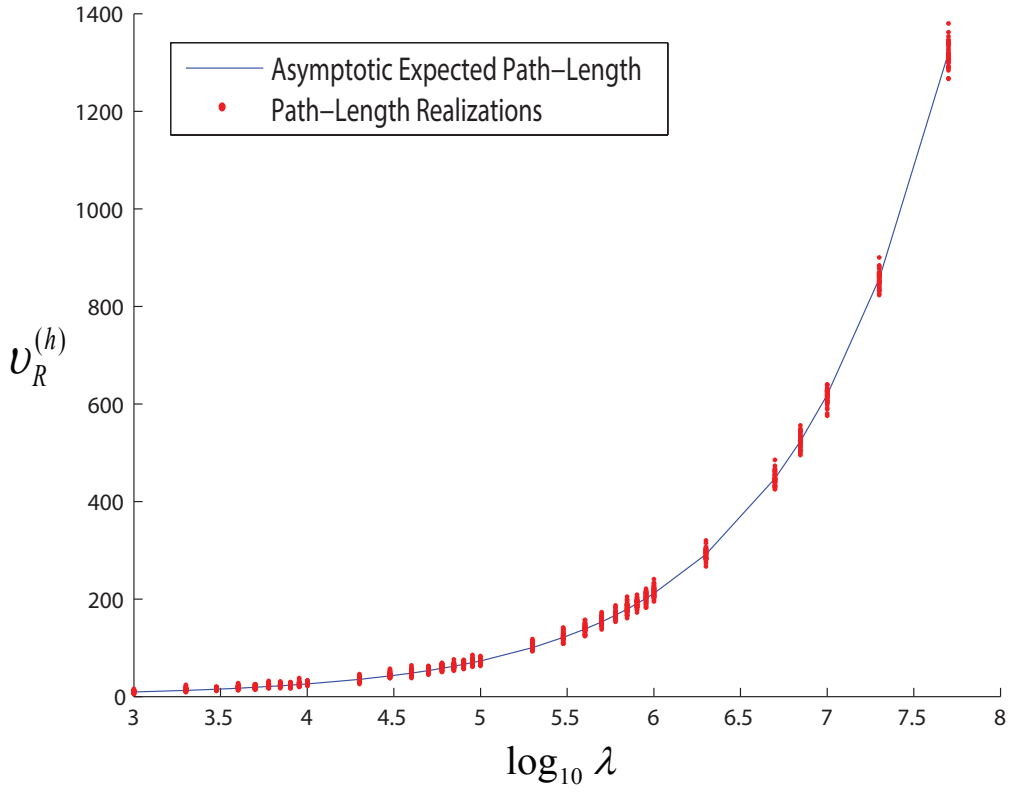

Figure 4.9: Random $\frac{1}{2}$disk routing realizations for $\lambda = 10^6$, $|A| = 1$, and $R = \sqrt{\frac{2 \log \lambda}{\lambda}}$, when the source is located at $(-1/4, -1/4)$ and its destination is located at $(1/4, 1/4)$.

paths generated by the random $\frac{1}{2}$disk routing scheme for source-destination pairs a) $S - Dst_1$ and b) $S - Dst_2$. Comparing these figures with Figs. 4.7 and 4.8, we observe that given a fixed h, routing close to the network edge does not affect the *asymptotic* path statistics. Intuitively, as shown in Remark 4.4.2, the distances between source-destination pairs will be of order $h = \Theta(L)$ with high probability where $h/R \to 0$ as $N \to \infty$. Therefore, for large enough N, it is very unlikely that a considerable portion of the path connecting a source to its destination traverses close to the network edge. As such, the effect of the routing close to the boundary on path statistics is relatively negligible for large network sizes. However, for small

network sizes (when h and R are comparable), the empirical mean of the path length is smaller than the value predicted in (4.14).

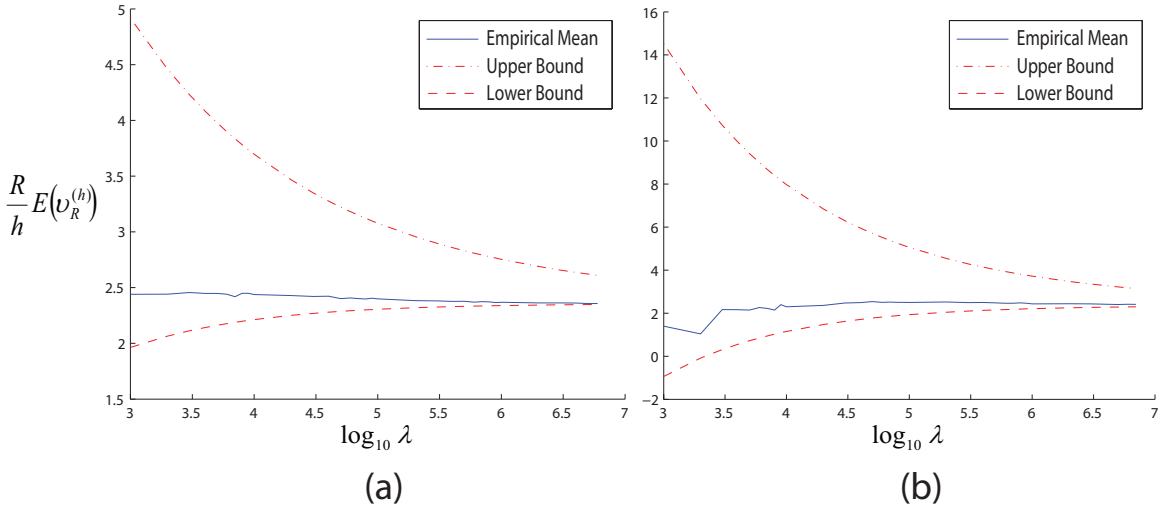

Figure 4.10: Numerical comparison between analytical bounds derived in Eq. (4.13) and the (normalized) empirical mean of the path length generated by the random $\frac{1}{2}$disk routing scheme for source-destination pairs that are close to the network boundary when a) $h = \sqrt{2}/2$ and b) $h = \sqrt{2}/33$. In both cases $|A| = 1$, $R = \sqrt{\frac{2\log\lambda}{\lambda}}$, and $\|S\| = \|Dst\| \simeq 0.95L$.

4.6 Generalization

In the previous sections we derived sufficient conditions for the network to be connected deploying the random $\frac{1}{2}$disk routing scheme and quantified the mean and variance asymptotes of the routing path generated the random $\frac{1}{2}$disk routing scheme. In this section we present some guidelines that generalize the aforementioned results for some other variants of the geometric routing schemes such as MFR, DIR, NFP, and the random ηdisk routing scheme, where the latter one is the generalized version of the random $\frac{1}{2}$disk routing scheme with an ηdisk as its RSR.

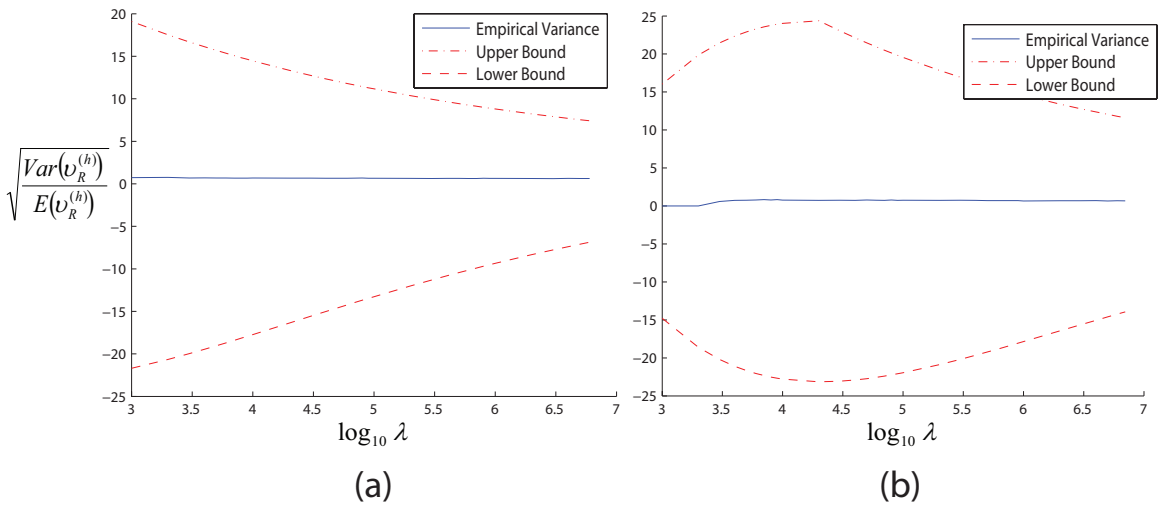

Figure 4.11: Numerical comparison between analytical bounds derived in Eq. (4.19) and the (normalized) empirical standard deviation of the path length generated by the random $\frac{1}{2}$disk routing scheme for source-destination pairs that are close to the network boundary when a) $h = \sqrt{2}/2$ and b) $h = \sqrt{2}/33$. In both cases $|A| = 1$, $R = \sqrt{\frac{2\log\lambda}{\lambda}}$, and $\|S\| = \|Dst\| \simeq 0.95L$.

Observe that the results of Section 4.3 were derived for the general ηdisks relay selection region which encompasses most of the geometric routing schemes such as MFR, DIR, NFP, and the random ηdisk routing scheme. Let Δ be the set of all nodes (in the RSR of a specific transmitting node) that can be selected as the next relay by the relay selection rule (RSL) of the geometric routing scheme. For example, in the cases of MFR, DIR, NFP, and the random ηdisk routing scheme we have: $\Delta_{\text{MFR}} := \{(x'_n, y'_n) \in \frac{1}{2}\text{RSR} : x'_n \geq x, \text{ for all } (x,y) \in \frac{1}{2}\text{RSR}\}$, $\Delta_{\text{DIR}} := \{(x'_n, y'_n) \in \frac{1}{2}\text{RSR} : |\tan^{-1}(y'_n/x'_n)| \leq |\tan^{-1}(y/x)|, \text{ for all } (x,y) \in \frac{1}{2}\text{RSR}\}$, $\Delta_{\text{NFP}} := \{(x'_n, y'_n) \in \frac{1}{2}\text{RSR} : \sqrt{(x'_n)^2 + (y'_n)^2} \leq \sqrt{(x)^2 + (y)^2}, \text{ for all } (x,y) \in \frac{1}{2}\text{RSR}\}$, and $\Delta_\eta = \{(x'_n, y'_n) \in \eta\text{RSR}\}$, respectively. Since the nodes in Δ (if more than one) are indistinguishable by the RSL, the transmitting node selects one of the nodes in Δ randomly as the next relay. Next, we present the generalized results for the network

connectivity and the mean and variance asymptotes of routing paths generated by the general geometric routing schemes.

Corollary 4.6.1. *Let Δ be the set of all nodes that can be selected by the relay selection rule as the next relay. Then the network is connected employing the geometric routing scheme a.a.s. if* $\mathrm{E}\left(g(R,x',y')\mathbf{1}_{\Delta}\right) < 0$.

Proof. The proof is immediate due to (4.11). □

Corollary 4.6.2. *If* $\mathrm{E}\left(g(R,x',y')\mathbf{1}_{\Delta}\right) < 0$ *and* $\mathrm{E}\left((y')^2\mathbf{1}_{\Delta}\right) \leq R\,\mathrm{E}\left(x'\mathbf{1}_{\Delta}\right)$*, the expected length of the routing path generated by the general geometric routing scheme connecting a source-destination pair that is h-distance apart scales as* $\mathrm{E}\left(\nu \mid h\right) \sim h/\mathrm{E}\left(x'\mathbf{1}_{\Delta}\right)$ *as* $N \to \infty$.

Proof. The proof follows directly from (4.12) and noting that if $\mathrm{E}\left((y')^2\mathbf{1}_{\Delta}\right) \leq R\,\mathrm{E}\left(x'\mathbf{1}_{\Delta}\right)$, using the intermediate value theorem, we can find r such that $\frac{2R(r-h)}{\mathrm{E}((y')^2\mathbf{1}_{\Delta})} = \frac{R}{\mathrm{E}(x'\mathbf{1}_{\Delta})}\left(\sqrt{\frac{h}{2R}}+1\right)$, which yields the bound in Eq. (4.13) and hence the desired result. □

Corollary 4.6.3. *If* $\mathrm{E}\left(g(R,x',y')\mathbf{1}_{\Delta}\right) < 0$*, the variance of the path length generated by the general geometric routing scheme, normalized by its mean, scales as* $\mathrm{Var}\left(\nu\right)/\mathrm{E}\left(\nu\right) \sim \mathrm{Var}\left(x'\mathbf{1}_{\Delta}\right)/\left(\mathrm{E}\left(x'\mathbf{1}_{\Delta}\right)\right)^2$ *as* $N \to \infty$.

Proof. The proof follows the same steps as in Section 4.4.3. □

4.7 Conclusion

In this section, we presented a simple methodology employing statistical analysis and stochastic geometry to study geometric routing schemes in wireless ad-hoc networks, and in particular, analyzed the network layer performance of one such scheme named the random $\frac{1}{2}$disk routing scheme. We defined a notion of network connectivity considering the special local properties of geometric routing schemes and

determined some sufficient conditions that guarantee network connectivity when each node finds its next relay in the so-defined $\frac{1}{2}$disk. More specifically, if all nodes transmit at a power that covers a normalized area d and the expected number of nodes in the network is N, the network is connected a.a.s. if $\eta dN + \log d \to \infty$ when $N \to \infty$. Furthermore, we proved that the routing path progress conditioned on the previous two hops can be approximated with a Markov process. Then using this Markovian approximation, we derived exact asymptotic expressions for the mean and variance of the path length generated by the random $\frac{1}{2}$disk routing scheme. Furthermore, we provided guidelines to extend these results to other variants of geometric routing schemes such as MFR, DIR, and NFP.

5. CONCLUSION

5.1 Summary of Contributions

In this dissertation, we adopted the opportunistic spectrum access strategy and studied the throughput performance of a specific type of cognitive radio network, namely the wireless ad-hoc CRNs, which possesses the following specifications:

- Decentralized, distributed, and Self governed (i.e., Ad-Hoc); this specific network configuration is chosen due to the foreseeable autonomous property of the secondary users. It is desirable for the secondary networks to be decentralized due to cost considerations; It is desirable for the secondary networks to be distributed to retain robustness, i.e., the capability of operation in a way that does not depend on the presence of a specific type of nodes and nodes be able to come and go as they please.

- Transparent to the primary network; so that the primary users allow the secondary users to use their resources.

- Technologically feasible; based on today's technology, it is extremely challenging and costly to produce wide-band spectrum sensors. So the system that we consider has a limited sensing capability.

In this dissertation, We first investigate the effect of spectrum sensing errors and the benefit of wide-band spectrum sensing and access capability. To this end, we considered an overlaid network scenario, where N licensed frequency bands are made available to a secondary network, contingent upon adherence to certain inter-network interference constraints. To limit the interference to the primary network, secondary nodes are equipped with spectrum sensors and are capable of sensing

and accessing a limited number of channels simultaneously. We considered both the error-free and the erroneous spectrum detection scenarios and established the jointly optimal random sensing and access scheme, which maximizes the secondary network expected sum throughput while abiding by the primary interference constraint. We have shown that in the case of error-free spectrum detection, when the number of secondary users times the number of channels that they can access is larger than the number of primary frequency bands, the optimal sensing and access scheme is independent of the channel bandwidths and usage statistics; otherwise they follow water-filling-like strategies. In the case of erroneous spectrum detection, we have shown similar characteristics for the optimal sensing and access scheme under slightly different conditions. Moreover, we derived the optimal number of secondary users that can co-exist with the primary network, and demonstrated a binary behavior for the optimal access scheme at each channel depending on whether the opportunity-detection probability or the mis-detection probability is larger in that channel.

The design and deployment of cognitive radio networks mandates an understanding of the following fundamental questions: What is an appropriate metric to evaluate the performance of cognitive radio networks? What type of performance assurances can secondary users provide the primary users? and How secondary users can deliver these assurances?

In Section 3, we studied how the performance of cognitive radio networks scale for very large network sizes and investigate the question of what is an appropriate performance metric for cognitive radio networks. We show that the conventional throughput scaling which has been broadly used in the literature is not sufficient and to be descriptive enough the constant behind the scaling should also be considered. In particular, we showed that regardless of the spectrum sensing settings, both networks can achieve their stand-alone throughput scalings. Furthermore, with

the newly defined performance metric, the asymptotic multiplexing gain (AMG), we quantified how the asymptotic network performances is affected by the mutual interference between the two networks. In addition, we derived the spatial throughput of an ad-hoc overlaid cognitive network with exact expressions for the pre-constant multipliers. We showed that employing the proper spectrum sensing and medium access probability settings, secondary users can achieve a reasonable throughout performance while satisfying the primary AMG requirement when the secondary network is denser; However, when the secondary network is sparser, the spectrum sensing cannot improve the throughput performance of the secondary users. As such, secondary users should satisfy the primary AMG requirement by appropriate selection of medium access probability, which results in a significant secondary throughput degradation.

Finally, in the last section we introduced a methodology to systematically derive path statistics for geometric routing schemes in wireless ad hoc networks. These results are the key enablers for rigorous throughput performance analysis of large scale wireless networks. We defined a notion of network connectivity considering the special local properties of geometric routing schemes and determined some sufficient conditions that guarantee network connectivity when each node finds its next relay in the so-defined $\frac{1}{2}$disk. More specifically, if all nodes transmit at a power that covers a normalized area d and the expected number of nodes in the network is N, the network is connected a.a.s. if $\eta dN + \log d \to \infty$ when $N \to \infty$. Furthermore, we proved that the routing path progress conditioned on the previous two hops can be approximated with a Markov process. Then using this Markovian approximation, we derived exact asymptotic expressions for the mean and variance of the path length generated by the random $\frac{1}{2}$disk routing scheme. Furthermore, we provided guidelines to extend these results to other variants of geometric routing schemes such as MFR,

DIR, and NFP.

5.2 Future Work

In our investigation of the effect of erroneous and wide-band spectrum sensing we assumed that all the secondary users adopt the same physical-layer transmission scheme, such that the achievable rate at each channel, only depends on the bandwidth of that channel, and is constant across different secondary users. As a future endeavor, the cases with per-user adaptive modulations can be considered. Furthermore, we assumed that no acknowledgment is required to complete a packet transmission, and secondary transmitters do not re-transmit the data lost in the channel. Moreover, the spectrum occupancy statistics of primary networks are assumed to be known at the secondary users. The secondary network is time-slotted and synchronized with the primary network clock. We assume that the secondary users operate under a heavy traffic model, i.e., they always have packets to transmit, to focus on the maximum usage of spectrum opportunities. As a future direction, one can consider the effect that relaxing any of these idealized assumptions have on the performance of the cognitive radio networks.

In Section 3 we studied how the performance of cognitive radio networks scale for very large network sizes. However, we only considered the case where the secondary users were equipped with perfect spectrum sensors. The detailed analysis of overlaid networks with spectrum sensing errors is non-trivial due to the complex spatial correlation among primary and secondary users caused by non-perfect sensing. As part of future research, the analysis and the effect of spectrum sensing errors on the performance of the cognitive radio network can be investigated. Furthermore, we observed in Section 3.3 that if packets are not being stored indefinitely in some nodes in the network, the spatial throughput of the network is equivalent to the transport

capacity defined in [42]. This requires an intricate queuing and temporal analysis of the system, which is a worthwhile endeavor for a future work, since it can provide a comprehensive and indepth understanding regarding the behavior of the large scale cognitive radio networks.

In Section 4 we introduced a methodology to systematically derive path statistics for Geometric routing schemes in wireless ad hoc networks. We only derived the mean and variance statistics of the paths generated by the random $\frac{1}{2}$disk routing scheme. However, we pointed out that there exist a trade-off between the existence of a disconnected network node and the expected length of the routing path parameterized by the angle of the relay selection region. An explicit characterization of this trade-off can provide us with valuable design guidelines as it highlights the trade-off between the throughput, latency and reliability of the such network. Furthermore, in the proof of the results presented in this section, we made a key assumption that the process of route establishment by the random $\frac{1}{2}$disk routing scheme can be asymptotically approximated by a Markov process. We proved that this assumption is correct if we only consider the history of the routing path up to the two previous relaying nodes. We also argued that this assumption is correct in general if the number of the previous relaying nodes that their RSR intersect with the current transmitting node scales as $k_n = o\left(\sqrt{dN}\right)$. Simulations indicate that k_n should in fact remain in the order of $o\left(\sqrt{dN}\right)$; however, we could not establish an explicit proof for this claim, which can be an insightful effort for a future work.

REFERENCES

[1] "Cisco Visual Networking Index: Global Mobile Data Traffic Forecast Update, 2013–2018", Feb. 2014. Available: http://www.cisco.com/c/en/us/solutions/collateral/service-provider/visual-networking-index-vni/white_paper_c11-520862.html

[2] NTIA, "US Frequency Allocation Chart," 2003. Available: http://www.ntia.doc.gov/osmhome/allochrt.html

[3] Federal Communications Commission, Spectrum Policy Task Force, "Rep. ET Docket no. 02-135," Nov. 2002. Available: http://www.fcc.gov/sptf/reports.html

[4] FCC, "FCC Spectrum Policy Task Force Report, ET Docket no. 02-155," Nov. 2002. Available: http://transition.fcc.gov/headlines2002.html

[5] D. Cabric, S. Mishra, and R. Brodersen, "Implementation Issues in Spectrum Sensing for Cognitive Radios," in *Proc. of the Asilomar Conference on Signals, Systems and Computers*, vol. 1, pp. 772–776, Nov. 7-10, 2004.

[6] M. Islam, C. L. Koh, O. Ser Wah, Q. Xianming, Y. Y. Lai, *et al.*, "Spectrum Survey in Singapore: Occupancy Measurements and Analyses," in *Proc. of the International Conference on Cognitive Radio Oriented Wireless Networks and Communications (CrownCom)*, pp. 1-7, May 15-17, 2008.

[7] V. Valenta, R. Marsalek, G. Baudoin, M. Villegas, M. Suarez, and F. Robert, "Survey on Spectrum Utilization in Europe: Measurements, Analyses and Obser-

vations," in *Proc. of the International Conference on Cognitive Ra- dio Oriented Wireless Networks Communications (CrownCom)*, pp. 1-5, Jun. 911, 2010.

[8] M. McHenry, "Spectrum White Space Measurements," New America Foundation Broadband Forum, Jun. 2003. Available: `http://www.newamerica.net/files/nafmigration/archive/Doc_File_185_1.pdf`

[9] D. Cabric, S. M. Mishra, and R. W. Brodersen, "Implementation Issues in Spectrum Sensing for Cognitive Radios," in *Proc. of 38th Asilomar Conference on Signals, Systems and Computers*, pp. 772–776, Pacific Grove, CA, Nov. 2004.

[10] T. C. Clancy III, "Dynamic Spectrum Access in Cognitive Radio Networks", PhD Dissertation, University of Maryland, College Park, 2006.

[11] G. Faulhaber and D. Farber, "Spectrum Management: Property Rights, Markets, and the Commons," in *Telecommunications Policy Research Conference Proceedings*, 2003.

[12] Y. Benkler, "Overcoming Agoraphobia: Building the Commons of the Digitally Networked Environment," in *Harvard Journal of Law & Technology*, vol. 11, pp. 287–400, Winter 1998.

[13] I. Akyildiz, W. Lee, M. Vuran, and S. Mohanty, "Next Generation/Dynamic Spectrum Access/Cognitive Radio Wireless Networks: A Survey," *Elsevier Computer Networks*, vol. 50, pp. 2127–2159, 2006.

[14] A. Sahai, N. Hoven, and R. Tandra, "Some Fundamental Limits on Cognitive Radio," in *Proc. of the Allerton Conf. on Commun., Control and Computing 2004*, pp. 1662–1671, Oct. 2004.

[15] R. Etkin, A. Parekh, and D. Tse, "Spectrum Sharing for Unlicensed Bands," *IEEE Journal on Selected Areas in Communications*, vol. 25, no. 3, pp. 517–528, Apr. 2007.

[16] T. C. Clancy, "Dynamic Spectrum Access Using the Interference Temperature Model," *Annals of Telecommunications*, vol. 64, no. 7-8, pp. 573–592, Aug. 2009.

[17] J. Mitola and G. Maguire, Jr., "Cognitive Radio: Making Software Radios More Personal," *IEEE Personal Communications Magazine*, vol. 6, no. 6, pp. 13–18, Aug. 1999.

[18] J. Mitola III, "Cognitive Radio: An Integrated Agent Architecture for Software Defined Radio," Ph.D. Thesis, KTH Royal Inst. Technology, Stockholm, Sweden, 2000.

[19] C. J. Rieser, "Biologically Inspired Cognitive Radio Engine Model Utilizing Distributed Genetic Algorithms for Secure and Robust Wireless Communications and Networking," Ph.D. Thesis, Virginia Polytechnic Institute and State University, Blacksburg, 2004.

[20] FCC, "FCC 03-322," Dec. 2003. Available: `http://hraunfoss.fcc.gov/edocspublic/attachmatch/FCC-03-322A1.pdf`

[21] "Spectrum Access and the Promise of Cognitive Radio Technology," in *Federal Communications Commission (FCC) Cognitive Radio Technologies Proceeding (CRTP)*, ET Docket No. 03–108, May 2003.

[22] C. Stevenson, G. Chouinard, Z. Lei, W. Hu, S. Shellhammer, and W. Caldwell, "IEEE 802.22: The First Cognitive Radio Wireless Regional Area Networks

(WRANs) Standards," *IEEE Communications Magazine*, vol. 47, no. 1, pp. 130–138, Jan. 2009.

[23] L. Ma, X. Han, and C. Shen, "Dynamic Open Spectrum Sharing MAC Protocol for Wireless Ad-Hoc Networks," in *Proc. of IEEE Symposium on New Frontiers in Dynamic Spectrum Access Networks (DySPAN05)*, pp. 203–213, Baltimore, MD, Nov. 2005.

[24] J. Zhao, H. Zheng, and G. H. Yang "Distributed Coordination in Dynamic Spectrum Allocation Networks," in *Proc. of IEEE DySPAN'05*, pp. 259–268, Baltimore, MD, Nov. 2005.

[25] H. Su and X. Zhang, "Cross-Layer Based Opportunistic MAC Protocols for QoS Provisionings Over Cognitive Radio Wireless Networks," *IEEE Journal on Selected Areas in Communications*, vol. 26, no. 1, pp. 118–129, Jan. 2008.

[26] D. Hu and S. Mao, "A Sensing Error Aware MAC Protocol for Cognitive Radio Networks," *EAI Endorsed Transactions on Mobile Communications and Applications*, vol. 12, no. 2, p. e1, Aug. 2012.

[27] Y. Chen, Q. Zhao, and A. Swami, "Joint Design and Separation Principle for Opportunistic Spectrum Access in the Presence of Sensing Errors," *IEEE Transactions on Information Theory*, vol. 54, no. 5, pp. 2053-2071, May 2008.

[28] L. Le and E. Hossain, "A MAC Protocol for Opportunistic Spectrum Access in Cognitive Radio Networks," in *Proc. of WCNC'08*, pp. 1426-1430, Las Vegas, NV, Mar./Apr. 2008.

[29] P. Kyasanur, and N. H. Vaidya, "Capacity of Multi-Channel Wireless Networks: Impact of Number of Channels and Interfaces" in *Proc. of MobiCom'05*, pp. 43-57, New York, New York, Aug. 2005.

[30] A. Proutiere, Y. Yi, T. Lan, and M. Chiang, "Resource Allocation over Network Dynamics without Timescale Separation," in *Proc. of IEEE INFOCOM'10*, pp. 1-5, San Diego, CA, Mar. 2010.

[31] A. Asterjadhi, F. Librino, and M. Zorzi, "Analysis of Random Access Protocols for Multi Channel Wireless Networks," in *Proc. of IEEE GLOBECOM'11*, pp. 1-6, Houston, TX, Dec. 2011.

[32] T. Bonald and M. Feuillet, "Performance of CSMA in Multi-Channel Wireless Networks," *Queueing Systems*, vol. 72, no. 1, pp. 139-160, Oct. 2012.

[33] L. Jiang and J. Walrand, "Approaching Throughput-Optimality in Distributed CSMA Scheduling Algorithms with Collisions," *IEEE/ACM Transactions on Networking*, vol. 19, no. 3, pp. 816-829, Jun. 2011.

[34] J. Ni and R. Srikant, "Distributed CSMA/CA Algorithms for Achieving Maximum Throughput in Wireless Networks," in *Proc. of Information Theory Application Workshop*, p. 250, San Diego, CA, Feb. 2009.

[35] T. A. Weiss and F. K. Jondral, "Spectrum Pooling: An Innovative Strategy for the Enhancement of Spectrum Efficiency, " *IEEE Communications Magazine*, vol. 42, no. 3., pp. 8-14, Mar. 2004.

[36] T. A. Weiss, A. Krohn, F. Capar, I. Martoyo, and F. K. Jondral, "Synchronization Algorithms and Preamble Concepts for Spectrum Pooling Systems," in *Proc.*

of IST Mobile and Wireless Telecommunications Summit, pp. 788-792, Aveiro, Portugal, Jun. 2003.

[37] S. Boyd and L. Vandenberghe, *Convex Optimization*, Cambridge University Press, New York, NY, 2004.

[38] Q. Zhao and B. M. Sadler, "A Survey of Dynamic Spectrum Access," *IEEE Signal Processing magazine*, vol. 24, no. 3, pp. 79-89, May 2007.

[39] M. Vu, N. Devroye, M. Sharif, and V. Tarokh, "Scaling Laws of Cognitive Networks," in *Proc. of CrownCom*, pp. 2–8, Orlando, FL, Aug. 2007. (Invited)

[40] S.-W. Jeon, N. Devroye, M. Vu, S.-Y. Chung, and V. Tarokh, "Cognitive Networks Achieve Throughput Scaling of a Homogeneous Network," *IEEE Transactions on Information Theory*, vol. 57, no. 8, pp. 5103–5115, Aug. 2011.

[41] C. Yin, L. Gao, and S. Cui, "Scaling Laws of Overlaid Wireless Networks: A Cognitive Radio Network vs. A Primary Network," *IEEE/ACM Transactions on Networking*, vol. 18, no. 4, pp. 1317–1329, Aug. 2010.

[42] P. Gupta and P. R. Kumar, "The Capacity of Wireless Networks, " *IEEE Transactions on Information Theory*, vol. 46, no. 2, pp. 388-404, Mar. 2000.

[43] H. Takagi and L. Kleinrock, "Optimal Transmission Ranges for Randomly Distributed Packet Radio Terminals," *IEEE Transactions on Communications*, vol. 32, no. 3, pp. 246–257, Mar. 1984.

[44] R. Nelson and L. Kleinrock, "The Spatial Capacity of a Slotted ALOHA Multihop Packet Radio Network with Capture," *IEEE Transactions on Communications,* vol. 32, no. 6, pp. 684–694, Jun. 1984.

[45] S. Weber, J. G. Andrews, and N. Jindal, "An Overview of the Transmission Capacity of Wireless Networks," *IEEE Transactions on Communications*, vol. 58, no. 12, pp. 3593–3604, Dec. 2010.

[46] F. Baccelli, B. Blaszczyszyn, and P. Mühlethaler, "An Aloha Protocol for Multihop Mobile Wireless Networks," *IEEE Transactions on Information Theory*, vol. 52, no. 2, pp. 421-436, Feb. 2006.

[47] S. A. R. Zaidi, M. Ghogho, D. C. McLernon, and A. Swami, "Achievable Spatial Throughput in Multi-Antenna Cognitive Underlay Networks with Multi-Hop Relaying," *IEEE Journal on Selected Areas in Communications*, vol. 31, no. 8, pp. 1543–1558, Aug. 2013.

[48] C.-H. Lee and M. Haenggi, "Interference and Outage in Poisson Cognitive Networks," *IEEE Transactions on Wireless Communications*, vol. 11, no.4, pp. 1392–1401, Apr. 2012.

[49] T.-C. Hou and V. Li, "Transmission Range Control in Multihop Packet Radio Networks," *IEEE Transactions on Communications*, vol. 34, no. 1, pp. 38–44, Jan. 1986.

[50] E. Kranakis, H. Singh, and J. Urrutia, "Compass Routing on Geometric Networks," in *Proc. of 11th Canadian Conference on Computational Geometry*, pp. 51–54, Aug. 1999.

[51] P.-J. Wan, C.-W. Yi, F. Yao, and X. Jia, "Asymptotic Critical Transmission Radii for Greedy Forward Routing in Wireless Ad-Hoc Networks," *IEEE Transactions on Communications*, vol. 57, no. 5, pp. 1433–1443, May 2009.

[52] S. Subramanian and S. Shakkottai, "Geographic Routing With Limited Information in Sensor Networks," *IEEE Transactions on Information Theory*, vol 56, no. 9, pp. 4506–4519, Aug. 2010.

[53] S. I. Resnick, *A Probability Path,* Birkhuser Boston, 1999.

[54] A. Banaei, D. B.H. Cline, C. N. Georghiades, and S. Cui, "On Asymptotic Statistics for Geometric Routing Schemes in Wireless Ad-Hoc Networks," *IEEE/ACM Transactions on Networking*, to be published. Available: `arXiv:1211.2496v2`

[55] Glen E. Bredon, *Topology and Geometry,* Graduate Texts in Geometry, Springer Verlog, 1993.

[56] E. W. Dijkstra, "A Note on Two Problems in Connexion with Graphs," *Numerische Mathematik*, vol. 1, no. 1, pp. 269–271, Dec. 1959.

[57] C. E. Perkins and E. M. Royer, "Ad-Hoc On-Demand Distance Vector Routing," in *Proc. of the 2nd IEEE Workwhop on Mobile Computing Systems and Applications*, pp. 90–100, New Orleans, LA, Feb. 1997.

[58] R. Jain, A. Puri, and R. Sengupta, "Geographical Routing Using Partial Information for Wireless Ad-Hoc Networks," *IEEE Personal Communications*, vol. 8, no. 1, pp. 48–57, Feb. 2001.

[59] B. Karp and H. T. Kung, "GPSR: Greedy Perimeter Stateless Routing for Wireless Networks," in *Proc. 6th Annual International Conference on Mobile Computing and Networking*, pp. 243–254, Boston, MA, Aug. 2000.

[60] P. Gupta and P. R. Kumar, "Critical Power for Asymptotic Connectivity," in *Proc. of 37th IEEE Conference on Decision and Control*, pp. 1106– 1110, Tampa, Florida, Dec. 1998.

[61] G. Xing, C. Lu, R. Pless, and Q. Huang, "On Greedy Geographic Routing Algorithms in Sensing Covered Networks," in *Proc. of 5th ACM International Symposium on Mobile Ad-Hoc Networking and Computing*, pp. 31–42, Tokyo, Japan, May 2004.

[62] C. Bordenave, "Navigation on a Poisson Point Process," *The Annals of Applied Probability*, vo. 18, no. 2, pp. 708–746, 2008.

[63] F. Baccelli, B. Blaszczyszyn, and P. Mühlethaler, "Time-Space Opportunistic Routing in Wireless Ad Hoc Networks, Algorithms and Performance," *The Computer Journal*, vol. 53, no. 5, pp. 592–609, Jun. 2009.

[64] K. V. Mardia, *Statistics of Directional Data,* Academic Press, London, 1972.

[65] T. K. Philips, S. S. Panwar, and A. N. Tantawi, "Connectivity Properties of a Packet Radio Network Model," *IEEE Transactions on Information Theory,* vol. 32, no. 5, pp. 1044–1047, Sep. 1989.

[66] H. P. Keeler, "A Stochastic Analysis of Greedy Routing in a Spatially Dependent Sensor Network", *European Journal of Applied Mathematics,* vol. 23, no. 4, pp. 485–514, Jul. 2012.

[67] H. P. Keeler and P. G. Taylor, "A Stochastic Analysis of a Greedy Routing Scheme in Sensor Networks," *SIAM Journal on Applied Mathematics,* vol. 70, no. 7, pp. 2214–2238, Apr. 2010.

[68] H. P. Keeler and P. G. Taylor, "A Model Framework for Greedy Routing in a Sensor Network with a Stochastic Power Scheme," *ACM Transactions on Sensor Networks,* vol. 7, no. 4, pp. 1–34, Feb. 2011.

[69] L. A. Santalo, *Integral Geometry and Geometric Probability,* Encyclopedia of Mathematics and its Applications, vol. 1, Addison-Wesley Publishing Co., Reading, Mass.-London-Amsterdam, 1976.

[70] H. P. Keeler and P. G. Taylor, "Random Transmission Radii in Greedy Routing Models for Ad-Hoc Sensor Networks," *SIAM Journal on Applied Mathematics,* vol. 72, no. 2, pp. 535–557, Mar. 2012.

[71] G. R. Grimmett and D. R. Stirzaker, *Probability and Random Processes,* 3rd ed., Oxford Univ. Press, USA, 1992.

[72] F. Baccelli and B. Blaszczyszyn, "Stochastic Geometry and Wireless Networks Volume 1: Theory," *Foundations and Trends in Networking*, vol. 3, no. 3–4, pp. 249-449, 2009.

APPENDIX A

PROOF OF PROPOSITION 3.4.1

Let σ_n denote the event that no primary transmitters fall into $B_{R_D+R_I^{(sp)}}(X_{n+1}^{(p)})$ and let $\hat{\Lambda}_{2,X_{n+1}^{(p)}}$ denote the event that no primary users in $B_{R_I^{(p)}}(X_{n+1}^{(p)}) - B_{R_D+R_I^{(sp)}}(X_{n+1}^{(p)})$, except $X_n^{(p)}$, initiate transmissions. Note that $B_{R_I^{(p)}}(X_{n+1}^{(p)}) - B_{R_D+R_I^{(sp)}}(X_{n+1}^{(p)})$ might be a null area. We have that $\Lambda_{1,X_n^{(p)}}$ and $\hat{\Lambda}_{2,X_{n+1}^{(p)}}$ are independent of σ_n, $X_n^{(p)}$, and $X_{n+1}^{(p)}$. In addition, given σ_n, the secondary users located inside $B_{R_I^{(sp)}}(X_{n+1}^{(p)})$ detect *no* primary transmitters and initiate transmissions with probability $q^{(s)}$ independent of $\Lambda_{1,X_n^{(p)}}$ and $\hat{\Lambda}_{2,X_{n+1}^{(p)}}$. Together with (3.3) and (3.12), we have

$$
\begin{aligned}
C_{\beta>1}^{(p)} &= \lambda^{(p)}|A|\mathrm{E}\left(\frac{1}{\nu+1}\sum_{n=0}^{\nu}\mathrm{E}\left(Y_{X_n^{(p)}}\mathbf{1}_{\Lambda_{X_n^{(p)}}}\right)\right) \\
&\sim \lambda^{(p)}|A|\mathrm{E}\left(\frac{1}{\nu+1}\sum_{n=0}^{\nu}\mathrm{E}_{\sigma_n}\left(Y_{X_n^{(p)}}\mathbf{1}_{\Lambda_{X_n^{(p)}}}\right)\right) \\
&\sim \lambda^{(p)}|A|\mathrm{E}\left(\frac{1}{\nu+1}\sum_{n=0}^{\nu}\mathrm{E}_{\sigma_n}\left(Y_{X_n^{(p)}}\mathbf{1}_{\Lambda_{1,X_n^{(p)}}\hat{\Lambda}_{2,X_{n+1}^{(p)}}}\right)\Pr\left(\Lambda_{3,X_{n+1}^{(p)}}\right)\right) \\
&= \lambda^{(p)}|A|\mathrm{E}\left(\frac{1}{\nu+1}\sum_{n=0}^{\nu}\mathrm{E}_{\{|X_n^{(p)}-X_{n+1}^{(p)}|>R_D+R_I^{(sp)}\}}\left(Y_{X_n^{(p)}}\right)\right)\Pr\left(\Lambda_{1,X_n^{(p)}}\hat{\Lambda}_{2,X_{n+1}^{(p)}}\right) \\
&\qquad \Pr\left(\Lambda_{3,X_{n+1}^{(p)}}\right) \\
&\sim C^{(p)}e^{-\lambda^{(s)}q^{(s)}(R_I^{(sp)})^2},
\end{aligned}
$$

where the second line is due to $\Pr(\overline{\sigma}_n) = 1 - \exp(-\lambda^{(p)} q^{(p)} (R_D + R_I^{(sp)})^2) \to 0$ and the last line is due to

$$\mathrm{E}(Y_{X_n^{(p)}} : |X_n^{(p)} - X_{n+1}^{(p)}| > R_D + R_I^{(sp)}) \to \mathrm{E}(Y_{X_n^{(p)}}),$$
$$\Pr(\hat{\Lambda}_{2,X_{n+1}^{(p)}}) \to \Pr(\Lambda_{2,X_{n+1}^{(p)}}),$$

as $\lambda^{(p)} \to \infty$ since $R_D = o(R_r^{(p)})$ and $R_r^{(sp)} = o(R_r^{(p)})$. By an abuse of notation, we abbreviate $\nu_{R_r^{(p)}}$ and $\nu_{R_r^{(s)}}$ with ν when the correct form is clear from context. Now choosing $q^{(s)} = \alpha_1 (\lambda^{(s)} \pi (R_I^{(s)})^2)^{-1}$ with $\alpha_1 > 0$ and taking $\lambda^{(p)} \to \infty$, we have (3.16).

APPENDIX B

PROOF OF PROPOSITION 3.4.2

Define $\sigma_{1,n} := \{|X_n^{(p)} - X_{n+1}^{(p)}| \leq R_D - R_I^{(sp)}\}$, $\sigma_{2,n} := \{R_D - R_I^{(sp)} \leq |X_n^{(p)} - X_{n+1}^{(p)}| \leq R_D + R_I^{(sp)}\}$, and $\sigma_{3,n} := \{|X_n^{(p)} - X_{n+1}^{(p)}| \geq R_D + R_I^{(sp)}\}$. Given $\sigma_{1,n}$, all secondary users in $B_{R_I^{(sp)}}(X_{n+1}^{(p)})$ will detect the transmission of $X_n^{(p)}$ and refrain from transmission. In this case, $X_{n+1}^{(p)}$ does not perceive any inter-network interference from the secondary network and we can apply the separation principle to compute the conditional spatial throughput for the primary network. Given $\sigma_{3,n}$, we have that $X_n^{(p)}$ is out of the detection ranges of all secondary users in $B_{R_I^{(sp)}}(X_{n+1}^{(p)})$ and consequently, the event $\Lambda_{X_n^{(p)}}$ is independent of $X_n^{(p)}$ and $X_{n+1}^{(p)}$. Also note that in this case, additionally given $\Lambda_{2,X_{n+1}^{(p)}}$, the secondary users in $B_{R_I^{(sp)}}(X_{n+1}^{(p)})$ detect no primary transmitters (since $R_D + R_I^{(sp)} \leq |X_n^{(p)} - X_{n+1}^{(p)}| \leq R_r^{(p)} \leq R_I^{(p)}$) and initiate transmissions with probability $q^{(s)}$. Hence, using (3.3) we obtain the primary network spatial throughput as

$$
\begin{aligned}
C_{\beta>1}^{(p)} &= \lambda^{(p)}|A|\mathrm{E}\left(\frac{1}{\nu+1}\sum_{n=0}^{\nu}\sum_{i=1}^{3}\mathrm{E}_{\sigma_{i,n}}\left(Y_{X_n^{(p)}}\mathbf{1}_{\Lambda_{X_n^{(p)}}}\right)\Pr\left(\sigma_{i,n}\right)\right) \\
&= \lambda^{(p)}|A|\mathrm{E}\Bigg(\frac{1}{\nu+1}\sum_{n=0}^{\nu}\Bigg[\mathrm{E}_{\sigma_{1,n}}\left(Y_{X_n^{(p)}}\right)\Pr\left(\Lambda_{1,X_n^{(p)}}\Lambda_{2,X_{n+1}^{(p)}}\right)\Pr\left(\sigma_{1,n}\right) \\
&\qquad + \mathrm{E}_{\sigma_{2,n}}\left(Y_{X_n^{(p)}}\mathbf{1}_{\Lambda_{X_n^{(p)}}}\right)\Pr\left(\sigma_{2,n}\right) \\
&\qquad + \mathrm{E}_{\sigma_{3,n}}\left(Y_{X_n^{(p)}}\right)\Pr\left(\Lambda_{1,X_n^{(p)}}\Lambda_{2,X_{n+1}^{(p)}}\right)\Pr\left(\Lambda_{3,X_{n+1}^{(p)}} \mid \Lambda_{2,X_{n+1}^{(p)}}\right)\Pr\left(\sigma_{3,n}\right)\Bigg]\Bigg) \\
&\sim C^{(p)}\left(\alpha_2^3 + (1-\alpha_2^3)e^{-\lambda^{(s)}q^{(s)}\pi(R_I^{(sp)})^2}\right),
\end{aligned}
$$

where the last line is due to

$$\begin{aligned}
\mathrm{E}_{\sigma_{1,n}}\left(Y_{X_n^{(p)}}\right) &= \frac{4}{3\pi}(R_D - R_I^{(sp)})\,, \\
\mathrm{E}_{\sigma_{3,n}}\left(Y_{X_n^{(p)}}\right) &= \frac{4}{3\pi}\frac{(R_r^{(p)})^3 - (R_D + R_I^{(sp)})^3}{(R_r^{(p)})^2 - (R_D + R_I^{(sp)})^2}\,, \\
\Pr(\sigma_{2,n}) &= O\left((\lambda^{(p)})^{1-\beta}\right)\,.
\end{aligned}$$

APPENDIX C

PROOF OF PROPOSITION 3.4.3

In Proposition 3.4.6, we show that the secondary users initiate transmission with probability no less than $\tilde{q}^{(s)}$ and no greater than $\check{q}^{(s)}$ (as defined in (E.1b)) when $\beta < 1$. Together with the fact that $\check{q}^{(s)} \to \tilde{q}^{(s)}$ as $\lambda^{(p)} \to \infty$, we obtain that

$$\begin{aligned} C_{\beta<1}^{(p)} &= \lambda^{(p)}|A|\mathrm{E}\left(\frac{1}{\nu+1}\sum_{n=0}^{\nu}\mathrm{E}\left(Y_{X_n^{(p)}}\mathbf{1}_{\Lambda_{X_n^{(p)}}}\right)\right) \\ &\sim \lambda^{(p)}|A|\mathrm{E}\left(\frac{1}{\nu+1}\sum_{n=0}^{\nu}\mathrm{E}\left(Y_{X_n^{(p)}}\mathbf{1}_{\Lambda_{1,X_n^{(p)}}\Lambda_{2,X_{n+1}^{(p)}}}\right)\right)\Pr\left(\Lambda_{3,X_{n+1}^{(p)}}\right) \\ &\sim C^{(p)}e^{-\lambda^{(s)}\tilde{q}^{(s)}\pi(R_I^{(sp)})^2}. \end{aligned}$$

APPENDIX D

PROOF OF PROPOSITION 3.4.5

Let us first consider the case where $R_D \leq R_I^{(ps)} - R_I^{(s)}$. In this case, given $\Lambda_{3,X_{n+1}^{(s)}}$, all secondary users in $B_{R_I^{(s)}}(X_{n+1}^{(s)})$ together with $X_n^{(s)}$ and $X_{n+1}^{(s)}$ detect no primary users and independently initiate transmissions with probability $q^{(s)}$. Hence, using the separation principle and (3.3), we have

$$\begin{aligned} C_{\beta>1}^{(s)} &= \lambda^{(s)}|A|\mathrm{E}\left(\frac{1}{\nu+1}\sum_{n=0}^{\nu}\mathrm{E}\left(Y_{X_n^{(s)}}\mathbf{1}_{\tilde{\Lambda}_{X_n^{(s)}}}\right)\right) \\ &= \lambda^{(s)}|A|\mathrm{E}\left(\frac{1}{\nu+1}\sum_{n=0}^{\nu}\mathrm{E}_{\Lambda_{3,X_{n+1}^{(s)}}}\left(Y_{X_n^{(s)}}\mathbf{1}_{\tilde{\Lambda}_{1,X_n^{(s)}}\tilde{\Lambda}_{2,X_{n+1}^{(s)}}}\right)\right)\Pr\left(\Lambda_{3,X_{n+1}^{(s)}}\right) \\ &= \lambda^{(s)}|A|\mathrm{E}\left(\frac{1}{\nu+1}\sum_{n=0}^{\nu}\mathrm{E}_{\Lambda_{3,X_{n+1}^{(s)}}}\left(Y_{X_n^{(s)}}\mathbf{1}_{\Lambda_{1,X_n^{(s)}}\Lambda_{2,X_{n+1}^{(s)}}}\right)\right)\Pr\left(\Lambda_{3,X_{n+1}^{(s)}}\right) \\ &= C^{(s)}e^{-(\frac{R_I^{(ps)}}{R_I^{(p)}})^2}. \end{aligned} \tag{D.1}$$

Now consider the case with $R_D > R_I^{(ps)} - R_I^{(s)}$. In this case, observe that $\tilde{\Lambda}_{1,X_n^{(s)}}\tilde{\Lambda}_{2,X_{n+1}^{(s)}}\hat{\Lambda}_{3,X_{n+1}^{(s)}} \subseteq \tilde{\Lambda}_{1,X_n^{(s)}}\tilde{\Lambda}_{2,X_{n+1}^{(s)}}\Lambda_{3,X_{n+1}^{(s)}}$, where $\hat{\Lambda}_{3,X_{n+1}^{(s)}}$ denotes the event that there are no primary transmitters within a $R_D + R_I^{(s)}$ radius of $X_{n+1}^{(s)}$; again, given $\hat{\Lambda}_{3,X_{n+1}^{(s)}}$, $\tilde{\Lambda}_{1,X_n^{(s)}}\tilde{\Lambda}_{2,X_{n+1}^{(s)}}$ is independent of the spectrum sensing outcome. Hence, using the separation principle, we obtain the following lower bound for the secondary

network sum spatial throughput:

$$
\begin{aligned}
C_{\beta>1}^{(s)} &= \lambda^{(s)}|A|\mathrm{E}\left(\frac{1}{\nu+1}\sum_{n=0}^{\nu}\mathrm{E}\left(Y_{X_n^{(s)}}\mathbf{1}_{\tilde{\Lambda}_{X_n^{(s)}}}\right)\right) \\
&\geq \lambda^{(s)}|A|\mathrm{E}\left(\frac{1}{\nu+1}\sum_{n=0}^{\nu}\mathrm{E}_{\hat{\Lambda}_{3,X_{n+1}^{(s)}}}\left(Y_{X_n^{(s)}}\mathbf{1}_{\tilde{\Lambda}_{1,X_n^{(s)}}\tilde{\Lambda}_{2,X_{n+1}^{(s)}}}\right)\Pr\left(\hat{\Lambda}_{3,X_{n+1}^{(s)}}\right)\right) \\
&= \lambda^{(s)}|A|\mathrm{E}\left(\frac{1}{\nu+1}\sum_{n=0}^{\nu}\mathrm{E}\left(Y_{X_n^{(s)}}\mathbf{1}_{\Lambda_{1,X_n^{(s)}}\Lambda_{2,X_{n+1}^{(s)}}}\right)\Pr\left(\hat{\Lambda}_{3,X_{n+1}^{(s)}}\right)\right) \\
&= C^{(s)}e^{-(\frac{R_D}{R_I^{(p)}})^2}. \qquad \text{(D.2)}
\end{aligned}
$$

Next we derive an upper bound for the secondary network sum spatial throughput when $R_D > R_I^{(ps)} - R_I^{(s)}$. Assume there are N secondary users $\{X_1, X_2, \ldots, X_N\}$ located inside $B_{R_I^{(s)}}(X_{n+1}^{(s)})$ including $X_{n+1}^{(s)}$ itself and excluding $X_n^{(s)}$. Let σ_i denote the event that X_i initiates a transmission, $\overline{\sigma}_i$ denotes the event that X_i remains silent, and σ_{-i} denote the event that at least one of $\{X_1, X_2, \ldots, X_N\}\backslash\{X_i\}$ initiate a transmission. Given $\Lambda_{3,X_{n+1}^{(s)}}$ and $\tilde{\Lambda}_{1,X_n^{(s)}}$, the probability that X_i remains idle is no more than $\Pr(\overline{\sigma}_i) \leq 1 - \hat{q}^{(s)}$ (i.e., when X_i and $X_n^{(s)}$ are farthest away) and no less than $\Pr(\overline{\sigma}_i) \geq 1 - q^{(s)}$, where $\hat{q}^{(s)} := q^{(s)}\exp(-\lambda^{(p)}q^{(p)}|B_{R_D}(R_I^{(s)}, 0) - B_{R_D}(-R_I^{(s)}, 0) - B_{R_I^{(ps)}}(0,0)|)$. Similarly, given $\Lambda_{3,X_{n+1}^{(s)}}$ and $\tilde{\Lambda}_{1,X_n^{(s)}}$, the probability that X_i initiates a transmission is no less than $\Pr(\sigma_i) \geq \hat{q}^{(s)}$. Consequently, given $\Lambda_{3,X_{n+1}^{(s)}}$ and $\tilde{\Lambda}_{1,X_n^{(s)}}$,

we have

$$
\begin{aligned}
N(1-\hat{q}^{(s)}) \geq \sum_{i=1}^{N} \Pr\left(\overline{\sigma}_i\right) &= \sum_{i=1}^{N} \Pr(\overline{\sigma}_i \cap \overline{\sigma}_{-i}) + \sum_{i=1}^{N} \Pr\left(\overline{\sigma}_i \cap \sigma_{-i}\right) \\
&= \sum_{i=1}^{N} \Pr(\bigcap_{j=1}^{N} \overline{\sigma}_j) + \sum_{i=1}^{N} \Pr\left(\overline{\sigma}_i\right) \Pr\left(\sigma_{-i} \mid \overline{\sigma}_i\right) \\
&\geq N\Pr(\bigcap_{j=1}^{N} \overline{\sigma}_j) + N(1-q^{(s)}) \sum_{j=1}^{N-1} \binom{N-1}{j} \\
&\quad (\hat{q}^{(s)})^j (1-q^{(s)})^{N-1-j} \\
&= N\Pr(\bigcap_{j=1}^{N} \overline{\sigma}_j) + N(1-q^{(s)}) \\
&\quad \left[(1-q^{(s)}+\hat{q}^{(s)})^{N-1} - (1-q^{(s)})^{N-1}\right]. \qquad \text{(D.3)}
\end{aligned}
$$

Taking expectation over the number of nodes falling inside $B_{R_I^{(s)}}(X_{n+1}^{(s)})$, we obtain

$$
\begin{aligned}
\Pr\left(\tilde{\Lambda}_{2,X_{n+1}^{(s)}} \mid \tilde{\Lambda}_{1,X_n^{(s)}} \Lambda_{3,X_{n+1}^{(s)}}\right) &= \mathrm{E}(\Pr(\bigcap_{i=1}^{N} \overline{\sigma}_i \mid \Lambda_{3,X_{n+1}^{(s)}} \tilde{\Lambda}_{1,X_n^{(s)}})) \\
&\leq e^{-\lambda^{(s)} q^{(s)} \pi (R_I^{(s)})^2} + \\
&\quad \left[(1-\hat{q}^{(s)}) - (1-q^{(s)}) e^{-\lambda^{(s)}(q^{(s)}-\hat{q}^{(s)})\pi (R_I^{(s)})^2}\right]. \qquad \text{(D.4)}
\end{aligned}
$$

Hence, we have

$$
\begin{aligned}
C_{\beta>1}^{(s)} &= \lambda^{(s)}|A|\mathrm{E}\left(\frac{1}{\nu+1}\sum_{n=0}^{\nu} \mathrm{E}\left(Y_{X_n^{(s)}} \mathbf{1}_{\tilde{\Lambda}_{X_n^{(s)}}}\right)\right) \\
&\leq \lambda^{(s)}|A|\mathrm{E}\left(\frac{1}{\nu+1}\sum_{n=0}^{\nu} \mathrm{E}_{\tilde{\Lambda}_{1,X_n^{(s)}}\Lambda_{3,X_{n+1}^{(s)}} X_n^{(s)} X_{n+1}^{(s)}}\left(Y_{X_n^{(s)}} \mathbf{1}_{\tilde{\Lambda}_{2,X_{n+1}^{(s)}}}\right) q^{(s)} e^{-(\frac{R_D}{R_I^{(p)}})^2}\right) \\
&\leq \lambda^{(s)}|A| q^{(s)} e^{-(\frac{R_D}{R_I^{(p)}})^2} \mathrm{E}\left(\frac{1}{\nu+1}\sum_{n=0}^{\nu} \mathrm{E}\left(Y_{X_n^{(s)}}\right)\right)
\end{aligned}
$$

$$\max_{X_n^{(s)}, X_{n+1}^{(s)}} \Pr\left(\tilde{\Lambda}_{2,X_{n+1}^{(s)}} \mid \tilde{\Lambda}_{1,X_n^{(s)}} \Lambda_{3,X_{n+1}^{(s)}} X_n^{(s)} X_{n+1}^{(s)}\right)$$

$$= C^{(s)} e^{-(\frac{R_D}{R_I^{(p)}})^2} \left[1 + (1-\hat{q}^{(s)}) e^{\lambda^{(s)} q^{(s)} \pi (R_I^{(s)})^2} - (1-q^{(s)}) e^{\lambda^{(s)} \hat{q}^{(s)} \pi (R_I^{(s)})^2}\right]. \quad \text{(D.5)}$$

From (D.2), (D.5), and the fact that $\hat{q}^{(s)} \to q^{(s)}$ as $\lambda^{(p)} \to \infty$, we conclude that $C_{\beta>1}^{(s)} \sim C^{(s)} \exp(-(\frac{R_D}{R_I^{(p)}})^2)$ when $R_D > R_I^{(ps)} - R_I^{(s)}$. Finally, together with (D.1), we obtain (3.22).

APPENDIX E

PROOF OF PROPOSITION 3.4.6

Similar to the proof of Proposition 3.4.5, assume there are N secondary users $\{X_1, X_2, \ldots, X_N\}$ located inside $B_{R_I^{(s)}}(X_{n+1}^{(s)})$ including $X_{n+1}^{(s)}$ itself and excluding $X_n^{(s)}$. Define σ_i, $\overline{\sigma}_i$, and σ_{-i} as before. Let ς_i denote the event that there are no *secondary* users located inside $B_{2R_D}(X_i)$. Similar to (D.3), (D.4), and using the facts that

$$\Pr(\sigma_i) \geq \tilde{q}^{(s)}, \tag{E.1a}$$

$$\begin{aligned}\Pr(\sigma_i) &= \Pr(\sigma_i \mid \varsigma_i)\Pr(\varsigma_i) + \Pr(\sigma_i \mid \overline{\varsigma_i})\Pr(\overline{\varsigma_i}) \\ &\leq q^{(s)}\left(1 - e^{-\lambda^{(s)}\pi(2R_D)^2}\right) + \tilde{q}^{(s)}e^{-\lambda^{(s)}\pi(2R_D)^2} =: \check{q}^{(s)}, \end{aligned} \tag{E.1b}$$

when $\beta < 1$, we obtain

$$\Pr\left(\tilde{\Lambda}_{X_n^{(s)}}\right) \leq \check{q}^{(s)}\left(e^{-\lambda^{(s)}\check{q}^{(s)}\pi(R_I^{(s)})^2} + \left[(1-\tilde{q}^{(s)}) - (1-\check{q}^{(s)})e^{-\lambda^{(s)}(\check{q}^{(s)}-\check{q}^{(s)})\pi(R_I^{(s)})^2}\right]\right) e^{-(\frac{R_I^{(ps)}}{R_I^{(p)}})^2}, \tag{E.2a}$$

$$\Pr\left(\tilde{\Lambda}_{X_n^{(s)}}\right) \geq \tilde{q}^{(s)}\left(e^{-\lambda^{(s)}\tilde{q}^{(s)}\pi(R_I^{(s)})^2} + \left[(1-\check{q}^{(s)}) - (1-\tilde{q}^{(s)})e^{-\lambda^{(s)}(\check{q}^{(s)}-\tilde{q}^{(s)})\pi(R_I^{(s)})^2}\right]\right) e^{-(\frac{R_I^{(ps)}}{R_I^{(p)}})^2}. \tag{E.2b}$$

Note that $\check{q}^{(s)} \to \tilde{q}^{(s)}$ as $\lambda^{(p)} \to \infty$ since $R_D = O(R_r^{(p)})$ and $R_r^{(p)} = o(R_r^{(s)})$ when

$\beta < 1$. As such, similar to (D.5) we obtain

$$C_{\beta<1}^{(s)} = \lambda^{(s)}|A|\mathrm{E}\left(\frac{1}{\nu+1}\sum_{n=0}^{\nu}\mathrm{E}\left(Y_{X_n^{(s)}}\mathbf{1}_{\tilde{\Lambda}_{X_n^{(s)}}}\right)\right)$$
$$\sim \tilde{C}^{(s)}e^{-(\frac{R_I^{(ps)}}{R_I^{(p)}})^2}.$$

APPENDIX F

PROOF OF PROPOSITION 4.4.1

First, let us consider the distribution of a Poisson point process conditioned on deleting one point. Let Φ be a homogeneous Poisson point process with intensity λ and assume a fixed region D. If $\phi(D) > 0$, one point in D is selected at random and removed. Let X be the location of that point. The distribution of Φ on D^c remains Poisson and independent of Φ on D, and thus independent of both $\phi(D)$ and X. Let Φ' be the (point) process with the point at X deleted. (Note that the distribution of Φ' is not the same as the reduced Palm distribution [72] of Φ, as the location of node X is random.)

Let $A_1, A_2, \ldots, A_k$ be a partition of D. Given $\phi(D) > 0$, the points in D are distributed uniformly. If one point is removed at random, the remaining points are still distributed uniformly on D. Hence,

$$\begin{aligned}\Pr\left(\bigcap_{j=1}^{k}\{\phi'(A_j) = n_j\} \;\middle|\; \phi(D) > 0, X\right) &= (1 - e^{-\lambda|D|})^{-1} \sum_{i=1}^{k} \frac{n_i + 1}{n_1 + \ldots + n_k + 1} \\ &\quad \cdot \prod_{j=1}^{k} \frac{(\lambda|A_j|)^{n_j + \mathbf{1}_{j=i}}}{(n_j + \mathbf{1}_{j=i})!} e^{-\lambda|A_j|} \\ &= \frac{\lambda|D|}{(1 - e^{-\lambda|D|})(n_1 + \ldots + n_k + 1)} \\ &\quad \prod_{j=1}^{k} \frac{(\lambda|A_j|)^{n_j}}{(n_j)!} e^{-\lambda|A_j|}, \end{aligned} \tag{F.1}$$

since $|A_1| + \ldots + |A_k| = |D|$. Therefore, conditional on $\phi(D) > 0$, Φ' is independent

of the location of the removed point (X). In particular,

$$\begin{aligned}\Pr\left(\phi'(D)=n \;\middle|\; \phi(D)>0, X\right) &= \frac{(\lambda|D|)^{n+1}}{(n+1)!(1-e^{-\lambda|D|})}e^{-\lambda|D|} \\ &= \Pr\left(\phi(D)=n+1 \;\middle|\; \phi(D)>0\right).\end{aligned}$$

Furthermore, given $n_1+\ldots+n_k=n>0$, we have

$$\Pr\left(\bigcap_{j=1}^{k}\{\phi'(A_j)=n_j\} \;\middle|\; \phi(D)>0, \phi'(D)=n, X\right) = \binom{n}{n_1\cdots n_k}\prod_{j=1}^{k}\left(\frac{|A_j|}{|D|}\right)^{n_j}.$$

Thus, for $A\subseteq D$ and given $\phi'(D)=n>0$, $\phi'(A)$ is conditionally Binomial $\left(n, \frac{|A|}{|D|}\right)$. Without knowing $\phi'(D)$, however, we obtain from (F.1) that

$$\begin{aligned}\Pr\left(\phi'(A)=k \;\middle|\; \phi(D)>0, X\right) &= \frac{\lambda|D|e^{-\lambda|D|}}{(1-e^{-\lambda|D|})}\sum_{j=0}^{\infty}\frac{1}{k+j+1}\frac{(\lambda|A|)^k}{k!}\frac{(\lambda|A^c\cap D|)^j}{j!} \\ &= \frac{\lambda|D|e^{-\lambda|D|}}{(1-e^{-\lambda|D|})}\frac{(\lambda|A|)^k}{k!}\int_0^1 y^k e^{\lambda|A^c\cap D|y}\mathrm{d}y\,, \qquad \text{(F.2)}\end{aligned}$$

where the second equality is due to

$$\begin{aligned}\sum_{j=0}^{\infty}\frac{1}{k+j+1}\frac{a^j}{j!} &= \sum_{j=0}^{\infty}\frac{1}{a^{k+1}}\int_0^a\frac{x^{k+j}}{j!}\mathrm{d}x \\ &= \int_0^a\frac{x^k}{a^{k+1}}e^x\mathrm{d}x \\ &= \int_0^1 y^k e^{ay}\mathrm{d}y\,.\end{aligned}$$

After the aforementioned preliminaries, we now proceed with the proof of Proposition 4.4.1. Suppose C is a random set that depends only on X.[1] The points of Φ', if any, which are in $CD := C\cap D$, are uniformly distributed and independent of the

[1]Note that D and C here correspond to D_{n-1} and D_n in Section 4.4, respectively.

points in CD^c, which are also uniformly distributed (if any). The combined points are uniformly distributed on C *only if* the expected proportion of points in CD is $\frac{|CD|}{|C|}$.

However, the expected proportion of points in CD is strictly less than $\frac{|CD|}{|C|}$ in our case as we now compute. Given $\phi'(C) > 0$, the probability that a randomly selected point in C is also in D is $\mathrm{E}(\frac{\phi'(CD)}{\phi'(C)} \mid \phi'(C) > 0, \phi(D) > 0, X)$. Let $\frac{\phi'(CD)}{\phi'(C)} = 0$ when $\phi'(C) = 0$. Using (F.2), we have

$$\begin{aligned}
\Pr\left(\phi'(C) > 0 \;\middle|\; \phi(D) > 0, X\right) &= 1 - \Pr\left(\phi'(CD) = 0, \phi'(CD^c) = 0 \;\middle|\; \phi(D) > 0, X\right) \\
&= 1 - \frac{\lambda|D|e^{-\lambda|D|}}{1 - e^{-\lambda|D|}} \frac{e^{\lambda|C^cD|} - 1}{\lambda|C^cD|} e^{-\lambda|CD^c|} \\
&= 1 - \frac{|D|}{|C^cD|} \frac{1 - e^{-\lambda|C^cD|}}{1 - e^{-\lambda|D|}} e^{-\lambda|C|}\,;
\end{aligned}$$

so we have

$$1 - \frac{|D|}{|C^cD|} e^{-\lambda|C|} \leq \Pr\left(\phi'(C) > 0 \;\middle|\; \phi(D) > 0, X\right) \leq 1 - e^{-\lambda|C|}\,.$$

Using the observation above and (F.2) we obtain

$$
\begin{aligned}
&\mathrm{E}\left(\frac{\phi'(CD)}{\phi'(C)}\mathbf{1}_{\phi'(C)>0} \;\middle|\; \phi(D)>0, X\right) \\
&\qquad = \sum_{n=0}^{\infty}\sum_{m=1}^{\infty}\frac{n}{n+m}\frac{(\lambda|CD^c|)^m}{m!}e^{-\lambda|CD^c|} \\
&\qquad\quad \frac{\lambda|D|e^{-\lambda|D|}}{1-e^{-\lambda|D|}}\frac{(\lambda|CD|)^n}{n!}\int_0^1 y^n e^{\lambda|C^cD|y}\mathrm{d}y \\
&\qquad = \frac{\lambda|D|e^{-\lambda|C\cup D|}}{1-e^{-\lambda|D|}}\sum_{n=1}^{\infty}\frac{(\lambda|CD|)^n}{(n-1)!} \\
&\qquad\quad \int_0^1 w^{n-1}\left(e^{\lambda|CD^c|w}-1\right)\mathrm{d}w\int_0^1 y^n e^{\lambda|C^cD|y}\mathrm{d}y \\
&\qquad = \frac{\lambda|D|e^{-\lambda|C\cup D|}}{1-e^{-\lambda|D|}}\int_0^1\int_0^1 \lambda|CD|y e^{\lambda(|CD|yw+|C^cD|y)}\left(e^{\lambda|CD^c|w}-1\right)\mathrm{d}w\mathrm{d}y
\end{aligned}
\tag{F.3}
$$

$$
\begin{aligned}
&< \frac{\lambda|D|e^{-\lambda|C\cup D|}}{1-e^{-\lambda|D|}}\int_0^1\int_0^1 \lambda|CD|y e^{\lambda(|CD|yw+|C^cD|y+|CD^c|w)}\mathrm{d}w\mathrm{d}y \\
&< \frac{\lambda|D|e^{-\lambda|C\cup D|}}{1-e^{-\lambda|D|}}\int_0^1 \frac{|CD|y}{|CD|y+|CD^c|}\left(e^{\lambda(|CD|y+|CD^c|)}-1\right)e^{\lambda|C^cD|y}\mathrm{d}y \\
&< \frac{|CD|}{|C|}\frac{\lambda|D|e^{-\lambda|C\cup D|}}{1-e^{-\lambda|D|}}\int_0^1 \left(e^{\lambda(|CD|y+|CD^c|)}-1\right)e^{\lambda|C^cD|y}\mathrm{d}y \\
&< \frac{|CD|}{|C|}\left(1-\frac{|D|}{|C^cD|}\frac{1-e^{-\lambda|C^cD|}}{1-e^{-\lambda|D|}}e^{-\lambda|C|}\right) \\
&= \frac{|CD|}{|C|}\Pr\left(\phi'(C)>0 \mid \phi(D)>0, X\right).
\end{aligned}
\tag{F.4}
$$

Therefore,

$$
\mathrm{E}\left(\frac{\phi'(CD)}{\phi'(C)} \;\middle|\; \phi'(C)>0, \phi(D)>0, X\right) < \frac{|CD|}{|C|}.
$$

Noting that

$$
1-\frac{1}{a} \le ae^{-a}\int_0^1 ye^{ay}\mathrm{d}y = 1-\frac{1-e^{-a}}{a} \le 1,
$$

and using (F.3), we could derive

$$
\begin{aligned}
&\mathrm{E}\bigg(\frac{\phi'(CD)}{\phi'(C)}\mathbf{1}_{\phi'(C)>0} \;\big|\; \phi(D)>0, X\bigg) \\
&\qquad = \frac{\lambda|D|e^{-\lambda|C\cup D|}}{1-e^{-\lambda|D|}}\bigg[\int_0^1 \frac{|CD|y}{|CD|y+|CD^c|}\left(e^{\lambda(|CD|y+|CD^c|)}-1\right)e^{\lambda|C^cD|y}\mathrm{d}y \\
&\qquad - \int_0^1\int_0^1 \lambda|CD|ye^{\lambda(|CD|yw+|C^cD|y)}\mathrm{d}w\mathrm{d}y\bigg] \\
&\qquad > \frac{\lambda|D|e^{-\lambda|C\cup D|}}{1-e^{-\lambda|D|}}\bigg[\int_0^1 \frac{|CD|}{|C|}y\left(e^{\lambda(|CD|y+|CD^c|)}-1\right)e^{\lambda|C^cD|y}\mathrm{d}y \\
&\qquad - \int_0^1 e^{\lambda|C^cD|y}\left(e^{\lambda|CD|y}-1\right)\mathrm{d}y\bigg] \\
&\qquad > \frac{|CD|}{|C|}\frac{1}{(1-e^{-\lambda|D|})}\bigg\{\lambda|D|e^{-\lambda|D|}\int_0^1 ye^{\lambda|D|y}\mathrm{d}y - \lambda|D|e^{-\lambda|C\cup D|}\int_0^1 ye^{\lambda|C^cD|y}\mathrm{d}y \\
&\qquad + \frac{|C|}{|CD|}\left(-e^{-\lambda|CD^c|}(1-e^{-\lambda|D|})+\frac{|D|}{|C^cD|}\left(e^{-\lambda|C|}-e^{-\lambda|C\cup D|}\right)\right)\bigg\} \\
&\qquad > \frac{|CD|}{|C|}\frac{1}{(1-e^{-\lambda|D|})}\bigg\{1-\frac{1}{\lambda|D|}-\frac{|D|}{|C^cD|}e^{-\lambda|C|} \\
&\qquad + \frac{|C|}{|CD|}\left(-e^{-\lambda|CD^c|}(1-e^{-\lambda|D|})+\frac{|D|}{|C^cD|}\left(e^{-\lambda|C|}-e^{-\lambda|C\cup D|}\right)\right)\bigg\} \\
&\qquad > \frac{|CD|}{|C|}\frac{1}{(1-e^{-\lambda|D|})}\left[1-\frac{1}{\lambda|D|}-\frac{|C|}{|CD|}\left(e^{-\lambda|CD^c|}+\frac{|D|}{|C^cD|}e^{-\lambda|C\cup D|}\right)\right] \\
&\qquad > \frac{|CD|}{|C|}\frac{1}{(1-e^{-\lambda|D|})}\left(1-\frac{1}{\lambda|D|}-\frac{|C||D|}{|CD||C^cD|}e^{-2\lambda|CD^c|}\right), \qquad \text{(F.5)}
\end{aligned}
$$

for large enough N such that $1-\frac{1}{\lambda|D|}-\frac{|C||D|}{|CD||C^cD|}\exp(-2\lambda|CD^c|)>0$. Hence we can ascertain that

$$
\mathrm{E}\left(\frac{\phi'(CD)}{\phi'(C)} \;\big|\; \phi'(C)>0, \phi(D)>0, X\right) > \left(1-\frac{1}{\lambda|D|}-\frac{|C||D|}{|CD||C^cD|}e^{-2\lambda|CD^c|}\right)\frac{|CD|}{|C|}\,.
$$

As such, the selected point is less likely to be in D than the case where we assume Φ' is Poisson on C.

APPENDIX G

DERIVATION OF INEQUALITY (4.10)

We have $(x'_n, y'_n) \stackrel{D}{=} (Rz\cos(\theta), Rz\sin(\theta))$, where $\theta \sim$ Uniform$(-\pi/2, \pi/2)$ and $z \sim$ Beta$(2, 1)$ are independent. Thus, we have

$$\mathrm{E}\,(x'_n) = R\frac{2}{\pi}\int_0^{\pi/2}\cos(\theta)\,\mathrm{d}\theta\int_0^1 2z^2\,\mathrm{d}z = \frac{4R}{3\pi}\,, \tag{G.1a}$$

$$\mathrm{E}\left((y'_n)^2\right) = \frac{R^2}{\pi}\int_{-\pi/2}^{\pi/2}\sin^2(\theta)\,\mathrm{d}\theta\int_0^1 2z^3\,\mathrm{d}z = \frac{R^2}{4}\,. \tag{G.1b}$$

Also, by first changing x to $1-x$ and then using polar coordinates, we obtain

$$\begin{aligned}
\frac{1}{R}\,\mathrm{E}\Big(g(R, x'_n, y'_n)\Big) + 1 &= \frac{4}{\pi}\int_0^1\int_0^1 \mathbf{1}_{x^2+y^2\le 1}\sqrt{(1-x)^2+y^2}\,\mathrm{d}x\mathrm{d}y \\
&= \frac{4}{\pi}\int_0^1\int_0^1 \mathbf{1}_{(1-x)^2+y^2\le 1}\sqrt{x^2+y^2}\,\mathrm{d}x\mathrm{d}y \\
&= \frac{2}{\pi}\int_0^{\pi/4}\int_0^{\sec\theta} 2z^2\,\mathrm{d}z\mathrm{d}\theta + \\
&\quad \frac{2}{\pi}\int_{\pi/4}^{\pi/2}\int_0^{2\cos\theta} 2z^2\,\mathrm{d}z\mathrm{d}\theta \\
&= \frac{4}{3\pi}\int_0^{\pi/4}\Big((\sec(\theta))^3 + (2\sin(\theta))^3\Big)\,\mathrm{d}\theta \\
&= \frac{3(2^{3/2}) + 6\log(1+\sqrt{2}) + 64 - 5(2^{7/2})}{9\pi} \\
&\approx 0.7499728\,.
\end{aligned}$$

Hence, $\mathrm{E}\,(g(R, x'_n, y'_n)) < -\frac{R}{4}$.